

Dissertation zur Erlangung des Doktorgrades
der Fakultät für Chemie und Pharmazie
der Ludwig-Maximilians-Universität München

***In vivo* and *ex vivo* approaches aimed at understanding the
physiological functions of APP**

Elena Montagna

aus

Rome, Italy

2018

Erklärung

Diese Dissertation wurde im Sinne von § 7 der Promotionsordnung vom 28. November 2011 von Herrn Prof. Dr. med. Jochen Herms betreut und von Herrn Prof. Dr. rer. nat. Martin Biel von der Fakultät für Chemie und Pharmazie vertreten.

Eidesstattliche Versicherung

Diese Dissertation wurde eigenständig und ohne unerlaubte Hilfe erarbeitet.

München, den 02 November 2018

.....
Elena Montagna

Dissertation eingereicht am 02 November 2018

1. Gutachterin / 1. Gutachter: Prof. Dr. rer.nat Martin Biel

2. Gutachterin / 2. Gutachter: Prof. Dr. med. Jochen Herms

Mündliche Prüfung am 17 December 2018

TABLE OF CONTENTS

TABLE OF CONTENTS	V
FIGURE LEGEND	VII
1 ZUSAMMENFASSUNG	1
2 SUMMARY	3
3 INTRODUCTION	5
3.1 APP	5
3.1.1 APP STRUCTURE	7
3.1.2 APP PROCESSING AND TRAFFICKING	8
3.1.3 APP FUNCTIONS	9
3.2 ASTROCYTES: THEIR ROLE IN THE CNS	10
3.2.1 MORPHOLOGY AND FUNCTIONS	10
3.2.2 ASTROCYTES Ca ²⁺ SIGNALS	12
3.2.3 PROGRESSES IN THE LAST DECADE IN STUDYING Ca ²⁺ TRANSIENTS AND ASTROCYTES	14
3.2.4 APP INTERFERES WITH ASTROCYTIC FUNCTIONS	15
3.3 MITOCHONDRIA	16
3.3.1 MITOCHONDRIAL ROLE IN THE REGULATION OF CYTOSOLIC FREE Ca ²⁺ CONCENTRATION	18
3.3.2 MITOCHONDRIA AND APP, STILL AN UNCLEAR RELATIONSHIP	19
3.4 DENDRITIC SPINE PLASTICITY AS A HALLMARK OF A HEALTHY BRAIN	20
3.4.1 DENDRITIC SPINE STRUCTURE	20
3.4.2 APP AND SPINE PLASTICITY: <i>IN VIVO</i> AND <i>EX VIVO</i> EVIDENCES	21
3.5 MICROSCOPY TECHNIQUES AND MOUSE LINES MAINLY INVOLVED IN THIS STUDY	22
3.5.1 FUNCTIONAL IMAGING: <i>IN VIVO</i> TWO PHOTON Ca ²⁺ MICROSCOPY	22
3.5.2 TWO PHOTON <i>IN VIVO</i> IMAGING OF DENDRITIC SPINES	26
4 AIM OF THE STUDY	28
5 METHODS	29
5.1 ANIMALS	29
5.2 GENOTYPING	29
5.3 CRANIAL WINDOW IMPLANTATION AND VIRUS INJECTION	31
5.4 TAMOXIFEN ADMINISTRATION	32
5.5 <i>IN VIVO</i> TWO PHOTON SPINE IMAGING	32
5.6 IMAGES, DATA PROCESSING	33
5.7 <i>IN VIVO</i> CALCIUM TWO PHOTON MICROSCOPY	34
5.8 EXTRACTION AND ANALYSIS OF Ca²⁺ TRANSIENTS	35
5.9 IMMUNOFLUORESCENCE	38
5.10 3D SHOLL ANALYSIS ON ASTROCYTES	38
5.11 MEASUREMENT OF THE VOLUME OF MOSSY FIBER IN APP FLOX X SLICK V MICE.	39
5.12 CORTICAL ASTROCYTIC CULTURE	39
5.13 IMMUNOFLUORESCENCE ON CULTURED CORTICAL ASTROCYTES	40
5.14 CONFOCAL CHARACTERIZATION OF MITOCHONDRIA MORPHOLOGY	40
5.15 EM CHARACTERIZATION OF MITOCHONDRIA MORPHOLOGY	41
5.16 IMMUNOHISTOCHEMICAL APPROACH TO QUANTIFY MCU PROTEIN	42
5.17 CONFOCAL MICROSCOPY AND DENDRITIC SPINE ACQUISITION	42

Table of contents

5.18	<i>IN VIVO</i> AND <i>EX VIVO</i> DENDRITIC SPINE ANALYSIS	42
5.19	PRIMARY ANTIBODY LIST FOR IMMUNOFLUORESCENCE	43
5.20	NOVEL OBJECT RECOGNITION TEST	44
5.21	ENVIRONMENTAL ENRICHMENT	44
5.22	STATISTICAL ANALYSIS	45
6	RESULTS	46
6.1	<i>IN VIVO</i> Ca^{2+} IMAGING TO UNRAVEL THE CRITICAL ROLE OF APP ALONG THE FINE PROCESSES OF ASTROCYTES	46
6.1.1	EXPRESSION OF MEMBRANE-ANCHORED GCaMP6f IN ASTROCYTES OF APP KO MICE	46
6.1.2	APP KO MICE SHOW IMPAIRED ASTROCYTIC CALCIUM TRANSIENTS ALONG THE FINE PROCESSES OF ASTROCYTES	47
6.1.3	MICRODOMAIN KINETICS ALONG THE FINE PROCESSES OF ASTROCYTES ARE ALTERED IN APP KO MICE	49
6.1.4	GFAP SIGNAL INCREASES IN APP KO ASTROCYTES SHOWING A MORE COMPLEX BRANCHING COMPARED TO WT	51
6.1.5	MITOCHONDRIA OF APP KO ASTROCYTES ARE FRAGMENTED AND DISTORTED	52
6.1.6	EXPRESSION OF APP ECTODOMAIN ALONE IN APP Δ CT15 MICE IS NOT SUFFICIENT TO RESTORE MITOCHONDRIA MORPHOLOGY	56
6.1.7	APP KO FRAGMENTED MITOCHONDRIA COLOCALIZE WITH CYTOCHROME C	58
6.1.8	MITOCHONDRIAL CALCIUM UNIPORTER EXPRESSION IS INCREASED IN ASTROCYTIC CULTURES OF APP KO MICE	60
6.1.9	SUMMARY OF THE FUNCTIONAL ROLE OF APP IN ASTROCYTES	61
6.2	POST SYNAPTIC APP AND APP ECTODOMAIN ARE NECESSARY FOR THE MAINTENANCE OF DENDRITIC SPINE PLASTICITY	63
6.2.1	FIVE DAYS TAMOXIFEN-TREATMENT DEPLETED APP FROM THY-1 YFP POSITIVE NEURONS IN APP-FLOX/SLICK V MICE	63
6.2.2	CONDITIONAL POST SYNAPTIC KO OF APP AFFECTS DENDRITIC SPINE DENSITY AND MORPHOLOGY	64
6.2.3	APP ECTODOMAIN IS CRUCIAL FOR SPINE DYNAMICS UPON EE STIMULATION	69
6.3	APPΔCT15 MICE CAN DISCRIMINATE BETWEEN FAMILIAR AND NOVEL OBJECTS DURING A NOVEL OBJECT RECOGNITION TEST	70
6.3.1	SUMMARY OF THE FUNCTIONAL ROLE OF APP IN MODULATING DENDRITIC SPINE PLASTICITY	71
7	DISCUSSION	73
8	ACKNOWLEDGEMENTS	82
9	LIST OF ABBREVIATIONS	84
10	REFERENCES	85
11	LIST OF PUBLICATIONS	A

Figure Legend

Figure 1: APP structure.	7
Figure 2: Golgi staining of astrocytes.	11
Figure 3: Time line of progresses done in regard to Ca ²⁺ investigation in astrocytes.	15
Figure 4: GCaMPs and loading approaches.	24
Figure 5: Two photon excitation microscope.	25
Figure 6: Example of GFP positive dendrites acquired through <i>in vivo</i> two photon microscopy.	27
Figure 7: Virus injection and cranial window implantation.	32
Figure 8: Cranial window and GFP positive dendrites.	33
Figure 9: La vision setup.	35
Figure 10: Representation of the protocol for the extraction and investigation of Ca ²⁺ transients.	37
Figure 11: Environmental housing condition.	45
Figure 12: <i>in vivo</i> setting and expression pattern of astrocytic viruses.	47
Figure 13: Altered ASCTs in the cortex of APPKO mice.	49
Figure 14: APP KO microdomains have impaired kinetics.	50
Figure 15: Sholl analysis on astrocytes.	52
Figure 16: APP KO astrocytic mitochondria display more fragmented morphology than WT, restored by full-length APP expression.	54
Figure 17: APP KO mitochondria show fragmented mitochondria and APP ectodomain cannot recover completely a normal phenotype.	58
Figure 18: APP KO mitochondria show "teardrop" like structures enriched with Cytochrome C.	59
Figure 19: Immunofluorescence of MCU shows enhanced number of MU-positive spots in APP KO astrocytic culture.	61
Figure 20: Experimental time line and proof of Tamoxifen- mediated recombination.	64
Figure 21: Conditional post synaptic KO of APP affects dendritic spines of the somatosensory cortex and of hippocampal CA1 pyramidal neurons.	67
Figure 22: APP ectodomain is necessary for spine plasticity upon EE stimulation.	70
Figure 23: APP Δ CT15 mice can discriminate between novel and familiar object during a NOR test.	71

Figure Legend

Figure 24: Schematic representation of the interplay between APP –mitochondria and calcium transients in fine processes of astrocytes. 76

Figure 25: APP and spine dynamic summary. 80

1 ZUSAMMENFASSUNG

Das Amyloid Vorläuferprotein (APP) ist ein transmembranes Protein, welches bisher hauptsächlich im Hinblick auf seine Rolle in der Pathogenese des Morbus Alzheimer untersucht wurde.

Dahingegen werden die physiologischen Funktionen von APP noch intensiv diskutiert, obwohl immer mehr Beweise seine essentielle Rolle während der Gehirnentwicklung aufzeigen. Beispielsweise hat das Vollängenprotein zelladhäsive und rezeptorenartige Eigenschaften, die für die Synapsenbildung und Synapsenstabilität grundlegend zu sein scheinen.

Trotz seiner ubiquitären Expression, konzentrieren sich die meisten Studien auf die Funktion von APP in Neuronen, wobei über seine Rolle in Astrozyten noch sehr wenig bekannt ist.

Um ein detaillierteres Verständnis über die Funktionen von APP zu bekommen, untersucht die vorliegende Studie die physiologischen Aktivitäten des Proteins sowohl in Neuronen, als auch in Astrozyten.

Das erste Ziel dieser Studie ist es, zu verstehen, ob und auf welche Weise APP intrazelluläre Ca^{2+} Mengen in Astrozyten *in vivo* beeinflusst. Hierfür verwendete ich die Kombination von Astrozyten-spezifischen Ca^{2+} -Indikatoren und Zweiphotonenmikroskopie *in vivo* an anästhesierten APP-Knock Out (KO) Mäusen. Die beobachteten Ergebnisse zeigen, dass das Fehlen von APP starken Einfluss auf die Ca^{2+} Transienten entlang der Zellfortsätze hat. Des Weiteren konnten durch einen Zellkulturansatz Mitochondrien als wichtige Mediatoren identifiziert werden. Es konnte eine starke Veränderung und Fragmentierung des Mitochondriennetzwerks zusammen mit einer Akkumulation von Cytochrom C in unmittelbarer Nähe von vergrößerten Mitochondrien beobachtet werden. Ein ähnlicher Phänotyp mit fragmentierten Mitochondrien wurde bereits in Astrozyten von mutierten Mäusen gefunden die eine APP Form ohne intrazelluläre Domäne exprimieren (APP Δ CT15). Diese Ergebnisse weisen auf die wichtige Rolle von APP als Modulator der Ca^{2+} Aktivität in astrozytischen Mikrodomänen hin.

Ein weiteres Ziel der Studie bestand darin die Rolle von postsynaptischem APP in der Plastizität dendritischer Dornfortsätze mit Hilfe konfokaler Mikroskopie zu

Zusammenfassung

untersuchen. Zu diesem Zweck diente eine Konditionale APP KO, mit Slick V gekreuzte Mauslinie. Diese ermöglicht es den Effekt von fehlendem APP in einzelnen kortikalen und hippocampalen Neuronen, die von APP positive Astrozyten umgeben sind, zu untersuchen. Das Fehlen von postsynaptischen APP führte sowohl zu einem Rückgang der Dichte als auch zu einer veränderten Morphologie der Dornfortsätze.

Da diese strukturellen Dornenphänotypen in konventionellen APP KO Mäusen nicht beobachtet werden können, war zu vermuten, dass es hier kompensierende Mechanismen gibt, die bei konditionalen KO Mäusen nicht auftreten.

Der letzte Punkt dieser Arbeit konzentriert sich auf einen Dornenphänotyp, der auch bei konventionellen APP KO Mäusen vorhanden ist – eine verminderte Dornenplastizität nach Haltung in einer angereicherten Umgebung.

Um zu zeigen, welche funktionale APP Domäne die Dornplastizität vor und nach Exposition gegenüber einer angereicherten Umgebung beeinflussen, wurden die apikalen Dornfortsätze des somatosensorischen Cortex von APP Δ CT15 mit GFP gekreuzten Mäusen mit Hilfe der *in vivo* Zweiphotonenmikroskopie untersucht.

Meine Ergebnisse identifizierten die APP Ektodomäne als wesentlich für die Erhaltung einer effizienten Dornenplastizität. Keine signifikante Unterschiede wurden hinsichtlich der Dornendichte zwischen der APP mutierten Linie und der Kontrollgruppe vor und nach der Exposition gegenüber angereicherter Umgebung gefunden.

Zusammengefasst stellt diese Studie neue Erkenntnisse vor, was die Rolle von APP bei der Regulierung der Funktion von Neuronen und Astrozyten im Gehirn betrifft.

“The brain: if it is cultivated, it works. If you let it go it will weaken. Its plasticity is terrific. That’s why you have to keep thinking.”

Rita Levi Montalcini, Italian neurologist, member of Italian Senate and Nobel Prize in Physiology or Medicine in 1986. From an interview for the Italian newspaper “*La Repubblica*”, 2006.

2 SUMMARY

Amyloid precursor protein (APP) is a transmembrane protein whose investigation has been mainly confined to the role played in Alzheimer’s disease (AD). By contrast, the physiological functions of APP are still matter of intensive debate, although compelling evidence strongly suggests its essential role during brain development. For instance, the full-length protein has cell-adhesion and receptor-like properties, which seem to be fundamental in synapse formation and stability. Furthermore, despite its ubiquitous expression, the majority of APP-related studies focused mostly on its role in neurons, whereas less is known about its functions in astrocytes. Thus, this study investigates the physiological actions executed by APP both in neurons and astrocytes, with the aim to provide a more detailed view of APP functions.

Astrocytes are electrically silent cells. They influence neuronal activity as well as morphology, thus defining the structure and the functionality of the brain network. Astrocytic function is primarily dependent on the intracellular free calcium concentration. The first aim of this study is to understand if and how APP modulates intracellular Ca^{2+} levels in astrocytes *in vivo*. My strategy combined astrocytic specific Ca^{2+} indicators and two photon *in vivo* microscopy on anesthetized APP knock-out (KO) mice. The *in vivo* results obtained indicate that lack of APP strongly influences Ca^{2+} transients along the fine processes of astrocytes. Additionally, through a cell culture approach, mitochondria have been identified as crucial mediator. A severe structural alteration and fragmentation of the mitochondrial network together with an accumulation of Cytochrome C was observed in close proximity of enlarged mitochondria. A similar fragmented mitochondria phenotype has been identified in astrocytes of mice expressing a mutated form of APP lacking its intracellular domain (APP Δ CT15). These results highlighted a prominent role of full length APP in the modulation of Ca^{2+} activity in astrocytic micro domains.

Summary

Secondly, confocal microscopy was applied to study the role of post-synaptic APP on dendritic spine plasticity. For this purpose, I used a conditional APP KO mouse crossed with Slick V mouse line which allows to investigate the effect of the APP KO in single cortical and hippocampal neurons having input and surrounded by cells that do express APP. It was observed that the lack of postsynaptic APP caused a decrease of spine density as well as an alteration in spine morphology. Since these structural spine phenotypes cannot be observed in conventional APP KO mice it was proposed that compensatory mechanisms occurred in APP KO mice that do not take place in adult mice where APP is conditionally knocked out.

The last part of this thesis focuses on one spine phenotype that is also seen in conventional APPKO mice, a reduced spine plasticity after environmental enrichment. By applying two photon *in vivo* spine imaging on apical dendrites of the somatosensory cortex on APP Δ CT15 mice crossed with mice expressing Green Fluorescence Protein (GFP), I aim to depict which functional domain of APP governs spine plasticity before and after exposure to enriched environment (EE). My findings identified the APP ectodomain as crucial for the maintenance of efficient spine plasticity, as no significant differences in terms of spine density were observed between the APP mutated line and the control group before and after exposure to EE.

Taken together, this study introduces new findings on the role by which the lack of APP modulates neuronal and glia functions in the brain.

3 INTRODUCTION

The Amyloid Precursor Protein (APP) and its cleavage products are primarily known for their involvement in Alzheimer's disease (AD), the leading cause of dementia worldwide (O'Brien and Wong, 2011). Around 47 million people worldwide are affected by dementia and AD may contribute to 60-70% of these cases (World Health Organization, 2014). In 1907 Alois Alzheimer reported the results of an autopsy on a 55 year old woman named August Deter, who died from a progressive behavioral and cognitive disorder. The "special substance in the cortex", found by Alzheimer in the brain of Deter, was later isolated and purified by Glenner & Wong in 1984. They detected a 40-42 amino acid long peptide. Few years later, in 1987, APP was cloned, and the small peptide was found to be a cleavage product of the larger APP precursor. Therefore, it was named amyloid- β ($A\beta$) peptide (O'Brien and Wong, 2011).

In the past 30 years, the biological functions of APP and of its cleavage products have been the subject of intense investigations.

3.1 APP

Amyloid precursor protein (APP) is a member of a family of conserved type I membrane proteins which also includes the APP like protein 1 (APLP1) and APP like protein 2 (APLP2) (Wasco et al., 1992, 1993; Slunt et al., 1994a). In adult mice, APP and APLP2 are ubiquitously expressed, but their highest concentrations have been observed in the nervous system and in the neuromuscular junction (NMJ) (Slunt et al., 1994b; Lorent et al., 1995; Thinakaran et al., 1995). Differently APLP1 is only expressed in the nervous system (Lorent et al., 1995).

APP was firstly describe in 1987 (Goldgaber et al., 1987; Kang et al., 1987; Tanzi et al., 1987). APP, similar to the other proteins of the APP-family, has a large extracellular domain and a short cytoplasmatic tail (Müller et al., 2017). The APP family member proteins are conserved across a variety of species, excluding prokaryotes, plants and yeast (Shariati and De Strooper, 2013). Very interestingly, the evolution of the APP family member proteins seems to be highly linked to the evolution of the first functional synapses and to the appearance of other cellular compounds as the lipoprotein receptors (Dieckmann et al., 2010).

Introduction

Alternative splicing of APP generates eight isoforms, of which three have been mainly characterized: APP₆₉₅, APP₇₅₁, APP₇₇₀. The isoform mainly expressed in neurons is 695 amino acids long, whereas astrocytes and microglia show roughly equal amounts of the three isoforms, and other peripheral tissues mainly express the longer isoforms (Haass et al., 1991; LeBlanc et al., 1997; Rohan de Silva et al., 1997).

APP can be cleaved by a large number of proteases, which are mainly grouped into α -, β -, and γ -secretases, depending on their cleavage site. However, proteases which cleave APP outside those three main sites also exist and have been described more recently (Vella and Cappai, 2012; Willem et al., 2015; Zhang et al., 2015; Baranger et al., 2016). Depending on the combination of proteases which process APP, a vast number of different cleavage products are generated, which have various biological properties (Andrew et al., 2016; Nhan et al., 2015). The cleavage products of the APP codomain are generally referred to as APPs, and alone represent at least 50% of the total forms of APP in the nervous system (Morales-Corraliza et al., 2009).

During the years a putative role in the progression of Alzheimer's disease (AD) has been assigned to APP, and in particular to one of the main APP-proteolytic fragments: amyloid- β (A β) (O'Brien and Wong, 2011; Zhang et al., 2011). Nowadays, APP and A β functions in AD pathogenesis are well characterized, and the two molecules are mainly investigated in the disease context. Nevertheless, APP and its cleavage products mediate also physiological functions, which are fundamental for brain development and neuronal plasticity (Müller and Zheng, 2012; Dawkins and Small, 2014; Müller et al., 2017). For instance, other proteolytic products, such as the soluble fragment sAPP α and C-terminal fragments (CTFs), show neuroprotective and transcriptional functions (Andrew et al., 2016; Chasseigneaux and Allinquant, 2012; Hick et al., 2015). Indeed, *in vitro* evidence suggests that CTFs induce axonal outgrowth by interacting with G-protein subunits, which in turn activate adenylyl cyclase/PKA-dependent pathways (Copenhaver and Kögel, 2017), although these findings have not been corroborated *in vivo*.

3.1.1 APP STRUCTURE

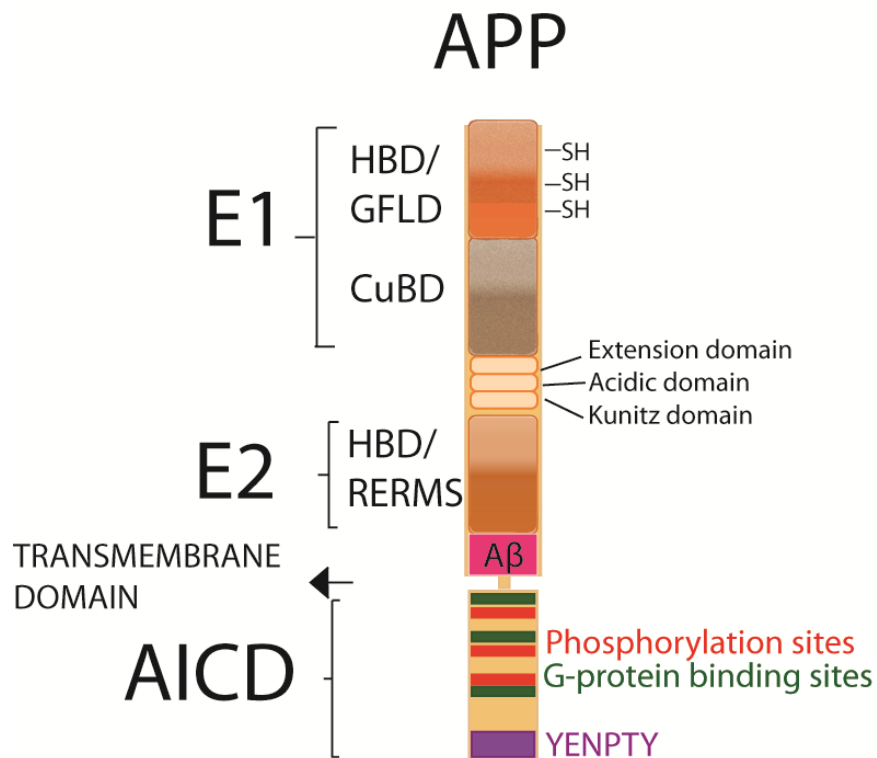


Figure 1: APP structure.

Modified from Montagna et al., 2017. Schematic representation of APP domain structure. APP is a type 1 transmembrane protein. From the N-terminal region; the E1 domain formed by: heparin binding domain (HBD), growth factor like domain (GFLD) and copper binding domain (CuBD). The E2 domain that includes the heparin binding domain and the pentapeptide sequence (RERMS). Aβ region and transmembrane region precede the AICD intracellular domain.

APP is a type I transmembrane protein, and in humans it is encoded by a gene located on the chromosome 21 and contains 18 exons spanning 290 kilobases. (Yoshikai et al., 1990; Lamb et al., 1993). APP protein structure has been extensively investigated during the years and comprises four major domains: the large extracellular domains E1 and E2 (Dahms et al., 2010; Coburger et al., 2014); a transmembrane sequence (Dulubova et al., 2004; Keil et al., 2004; Dahms et al., 2012); and the short APP intracellular domain (AICD) (Kroenke et al., 1997; Radzimanowski et al., 2008; Coburger et al., 2014) (Fig.1).

The E1 domain is composed of the growth factor-like domain (GFLD), which in turn contains the heparin binding domain (HBD) and the copper binding domain (CuBD).

The HBD and the CuBD are stabilized by the presence of several disulfide bridges (Müller et al., 2017).

The main neuronal APP isoform (APP₆₉₅) has a flexible acidic domain that connects E1 to E2. The other isoforms, present for example in astrocytes and microglia, show additionally a Kunitz domain and a short Ox-2 antigen domain, which are both lacking in the neuronal APP isoform (Müller et al., 2017).

The E2 domain of both neuronal and not isoforms contains another HBD and a RERMS motif (Ninomiya et al., 1993; Roch et al., 1993).

The intracellular domain of APP (APP-CTF) is further cleaved, generating the AICD fragment, which is known to regulate gene expression (Deyts et al., 2016).

The amyloidogenic and the non-amyloidogenic pathway is regulated by the β -secretase and the α -secretase, followed by the activity of the γ -secretase. β -secretase and α -secretase cleavage sites are found in the flexible region between the E2 domain and the transmembrane domain, whereas the cleavage site of γ -secretase is in the transmembrane domain.

3.1.2 APP PROCESSING AND TRAFFICKING

Nascent APP molecules, after sorting in the reticulum endoplasmaticum (ER) and Golgi apparatus are quickly transported towards the plasma membrane (PM) via the secretory pathway or directly to the endosomal compartment (O'Brien and Wong, 2011). During its trafficking, APP is post-translationally modified with N- and O-glycosylation, phosphorylation and tyrosine sulphatation (Haass et al., 2012). Usually no more than 10% of nascent APP reaches the PM, whereas the majority localizes into the Golgi apparatus and the trans-Golgi network (TGN) (Thinakaran and Koo, 2008; Haass et al., 2012). Recently it was found that APP has also a mitochondrial targeting sequence, which is most likely within the KPI domain (Wang et al., 2016). This causes APP accumulation in the mitochondria-associated membranes (MAM) (Anandatheerthavarada et al., 2003; Devi et al., 2006; Del Prete et al., 2017). In the PM, APP can be cleaved by the α -secretase, followed by γ -secretase cleavage, generating sAPP α and AICD fragments (Sisodia, 1992; Thinakaran and Koo, 2008). Otherwise, after exposure to the cell surface, APP is internalized within minutes through its YENPTY domain. Following endocytosis, APP is delivered to endosomes, where the secretase BACE1 is abundant and cleaves it, producing the majority of A β peptides (Perez et al., 1999).

3.1.3 APP FUNCTIONS

In the past years, numerous studies reported multiple APP functions, which vary from transcriptional regulation to synaptic functions and receptor-like activity.

In the brain, APP reaches its highest expression level during early postnatal development (from P1 to P36 in mice), and it preferentially localizes in the pre- and post-synaptic compartments (De Strooper and Annaert, 2000; Laßek et al., 2013). During this period, synaptogenesis occurs (that is, the formation of new synapses) and neuronal connections are formed (Hoe et al., 2009; Wang et al., 2009). Thus, many studies proposed putative roles of APP in the modulation of neurite outgrowth and synaptic connectivity (Moya et al., 1994; De Strooper and Annaert, 2000; Herms et al., 2004; Hoe et al., 2012; Müller and Zheng, 2012; Wang et al., 2014; Weyer et al., 2014; Hick et al., 2015).

The synapses are specialized structures that connect neurons. Recent studies have clearly demonstrated that during development and throughout life, synapses undergo continuous remodeling, both structurally and functionally, in a process known as synaptic plasticity. This process is essential for learning and memory. Neuronal inability to exhibit such plastic changes is often cause of neurodegenerative and physiological disorders (Munno and Syed, 2003). Synaptogenesis, neurite outgrowth and synaptic plasticity involve full-length APP, which has been shown to exhibit cell adhesion and receptor-like properties (Qiu et al., 1995; Ando et al., 1999; Turner et al., 2003; Soba et al., 2005; Müller and Zheng, 2012; Coburger et al., 2014; Deyts et al., 2016). There is convincing evidence that two distinct extracellular E1 domains from neighboring molecules of APP, APLP1 and APLP2 (Soba et al., 2005; Baumkötter et al., 2012; Deyts et al., 2016) can interact via their HBDs, and form a so called heparin cross-linked dimer (Coburger et al., 2014). The interaction of the E2 domains with heparin cross-linked dimers further strengthens the dimerization process (Wang et al., 2009; Hoefgen et al., 2014). As APP is present both in the pre- and postsynaptic terminals, a dimerization across the synapse may be relevant for synapse formation and stabilization (Wang et al., 2009; Baumkötter et al., 2014; Stahl et al., 2014). As trans-synaptic adhesion properties depend on the cell surface pool of APP, it is clear how mutations on the extracellular side of APP might alter these properties (Stahl et al., 2014).

In addition, APP has also been shown to be involved in synaptic plasticity of mature synapses. For instance, some AICD-proteolytic products can directly translocate into the nucleus and activate several transcription factors, like CP2/LSF/LBP1 or Tip60 (Müller et al., 2008a; Schettini et al., 2010; Pardossi-Piquard and Checler, 2012), which are known to be involved in the regulation of dendritic spine plasticity.

With regard to the APP receptor-like function, no enzymatic activity has been reported for APP so far, meaning that signal transduction requires interaction with other proteins. More than 200 binding partners, both intra and extracellular, have been identified (Müller et al., 2017). Growth factors and receptor-like proteins have been shown to interact with the APP-extracellular domains (Reinhard et al., 2005; Coburger et al., 2014; Deyts et al., 2016). Thus, activation of growth factor receptors could be one possible mode of action of how APP affects spine plasticity. Additionally, the intra-cellular domain AICD itself may mediate receptor-like activity (Cao and Südhof, 2001, 2004; McLoughlin and Miller, 2008; Müller et al., 2008a; Klevanski et al., 2015). Here, an intracellular response is triggered by the interaction of AICD-cleavage products with effector and adaptor proteins of the cytosolic compartment (Okamoto et al., 1990; Timossi et al., 2004; Deyts et al., 2012) (Figure 1). Besides the role of APP in neurons, only a few studies addressed its role in astrocytes. Investigations on astrocytic cell cultures from APP KO mice suggested a potential role of APP in modulating ATP production and the cytosolic-free Ca^{2+} concentration (Hamid et al., 2007; Linde et al., 2011; Wang et al., 2016). However, further studies are still needed to fully unravel the role of APP in astrocytes.

3.2 ASTROCYTES: THEIR ROLE IN THE CNS

3.2.1 MORPHOLOGY AND FUNCTIONS

The first description of neuroglia dates back to 1858 when Virchow wrote: “substance [...] which lies between the proper nervous parts, holds them together and gives the whole its form in a greater or lesser degree” (Virchow, 1858).

Thereafter, astrocytes have been often overlooked by many neurobiologists, and just recently they draw the attention of many researchers.

The first description of astrocytes morphology dates back to 1894, when the Golgi staining method made it possible to identify differences among astrocytes of the human brain (Retzius, 1894). One year later the term “astrocyte” was coined, that

Introduction

literally means “star-like cells” (from the Greek astron=star and kytos=cavity, cell), due to the complex and numerous processes characteristic of the astrocytes (von Lenhossek, 1895).

Astrocytes are glia cells (as oligodendrocytes, microglia and NG2 glia are) and occupy ~ 25%-50% of the brain volume, thereby being one of the most abundant cell types in the brain (Verkhratsky and Butt, 2013). They are classified into two different categories: “protoplasmic astrocytes”, with very complex and indistinguishable processes, mainly present in the grey matter; “fibrous astrocytes”, with clearly distinguishable processes and moderate branching, abundant in the white matter (Kettenmann and Verkhratsky, 2013).



Figure 2: Golgi staining of astrocytes.

Modified from Retzius; 1894; astrocytes as they appear after Golgi staining.

A recent classification divides astrocytes into nine different groups: tanycytes, radial cells, Bergmann glia, protoplasmic astrocytes, fibrous astrocytes, velate glia, marginal glia, perivascular glia, and ependymal glia. However this morphological classification does not reflect any specific distribution in the brain: within one region several types of astrocyte populations can coexist (Emsley and Macklis, 2006).

It is worth to mention that the majority of the morphological investigations were carried out on the human brain, where astrocytes are much more complex and bigger in their dimensions compared to rodent ones (Oberheim et al., 2006, 2009).

Differently, many studies on astrocytic functions have been conducted on cell cultures. Here astrocytes appear as flat cells, which possibly affects their behavior compare to astrocytes *in situ* that show a complex 3D structure (Cataldo and Broadwell, 1986).

Astrocytes perform a plethora of functions in the central nervous system and are the only cells able to store glycogen energy molecules in the brain. They are the main brain components of the brain blood barrier (BBB), and regulate the molecular trafficking across the endothelial cells. Besides their role in long term barrier induction and maintenance, astrocytes can release chemical factors to modulate endothelial permeability (Abbott, 2002).

Additionally they can regulate ion homeostasis, especially $[K]_o$, thus modulating neuronal activity as well (Ransom and Sontheimer, 1992; Ransom et al., 2000; Kofuji and Newman, 2004). Astrocytes are also involved in brain pH control mechanisms through several H^+/HCO_3^- transporters present on their membrane (Kimelberg and Nedergaard, 2010).

With regard to the way astrocytes communicate among them, it is known that they do not generate any electrical responses due to the low ratio of Na^+ to K^+ channels in mature astrocytes. Therefore, they developed a different communication system, including gap junctions, by which astrocytes are coupled (Magistretti and Ransom, 2002). Gap junctions consist of aqueous pores permeable to ions and other molecules with a molecular weight less than 1,000, able to keep astrocytic processes in contact (Magistretti J. and Ransom R). However astrocytes and neurons do not form any gap junctions. Thereby, their interaction is thought to happen only via the narrow extracellular space (ECS) (Kuffler and Nicholls, 1966). The brain ECS is a very dynamic compartment, where ions constantly diffuse almost instantly to adjacent cells (Kuffler and Nicholls, 1966). The fact that astrocytes express a broad variety of receptors for neuronal neurotransmitter allows astrocytes to sense and modulate synaptic transmission (Kettenmann and Ransom, 2005).

3.2.2 ASTROCYTES Ca^{2+} SIGNALS

The bidirectional communication between astrocytes and neurons gives rise to the concept called “tripartite synapse” (Perea et al., 2009). The model proposes that the

Introduction

information does not only travel between pre- and post-synaptic neurons, but also astrocytes can actively interfere and respond to those signals (Araque et al., 1999). In the early 1990s astrocytes became a main topic in the field of neuroscience, and pioneering studies revealed that astrocytes display a form of excitability based on the variation of intracellular calcium concentration (Cornell-Bell et al., 1990; Charles et al., 1991). The way astrocytes can respond to external stimuli is, indeed, by modulating intracellular calcium transients, often triggered by neurotransmitter release during synaptic activity (Cornell-Bell et al., 1990; Charles et al., 1991; Perea and Araque, 2005). Synaptic control over astrocytic Ca^{2+} is based on astrocytic expression of a variety of neurotransmitter receptors, such as for glutamate, GABA, norepinephrine and acetylcholine (Araque et al., 2002; Wang et al., 2006). These receptors are mainly metabotropic receptors which are linked to second messenger systems and activate phospholipase C, adenylyl-cyclase and production of IP_3 , Ca^{2+} and cAMP (Wang et al., 2009). Several evidence indicate that metabotropic glutamate receptors (mGluR) are involved in the mobilization of intracellular Ca^{2+} (Pasti et al., 1997; Porter and McCarthy, 1997).

In addition to the neurotransmitters receptors, both SOCE (store-operated Ca^{2+} entry), $\text{Na}^+/\text{Ca}^{2+}$ exchangers (NCXs) and voltage and ligand gated channels have been identified on the plasma membrane of astrocytes (Kukkonen et al., 2001; Parri et al., 2001; Reyes et al., 2012). As a consequence of Ca^{2+} increase within the cytosol of astrocytes, the secretory machine gets activated and neuroactive molecules like glutamate, D-serine, ATP, adenosine, GABA prostaglandins and other proteins and peptides are released in the ECS (Perea et al., 2009; Hamilton and Attwell, 2010; Zorec et al., 2012; Martineau et al., 2014). Both the intracellular compartments (like reticulum endoplasmaticum, ER, and mitochondria, MT) and the ECS play a role in controlling the cytosol free Ca^{2+} concentration. Prominent examples of molecules critically involved in the astrocytic calcium homeostasis are the SERCA (sarcolemmal/endoplasmic reticulum Ca^{2+} -ATPase), that moves calcium inside the lumen of the ER, the Ca^{2+} release channels inositol-1,4,5-triphosphate receptors (IP_3Rs), and the ryanodine/caffeine receptors (RYRs) (Camello et al., 2002; Beck et al., 2004; Bezprozvanny, 2005; Hamilton, 2005; Galione, 2011)

Mitochondria, as later discussed more in detail, can quickly sequester calcium from the cytoplasm. This is mediated by the mitochondrial calcium uniporter (MCU), leading to a slow calcium release via the mitochondrial NCX and the mitochondrial transition pore (Basso et al., 2005; Reyes and Parpura, 2008).

Overall, increased levels of intracellular Ca^{2+} are necessary for the release of gliotransmitters, thus shaping neuronal connectivity and contributing to neuronal network (Martineau et al., 2014; Bazargani and Attwell, 2016). Changes in cytosolic Ca^{2+} are dynamically regulated through the interplay between Ca^{2+} channels, pumps and transporters. Both the ER and mitochondria play an important role in this fine regulation (Srinivasan et al., 2016; Agarwal et al., 2017). Methodological advances in the past years have led to novel interest in astrocytic Ca^{2+} signaling with respect to brain functionality. Nevertheless astrocytic Ca^{2+} transients are still far away from being fully comprehended.

3.2.3 PROGRESSES IN THE LAST DECADE IN STUDYING Ca^{2+} TRANSIENTS AND ASTROCYTES

Pioneering studies on Ca^{2+} transients along the fine processes of Bergmann cells showed that, upon stimulation, the fluorescence of calcium indicators increases in small and specific areas, later called microdomains (Grosche et al., 1999).

The presence of mitochondria in each microdomain indicates that these microdomains are metabolically independent, as ATP and other sources of energy from the soma seem unlikely, due to the delay and decay in the transport (Grosche et al., 1999). The use of organic Ca^{2+} indicator dyes led to the erroneous conclusion that the majority of the spontaneous and GPCR-dependent Ca^{2+} fluctuations in astrocytes were mediated by inositol triphosphate receptor type 2 (IP3R2) on the ER membrane (Petraovicz et al., 2008; Agulhon et al., 2010, 2013).

However, the advent of *in vivo* imaging together with the development of cytoplasmic astrocytic Ca^{2+} indicators revealed that these Ca^{2+} transients are independent from IP3R2 and are only partially dependent on transmembrane Ca^{2+} fluxes (Srinivasan et al., 2015), thus shifting the attention to other possible candidates, like mitochondria.

In 2016 the differences between Ca^{2+} transients in the soma of astrocytes and Ca^{2+} transients along their processes were depicted (Srinivasan et al., 2016). Differences in Ca^{2+} dynamics might be ascribed to differences in the way they are initiated and

the way they propagate. A year later, the mechanisms behind the regulation of spontaneous Ca^{2+} transients occurring in microdomains along astrocytic processes were established, identifying mitochondria as main modulators. (Agarwal et al., 2017). More in detail, the inhibition of mitochondria Ca^{2+} exchangers and the modulation of the membrane potential of mitochondria resulted in a significant alteration in the number and in the activity of Ca^{2+} transients along microdomains (Agarwal et al., 2017). Interesting, less evident alterations were identified when knocking out IP3R2, thus suggesting a functional coupling between the ER and mitochondria, in which mitochondria play a pivotal role.

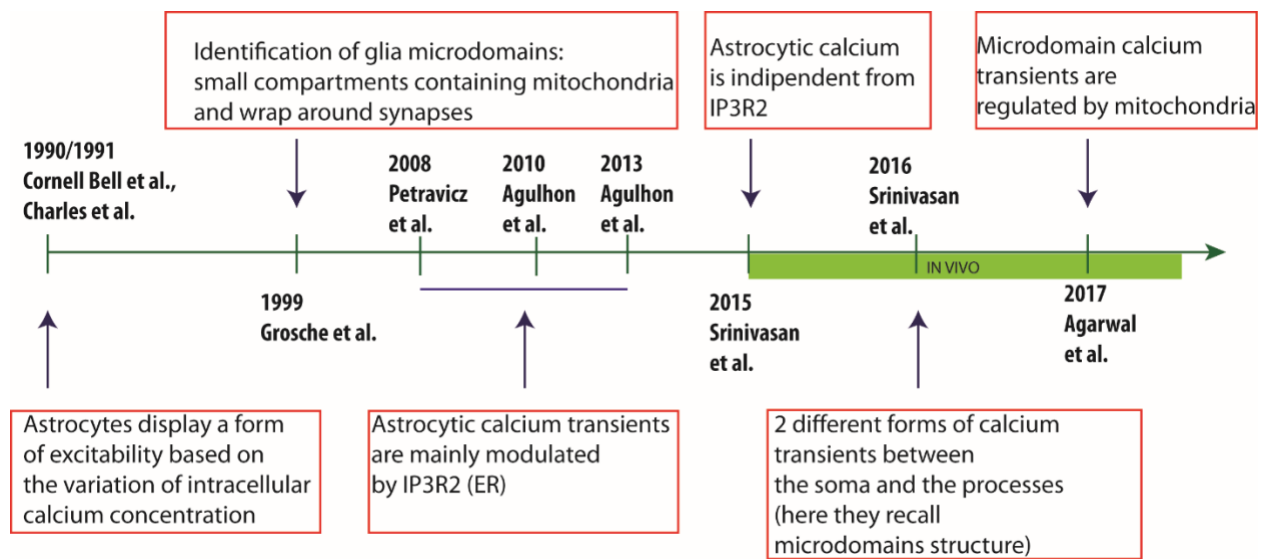


Figure 3: Timeline of the progresses achieved during recent investigations on the role of Ca^{2+} in astrocytes.

Scheme illustrating the chronological order of the progresses achieved to understand astrocytic Ca^{2+} mechanisms, from the 90s till today.

3.2.4 APP INTERFERES WITH ASTROCYTIC FUNCTIONS

APP isoforms are distributed in a cell-specific manner, with the KPI-containing isoforms (751,770) predominantly expressed in astrocytes (Rohan de Silva et al., 1997). Although its astrocytic expression has been proven (Haass et al., 1991; Rohan de Silva et al., 1997), APP physiological role in glia cells remains largely unknown. Pivotal studies on astrocytes showed increased levels of GFAP positive astrocytes in several brain areas of APP KO mice (Zheng et al., 1995). Additionally, cultured astrocytes of APP KO mice showed altered ATP and cytosolic Ca^{2+} contents (Hamid et al., 2007; Linde et al., 2011; Haass et al., 2012).

More recent findings tried to bridge the gap between astrocytes, dendritic spine plasticity and APP, investigating the release of glio-transmitters, like D-serine. As a glutamate co-agonist, the calcium-dependent astrocytic release of D-serine can in turn modulate post-synaptic NMDA-dependent long-term potentiation (LTP) (Henneberger et al., 2010), thus producing an effect on spine plasticity. Moreover, full-length APP and its fragments modulate D-serine secretion (Wu and Barger, 2004; Wu et al., 2004), and more recently, biosensor measurements in the cortex of 4-6 months old APP KO mice revealed alteration of D-serine homeostasis (Zou et al., 2016). Interestingly, a 5 week long oral D-serine treatment restores altered spine dynamics of APP KO mice both under standard housing conditions as well as in enriched environment. Taken together these data provided additional insights on the active role of astrocytes in the context of synaptic plasticity and APP expression (Zou et al., 2016).

3.3 MITOCHONDRIA

Mitochondria are double-membrane bound organelles present in the majority of the eukaryotic cells. They are thought to derive from eubacteria-like endosymbionts and carry their own DNA that forms structures known as “mitochondrial nucleoids” (Lang et al., 1997) .

Although mitochondria differ morphologically from cell to cell (Collins et al., 2002), they share common features, thus making them easily recognizable with the majority of the microscopy techniques. One typical mitochondrial structure is the double lipid membrane that divides the mitochondria in four different compartments: the outer membrane, the intermembrane space, the inner membrane, and the matrix. Each compartment conducts different functions (McCarron et al., 2013). Mitochondrial dimensions can vary from 0.75 to 3 μm , with a more round or a rod-shape morphology (McCarron et al., 2013).

Mitochondria are one of the main sources of energy for cells and play a crucial role in processes like apoptosis, free radical scavenging and Ca^{2+} signaling (Pagani and Eckert, 2011). The way mitochondria generate energy encompasses mainly two metabolic processes: tricarboxylic acid (TCA) cycle (producing NADH, FADH and less ATP) and the oxidative phosphorylation (OXPHOS), the main source of ATP production. The latter comprises the electron chain transport (ECT), which includes

Introduction

several complexes: complex I to IV plus the F1F0-ATP synthase (complex V) (Balaban et al., 2005; Benzi et al.; Pagani and Eckert, 2011).

Production of energy, such as ATP, requires the presence of Ca^{2+} , and the accumulation of mitochondrial Ca^{2+} is a tightly controlled process. While the outer membrane (OMM) is permeable for ions as Ca^{2+} as well as for small proteins, the inner membrane (IMM) is an impermeable membrane (Gincel et al., 2001; Frey et al., 2002). Therefore, Ca^{2+} can only pass through the IMM via the mitochondrial calcium uniporter (MCU), which takes calcium up and releases it into the mitochondrial matrix. For Ca^{2+} efflux two different routes have been identified: one sodium dependent (NCE) (that exchange Na^+ for calcium) and one sodium-independent (NICE) (that exchanges H^+ for calcium) (Bianchi et al., 2004).

Although Ca^{2+} is essential for ATP production, uncontrolled increased Ca^{2+} levels can activate the pro-apoptotic protein Cytochrome C (Jouaville et al., 1999; Szalai et al., 1999; Bianchi et al., 2004).

Furthermore, mitochondria are highly dynamic organelles, both in terms of shape and mobility within cells. This characteristic is extremely meaningful if we think that mitochondria need to reach those area that demand energy to provide them with ATP and Ca^{2+} (Jackson and Robinson, 2015).

Fusion and fission are part of the same cycle: a shift towards fusion favors generation of interconnected mitochondria, whereas a shift towards fission generates several fragmented mitochondria (Celis-Muñoz et al., 2016). During mitosis, mitochondrial fission is favored. Instead, mitochondrial fusion consists of OMM fusion followed by IMM fusion (Detmer and Chan, 2007). Fusion and fission are highly coordinated: for instance, inhibition of mitochondrial fission results in the formation of enlarged regions within the highly connected mitochondria network, due to clustering of nucleoids in fused mitochondria (Ban-Ishihara et al., 2013).

Remarkably, alterations in the mitochondrial morphology reflect altered mitochondria functionality, a hallmark in several neurological diseases (Swerdlow et al., 2010; Cai and Tammineni, 2016; Golpich et al., 2017). Moreover, as highly motile organelles, mitochondria can move around within a given cell, satisfying any needs of energy. Within astrocytes, mitochondrial trafficking is bidirectional (44% of mitochondria move retrogradly and 56% move anterogradly), whereas the opposite percentage of mitochondrial directions have been observed in neurons (Stephen et al., 2014).

Finally, it has been shown in organotypic slices (<600 nm), in astrocyte culture and *in vivo* that mitochondria are not uniformly distributed along the fine processes of astrocytes (Mathiisen et al., 2010; Jackson and Robinson, 2015).

3.3.1 MITOCHONDRIAL ROLE IN THE REGULATION OF CYTOSOLIC FREE Ca²⁺ CONCENTRATION

As aforementioned, mitochondria are very dynamic organelles that efficiently produce ATP and buffer intracellular Ca²⁺ (Agarwal et al., 2017; Hailong Li, Xiaowan Wang Nannan Zhanga, Manoj K. Gottipatic, Vladimir Parpura, 2005; Shigetomi et al., 2013).

The localization of mitochondria within astrocytes can determine the intracellular free Ca²⁺ concentration, thus influencing astrocytes Ca²⁺ signaling, Ca²⁺ wave propagation and Ca²⁺-dependent release of gliotransmitters (Wang et al., 2009; Shigetomi et al., 2013, 2016; Agarwal et al., 2017).

Mitochondria were the first organelles to be associated with Ca²⁺ handling (Rizzuto et al., 2012). In 1961, mitochondria were shown to accumulate Ca²⁺, whereas in 2004 the first mitochondrial Ca²⁺ uniporter (MCU) was identified (DeLuca and Engstrom, 1961; Vasington and Murphy, 1962; Kirichok et al., 2004). The driving force for the accumulation of Ca²⁺ into the mitochondria is the electrochemical proton gradient generated by the mitochondrial ETC (Rizzuto et al., 2012). The close apposition of mitochondria to both Ca²⁺ channels and ER allows a fast Ca²⁺ uptake (Rizzuto et al., 2004). ER and mitochondria are connected via the Mitofusin 2 protein, a component of the fission machinery of mitochondria, particularly enriched in mitochondria associated membranes (MAMs) (Raffaello et al., 2016; Filadi et al., 2017). Recent findings corroborate the hypothesis that ER and mitochondria are not simply morphologically associated, but rather act in concert involving special functional domains on both sides (Hayashi et al., 2009; de Brito and Scorrano, 2010).

In the context of Ca²⁺ transients along fine processes of astrocytes, it has been found that pharmacological modulation of mitochondria highly affects cytosolic Ca²⁺ dynamics (Kanemaru et al., 2014; Srinivasan et al., 2015; Agarwal et al., 2017).

Thus, mitochondria regulate several vital cellular functions through the modulation of intracellular Ca²⁺, like the cell metabolism (Rizzuto et al., 1999; Visch et al., 2004),

cell survival (Jacobson and Duchen, 2002), cell-cell signaling (Rizzuto et al., 1999; Martineau et al., 2014), and nuclear signaling (Ermak and Davies, 2002).

3.3.2 MITOCHONDRIA AND APP, STILL AN UNCLEAR RELATIONSHIP

APP and A β target to mitochondria, affecting mitochondrial morphology and functionality (Pavlov et al., 2011). Although it seems clear that APP is located on the mitochondrial membrane, the results regarding which APP-amino acids are determining this localization are still controversial. Several studies attributed such a function to the residues 40,44 and 51 (Anandatheerthavarada et al., 2003), whereas others propose the KPI domain as the responsible domain (Wang et al., 2016).

The formation of stable complexes between APP and components of the mitochondrial membrane, such as the translocase of outer mitochondrial membrane 40 (TOMM40) and translocase of the inner membrane 23 (TIM 23) (Pagani and Eckert, 2011) has been shown to modulate mitochondrial protein trafficking.

Although the functional role of APP for mitochondria needs to be further clarified, multiple observations have been highlighted in the AD context, where congruent mitochondrial-Ca²⁺ buffering alterations and oxidative stress have been reported (Devi et al., 2006; Pera et al., 2017). The presence of abnormal mitochondrial shape, transport and altered dynamics has also been reported (Du et al., 2010; Wang et al., 2014). In particular, the formation of “mitochondria on a string” (MOAS), that is, teardrop shaped mitochondria connected by a thin double membrane, has been described in AD human brain tissue (Zhang et al., 2016).

Nevertheless, it is not yet clear whether APP can localize and modulate mitochondria activity. A recent study on HeLa cells expressing truncated forms of APP carrying mutations in the KPI domain, showed altered mitochondrial morphology and altered APP distribution along the mitochondria membrane (Wang et al., 2016). In 2009, embryonic fibroblast from APP KO mice were studied in *in vitro* conditions (Sheng et al., 2009). Interestingly, lack of APP affected cell proliferation, mitochondrial membrane potential and electron transport chain IV activity, and led to reduced levels of reactive oxygen species (ROS). A possible connection between APP and mitochondria activity was also proposed in HEK293 cells, H4 cells and in astrocytic cultures derived from mice lacking APP. Here lower ATP levels and a

hyperpolarization of the inner membrane potential was observed (Hamid et al., 2007).

3.4 DENDRITIC SPINE PLASTICITY AS A HALLMARK OF A HEALTHY BRAIN

3.4.1 DENDRITIC SPINE STRUCTURE

Neurons can receive and transmit information through synapses, highly plastic components of the brain network (Foster and Sherrington, 1897).

An important structure of the brain to maintain its functionality is the dendritic spine. Specifically, dendritic spines are membrane-limited regions that project from the dendrites making contact with usually only one axon (Yuste et al., 2011). Most excitatory synapses occur at dendritic spines, thereby representing the main post synaptic excitatory compartment (Hering and Sheng, 2001). Although axons can directly communicate with dendrites (Yuste, 2015), spines greatly expand the surface of the dendrites (García-López et al., 2007; Yuste et al., 2011). Therefore, dendritic spines are thought to be necessary to implement a distributed circuit with widespread connectivity (Yuste et al., 2011).

Dendritic spines come in different shapes and sizes and act as subcellular compartments able to control, receive and process synaptic information (von Bohlen und Halbach, 2009). Additionally, the cytoplasm of dendritic spines contains F-actin, responsible for the regulation of morphological changes, maturation and stability of spines (Ebrahimi and Okabe, 2014) through the activity of several GTPases (Newey et al., 2005).

Depending on the shape and size of their head and neck, spines are usually divided in three main categories (Peters and Kaiserman-Abramof, 1970). Mushroom spines have a large head and a narrow neck; thin spines are characterized by a long neck and an almost absent head; stubby spines, instead, do not seem to have any obvious shrinkage between the base and the head. A fourth category named “filopodia” could be included. Filopodia have a hair-like morphology, are highly motile and can transform themselves into mushroom or thin spines, or initiate another dendritic branch formation (Skoff and Hamburger, 1974; Alvarez and Sabatini, 2007;

Montagna et al., 2017). Notably, spines with larger heads have greater synaptic strength than smaller spines; but it is not clear whether spines with different morphology serve different functions (Lai et al., 2016). The strength of a given spine, often measured by its head enlargement, is the consequence of rapid transport of specific mRNAs to the synapse, where local protein synthesis occurs.

Interestingly, spine plasticity depends also on external and environmental stimuli: processes like learning or exposure to Enriched Environment (EE) increase local protein synthesis at the spine, influencing stability and dynamics of dendritic spines (Johansson and Belichenko, 2002; Lai and Ip, 2013; Jung and Herms, 2014).

3.4.2 APP AND SPINE PLASTICITY: *IN VIVO* AND *EX VIVO* EVIDENCES

The physiological role of APP with regard to spine dynamics and plasticity is still controversial and a matter of debate.

So far, many transgenic mouse models have been employed to address this question: single, double and triple knock-out (KO), conditionally floxed alleles, and knock in (KI) lines. Among all of these models, the APP KO mouse (single KO of the APP locus) is probably the best studied. *Ex vivo* studies on brain sections of APP KO mice detected age-dependent deficits in neuronal morphology, synaptic plasticity and behavior (Dawson et al., 1999; Seabrook et al., 1999; Ring et al., 2007; Lee et al., 2010; Tyan et al., 2012).

APLP1 KO mice show postnatal growth deficits, whereas APLP 2 KO mice do not show any clear observable phenotype. However, APP/APLP2 double KO and APLP1/APLP2 double KO mice, as well as triple KO mice (APP, APLP1, and APLP2 KO) die shortly after birth, most probably due to severe neuromuscular deficits (Müller et al., 2017). Intriguingly, APP/APLP1 double KO mice are viable, indicating that APLP2 has unique properties that are required when either APP or APLP1 are absent. It also suggests that the APP family members can have redundant functions.

In vivo evidence are, unfortunately, more controversial. A recent *in vivo* study investigated the kinetic of spine dynamics of apical tufts dendrites of layer V pyramidal neurons of the somatosensory cortex in 4 months old APP KO-GFPm-crossed mice (Zou et al., 2016). The density and the turnover rate (TOR) of dendritic

spines were monitored over a period of 9 weeks in comparison to GFP-m control mice. Different from previous data (Bittner et al., 2009), no differences were detected in the overall spine densities between the two groups. However the fate of individual spines over time exhibited significant changes, resulting in reduced spine TOR in APP KO mice (Zou et al., 2016).

Furthermore, a recent study (Bittner et al., 2009) pointed out that APP might influence spine density in the somatosensory cortex of 4-6 months old APP KO mice crossed with YFP-H (Feng et al., 2000). In accordance, morphological analysis revealed a decrease in the fraction of thin spines and an increase of the relative number of mushroom spines (Zou et al., 2016).

In order to assess whether the reduced TOR in APP KO is a consequence of a developmental phenotype, mice were exposed to EE, which is known to enhance spine plasticity in several brain regions (Berman et al., 1996; Kozorovitskiy et al., 2005; Nithianantharajah and Hannan, 2006; Mora et al., 2007; Sale et al., 2014). Surprisingly, APP KO mice exposed to EE for 5 weeks did not exhibit any increase in spine density, thus delineating a novel role for APP in adaptive spine plasticity.

Taken together, *in vivo* and *ex vivo* results strongly suggest that APP and its functional domains are not only implicated in pathological aspects, but are also fundamental for dendritic spine plasticity.

3.5 MICROSCOPY TECHNIQUES AND MOUSE LINES MAINLY INVOLVED IN THIS STUDY

3.5.1 FUNCTIONAL IMAGING: *IN VIVO* TWO PHOTON Ca^{2+} MICROSCOPY

Genetically encoded Ca^{2+} indicators (GECIs) represent a biological and methodological milestone in the field of calcium imaging research. Their development relied on the establishment of multiple GFP color variants and the biochemical studies on Ca^{2+} binding proteins through a fusion of calmodulin with the peptide M13, derived from the myosin light chain kinase (Pérez Koldenkova and Nagai, 2013).

GECIs can be categorized in two classes according to the number of fluorescent proteins present in the indicator: some GECIs contains one single fluorophore, whereas others two (also used as ratiometric probes) (Pérez Koldenkova and Nagai,

2013). Single fluorescent protein-based GECIs typically share a common principle of action, which involves a change in fluorescence intensity upon Ca^{2+} binding. Ca^{2+} chelating properties in most of the available indicators are provided by the calmodulin fused with the fluorescent protein and the calmodulin-binding peptide M13 (Figure 4A).

GFP-based GCaMPs belong to the family of GECIs. They are a powerful tool for the investigation of cellular activity (Chen et al., 2013). They consist of a circular permuted enhanced green fluorescent protein (EGFP) that is flanked by the calcium binding protein calmodulin and by the calmodulin binding peptide (M13) (Nakai et al., 2001). Upon binding of 4 Ca^{2+} molecules, the interaction with the M13-calmodulin leads to conformational changes that induce an increase in the emitted fluorescence in a reversible manner (Nakai et al., 2001; Tian et al., 2009) (Figure 4A).

Selective expression of GCaMPs indicators can be achieved by viral transduction or by in utero electroporation. More recently, transgenic mice expressing GCaMP family members have been also developed (Gee et al., 2015) (Figure 4B). Stereotaxic injection of viruses determines the brain region to be targeted, whereas the selectivity of cells is regulated by the use of specific promoters. Within the same cell type, viral expression can be either cytoplasmic or limited to specific regions and/or specific cellular membranes (Grienberger and Konnerth, 2012). Efforts in optimizing GCaMPs and other indicators were often limited by physiologically relevant issues. Neurons, where calcium sensors are usually tested, have fast calcium dynamics and low peak calcium accumulations. However, during the years many improvements have been done in terms of sensitivity and speed (Chen et al., 2013). For instance, GCaMP6f, a genetically-encoded calcium indicator for free calcium in neurons, has a sensitivity comparable to the calcium dye oregon green BAPTA 1-AM (OGB1-AM).

Introduction

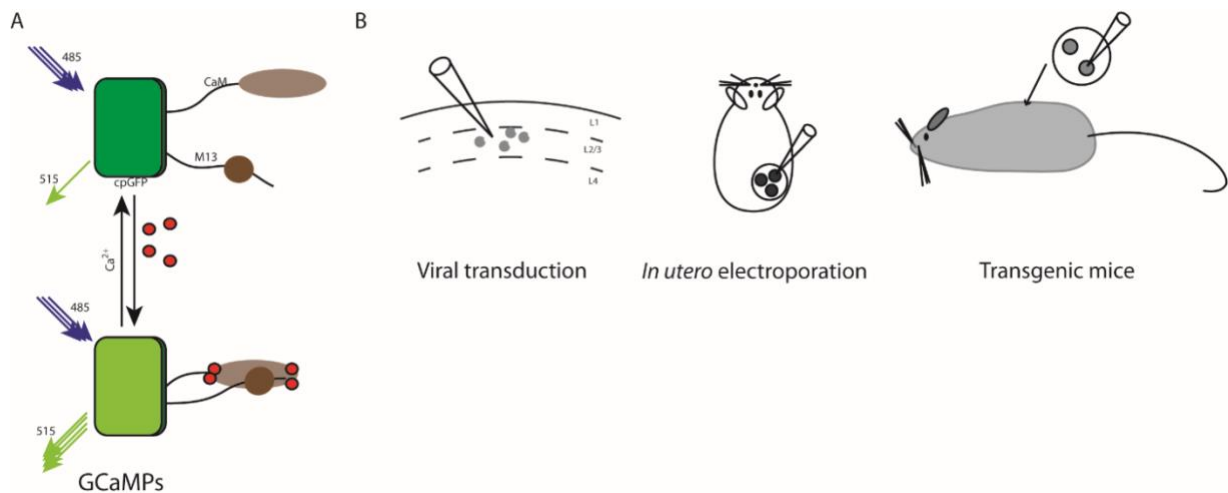


Figure 4: GCaMPs and loading approaches.

Schematic representation of GCaMP. Binding of 4 molecules of Ca^{2+} promotes intramolecular conformational rearrangement of calmodulin (CaM) and M13 changing the fluorescence intensity upon irradiation. Ca^{2+} affinity is conferred by Ca^{2+} -binding moieties derived from calmodulin (A); loading approaches of GCaMPs. Expression of genetically encoded calcium indicators (GECI) by viral transduction (left panel), in utero electroporation (middle panel), and generation of transgenic mouse lines (right panel) (B).

A further and fundamental step in understanding cellular networks within the brain has been achieved by combining sensitive and fast calcium indicators with two photon *in vivo* microscopy. This combination allows the investigation of calcium dynamics in whole cells within an intact brain and even in freely moving animals (Russell, 2011). To investigate Ca^{2+} dynamics in the cells of the brain of an alive animal, cranial windows need to be implanted on top of the skull. Although with this approach a smaller volume is visualized than when applying other *in vivo* imaging techniques, like Magnetic Resonance Imaging (MRI) and Positron Emission tomography (PET), the capability of two photon fluorescence microscopy to provide *in vivo* imaging at subcellular and subsecond resolutions is a unique advantage (Dunn and Sutton, 2008).

Two photon microscopy is based on the nonlinear optical approach that was originally proposed by the physicist Maria Göppert-Mayer in 1931. It states that a fluorophore can be stimulated by effectively simultaneous absorption of two photons, if the sum of their energies equals the required energy of excitation. In other words two low-energy photons (usually from the same laser) generate a high-energy electronic transition in a fluorescent molecule (Figure 5) (Svoboda and Yasuda, 2006).

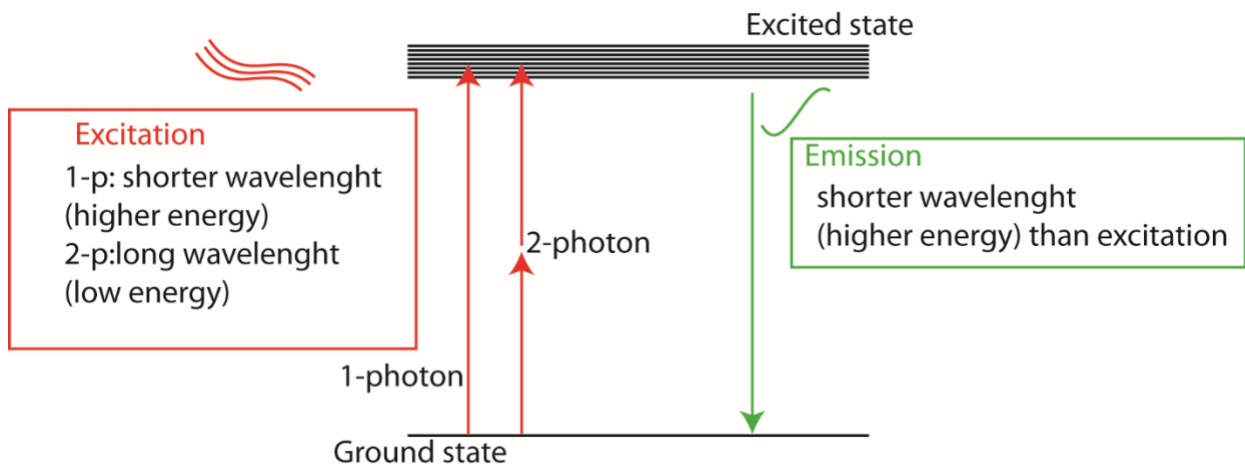


Figure 5: Two photon excitation microscope.

Diagram of 1-photon (1-p) and 2-photon (2-p) excitation. 2-p excitation of molecules can be elicited by simultaneous absorption of two long wavelengths (low energy). As main advantages the laser penetrates deeper into the tissue and only at the focal point, thus reducing bleaching and phototoxicity.

Moreover, besides the advantages of imaging at cellular and subcellular levels *in vivo*, the localization of the excitation of the fluorophore within the focal plane reduces bleaching and allows all the detected fluorescence photons to constitute useful signals (Svoboda and Yasuda, 2006).

Nevertheless, a unique interpretation of Ca^{2+} signals through two photon microscopy is not always easy and possible. It is important to consider the specific expression in the proper cell type, the exact subcellular compartment, the experimental conditions and the mouse age for a correct data interpretation. Different kind of anesthetics and the relative dose can differently influence intracellular Ca^{2+} dynamics (Ewald et al., 2011; Bindocci et al., 2017). Moreover, Ca^{2+} is known to be differently regulated according to the cell localization, so that a somatic localization differs from the dendrites of neurons or the processes of astrocytes. Therefore the investigation of Ca^{2+} dynamics in astrocytic processes needs to take into consideration the fact that Ca^{2+} dynamics here might differ from those detected in the soma, in terms of shape and regulatory mechanisms (Bindocci et al., 2017).

Notably, *in vivo* detection of Ca^{2+} transients along the fine processes of astrocytes has been challenging, mainly due to technical difficulties. The little amount of cytoplasm of the astrocytic processes made the *in situ* expression of cytosolic

GCaMPs very difficult. Nevertheless, the generation of membrane-tag Ca^{2+} indicators successfully overcame such limitation (Agarwal et al., 2017).

3.5.2 TWO PHOTON *IN VIVO* IMAGING OF DENDRITIC SPINES

Spine dynamics, including spine turnover and changes in spine shape and motility, occur throughout development and are vital for proper functioning of neural circuits in the adulthood (Calabrese, 2006). Although most of the spines are stable over very long time, a proportion of spines transiently appear and disappear. Many of these synaptic changes are driven by sensory experience and underline experience-dependent remodeling (Knott and Holtmaat, 2008).

Investigation on the number, morphology, and dynamics of healthy synapses along the brain provides researchers with information regarding neuronal development and functioning in specific brain regions.

The classification of dendritic spines must follow a constant criterium that can be summarized as following. Dendritic spines range from a volume less than $0.01 \mu\text{m}^3$ to $0,8 \mu\text{m}^3$, with a length between $0.5 \mu\text{m}$ and $2 \mu\text{m}$ (Hering and Sheng, 2001). Since spines are easily detectable, several staining and imaging methods have been developed so far.

In the past, visualization of dendritic spines was possible thanks to the Golgi staining, also called the “black staining” from Camillo Golgi himself (Mancuso et al., 2013). Afterwards, thanks to the introduction of more modern approaches, it became possible to obtain more valuable anatomical data of spine dynamics and morphology compared to those obtained from Golgi staining. Furthermore, for a simple investigation on spine density, bright field microscopy provides sufficient information, but the resolution of its images are not enough for investigating the morphology of spines (Perez-Costas et al., 2007). The advent of laser scanning confocal microscopy (LSCM) and electron microscopy (EM) have given researchers and neuroscientists a powerful tool to image changes in spine density and plasticity in brain slices and cultured neurons with nearly diffraction limited resolution (Moser et al., 1994; Papa et al., 1995).

Commonly LSCM and EM are used in combination with advanced staining techniques or injections of intracellular dyes. Additionally, by employing transgenic mice, it is nowadays possible to more precisely visualize dendritic spines, and differentiate population of neurons (Mancuso et al., 2013).

Introduction

However, two photon *in vivo* microscopy still represents the most innovative approach to study spine dynamics, as it reveals important features in the context of a living organism, with an intact brain and a functional network. Indeed, two photon microscopy allows to study spines longitudinally. Additionally, it permits to investigate the effects of the exposure to external stimuli, and to monitor aging or disease progressions (Jung and Herms, 2012). Finally, *in vivo* investigations revealed that there are populations of “persistent” spines that have a longer lifespan, and “transient” spines that appear and disappear more frequently. However, two photon *in vivo* microscopy shows drawbacks as well. For example, a reduced image resolution and the physical inaccessibility to the deep brain areas (Yuste et al., 2011) are still big limitations that need further improvement. Overall, two photon *in vivo* microscopy is the gold standard for analysing spine plasticity in living animals.

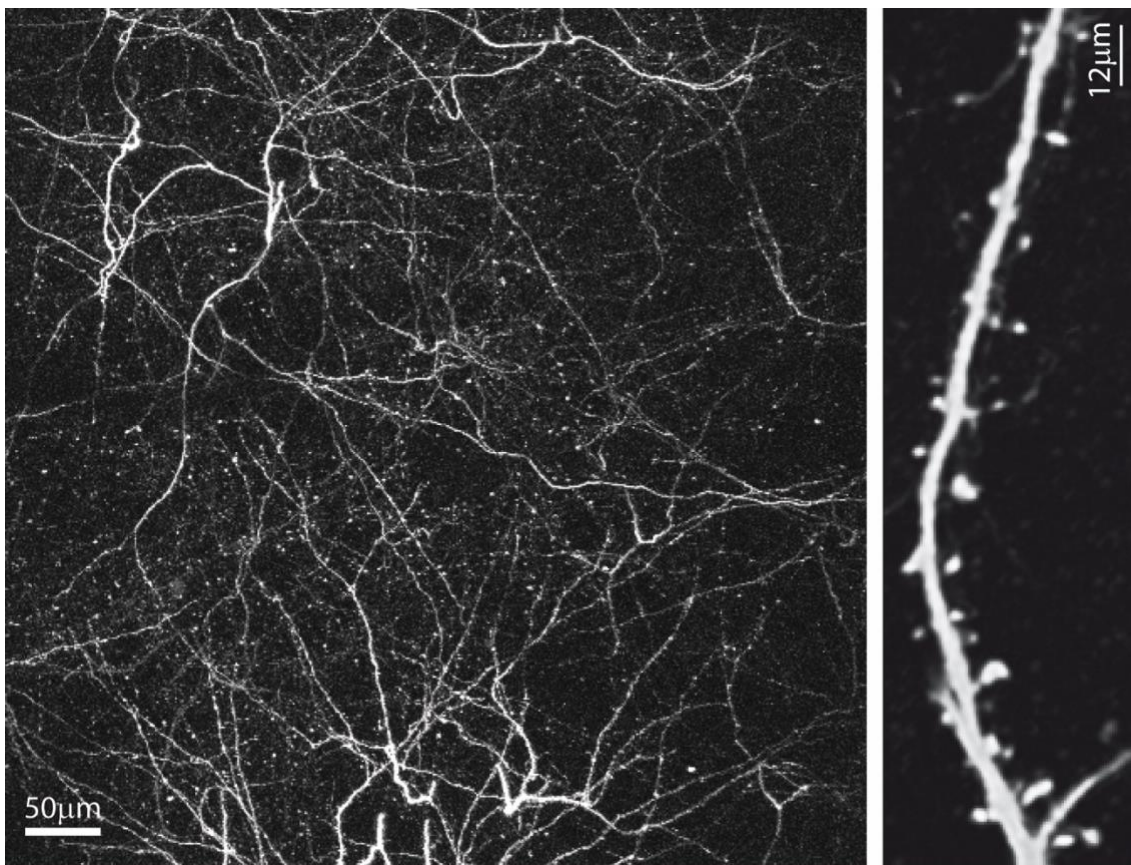


Figure 6: Example of GFP positive dendrites acquired through *in vivo* two photon microscopy. Z-stack of GFP-positive dendrites in the somatosensory cortex ($424\mu\text{m} \times 424\mu\text{m}$) acquired via two photon *in vivo* microscopy (LSM 7MP microscope Carl Zeiss, water immersion 20x objective, Leica); on the right panel z-stack of GFP-positive somatosensory dendrites and its spines ($512\mu\text{m} \times 256\mu\text{m}$).

4 AIM OF THE STUDY

With this study, I aimed at combining *in vivo* and *ex vivo* approaches to unravel the physiological function of APP in astrocytes and neurons, and to better characterize the key roles of APP in defining and influencing the overall brain network.

Firstly, this study investigates how APP modulates intracellular Ca^{2+} levels in astrocytes *in vivo*. Astrocytes are known to modulate activity and morphology of neurons, thus influencing the overall brain network. Through *in vivo* functional microscopy, I investigated Ca^{2+} dynamics in astrocytes of the somatosensory cortex of APP KO transgenic mice. With this approach I aimed at unraveling the role of APP as regulator of Ca^{2+} homeostasis in astrocytes, breaking ground for further investigations on APP function in astrocytes.

Secondly, through two photon *in vivo* microscopy on dendritic spines of APP Δ CT15 mice transgenic mouse line, where APP has been truncated at its C-terminal 15 aminoacids, I aimed at deciphering the role of APP in modulating dendritic spine dynamics in correlation with its specific functional domain, which is still matter of intensive debates.

Thirdly, to further explore the role of APP in regulating brain networking I applied confocal microscopy to investigate the density and morphology of dendritic spines of somatosensory and hippocampal neurons in conditional APP KO mice, highlighting the role of post-synaptic APP in modulating plasticity in the brain of adult mice.

Taken together, the goals of this thesis were to expand the knowledge on APP in astrocytes, a topic often overlooked in past studies, and neurons, underlining the reciprocal APP-mediated interaction between neurons and astrocytes to finely modulate the brain network.

Overall, this study aims at providing a detailed overview on APP physiological functionality, thus generating fundamental data for future investigations on AD and the development of efficacious treatments.

5 METHODS

5.1 ANIMALS

The studies were carried out in accordance with an animal protocol approved by the Ludwig-Maximilians-University Munich and the government of Upper Bavaria.

Amyloid precursor protein knock-out (APP KO) (Zheng et al., 1995), APP Δ CT15 (Ring et al., 2007), APP flox (Mallm et al., 2010) crossed with Slick V (Young et al., 2008) and wild type (WT) (C57BL/6) mice were used.

Prior to surgery mice were group-housed with three to six individuals in standard cages (30 × 15 × 20 cm), with standard bedding and additional nesting material under pathogen-free conditions. After cranial window implantation mice were singly housed in standard cages, with food and water provided ad libitum. Mice were kept under a 12/12-hour light/dark cycle. At the age of 2 months, virus injection and cranial window implantation were performed and at 3 months of age mice underwent *in vivo* imaging.

5.2 GENOTYPING

Mice were genotyped by polymerase chain reaction (PCR). Invisorb® DNA Tissue HTS 96 Kit/C (Stratagene molecular) was used for the extraction of DNA extraction from a small piece of tissue from each mouse. Briefly, 400 μ l of Lysis Buffer G was incubated with mouse tissue overnight under 52°C shaking condition, followed by 10 mins 1700g centrifugation. The supernatant was transferred into collection plate and mix with 200 μ l binding buffer A, followed by 1700 g centrifugation for 5 mins. After discarding the supernatant, the pellet was washed in 550 μ l washing buffer, followed by twice 5 mins centrifugation at 1700g. Finally, 100 μ l of warm (52°C) elution buffer was used to collect the DNA extraction.

The extracted DNA was used for PCR to identify the genotypes of each animal. The primers are listed in Table 1. The formulation of PCR solution is listed in Table 2. The PCR solution was placed in a thermocycler. The PCR program is listed in Table 3. PCR products were analyzed by gel electrophoresis. The samples were loaded to 1.5% agarose gel with SYBR® gold nucleic acid gel stain. The agarose gel was immersed into TAE running buffer. DNA migration was driven by 120-195 V electric

Methods

fields for 60-90 minutes. A photograph of the gel was taken under UV light source for documentation.

MOUSE LINE	PRIMER	SEQUENCE
APP KO	FORWARD	GAGACGAGGACGCTCAGTCCTAGGG
	REVERSE	ATCACCTGGTTCTAATCAGAGGCC
SLICKV	FORWARD	TCTGAGTGGCAAAGGACCTTAGG
	REVERSE	CGCTGAACTTGTGGCCGTTTACG
APP FLOX	FORWARD	TGCATGTCAGTCTAATGGAGGC
	REVERSE	ATCTGCCCTTATCCAGTGAAATGAACC
APP Δ CT15	FORWARD	CACACCTCCCCCTGAACCTGAAAC
	REVERSE	CTGCGAGAGAGCATCCCTACAACC

Table 1: Primers for genotyping.

ITEMS	VOLUME
Onetaq hotstart quickload	12.5 μ l
Forward primer	0.5 μ l
Reverse primer	0.5 μ l
Template DNA	0.5 μ l
Distilled water	10 μ l

Table 2: PCR mix.

STEP	TEMPERATURE ($^{\circ}$ C)	TIME(S)
1	94	180
2	94	30
3	60	60
4	68	20
5	68	120
6	10	∞

STEP 2-4 REPEATED 35
TIMES

Table 3: PCR program.

5.3 CRANIAL WINDOW IMPLANTATION AND VIRUS INJECTION

Cranial window implantation is a standard procedure commonly used for a number of *in vivo* imaging techniques (Fuhrmann et al., 2007; Holtmaat et al., 2009). Mice were anesthetized before undergoing surgery, by intraperitoneal injection of ketamine/xylazine (respectively 120 and 10 µg/g body weight; WDT/Bayer Health Care); inflammation and pain were reduced by the subcutaneously administration of the anti-inflammatory Rymadil (7.5 µg/g; Pfizer) and the antibiotic Baytril (7 µg/g body weight, Bayer Health care).

For the functional *in vivo* study 4 WT and 4 APP KO were injected in three different areas of the somatosensory cortex with: AAV5.GfaABC1D.cyto-tdTomato.SV40 (# 44332, Penn Vector, Philadelphia, PA, USA) and AAV2/5.GfaABC1D.Lck-GCaMP6f (# 52924, Penn Vector, Philadelphia, PA, USA) viruses, in a solution of 10% virus, 45% PBS (1x) and 45% of the original stock of mannitol solution, for a final volume of 300 µl/injection site. Viruses were injected at 200 µm depth from the brain surface with a speed of 30 nl/minute.

Protocol followed for cranial window implantation was the same for APP KO, WT and APP Δ CT15 mice and was done as following. A piece of skull, 4mm in diameter, above the somatosensory cortex was removed and a thin glass (VWR International GmbH, Darmstadt, De) was placed on top of the injected area and sealed by dental acrylic (Cyano-Veneer fast; Schein, Vienna, AU). A custom made small metal bar was cemented next to the coverslip to allow head-fixation during imaging sessions (Figure 7).

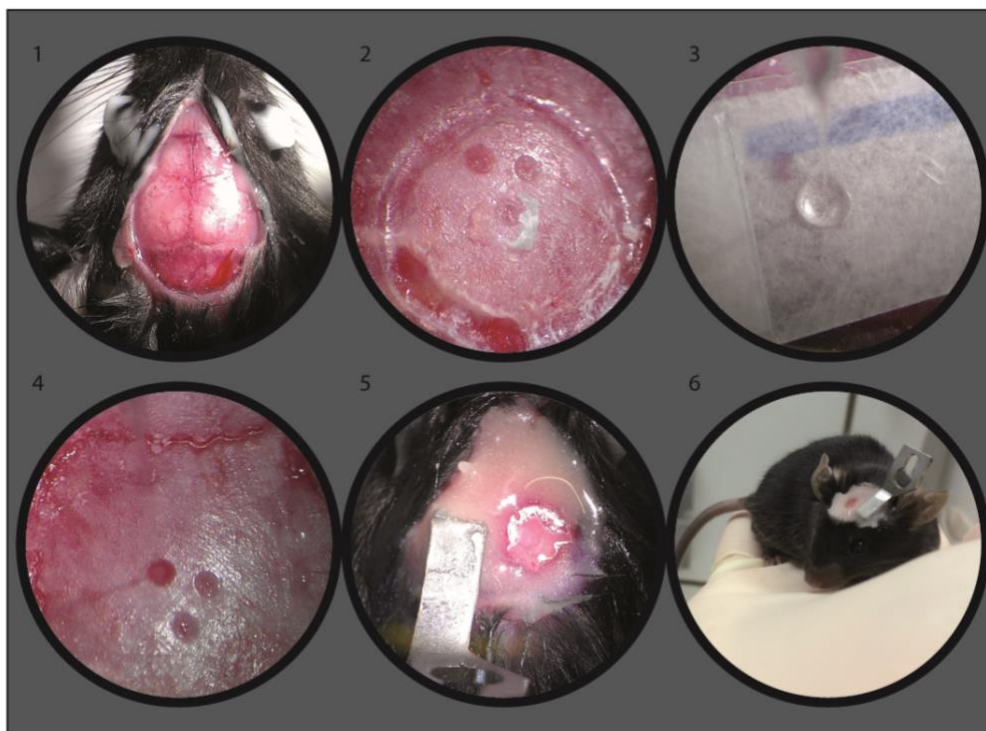


Figure 7: Virus injection and cranial window implantation.

Pictures taken during virus injection and cranial window implantation. From left to right, 1: skin on top of the skull is removed; 2: 3 mm diameter circle is delimiting the area on the somatosensory cortex where the three injections will be performed; 3: loading of the virus in a pulled glass micropipette; 4: virus is injected in three different spots; 5: after removal of 4 mm diameter skull window is implanted and sealed. Metal bar is cemented to allow head fixation during imaging sessions; 6: one month after surgery mouse is perfectly recovered.

5.4 TAMOXIFEN ADMINISTRATION

2 months old APP-flox homozygous crossed with Slick V (for control group) were daily forcedly feed with Tamoxifen (T5648, Sigma-Aldrich, Darmstadt, Germany) (0.25 mg/g) or peanut oil 5 days/week. Compounds were dissolved in a 1:10 ethanol: peanut oil mixture (Sigma-Aldrich, Darmstadt, Germany)

Control and tamoxifen treated mice were transcardially perfused and full KO of APP in YFP positive neurons was confirmed immunohistochemically (Figure 20).

5.5 *IN VIVO* TWO PHOTON SPINE IMAGING

Apical dendrites of layer V somatosensory pyramidal neurons have been considered in this investigation. Expression of eGFP and eYFP in GFP-M and SlickV mice

Methods

respectively, allows visualization of apical dendritic spines *in vivo*. LSM 7MP microscope (Carl Zeiss) equipped with water-immersion objective (20x, NA=1.0; Carl Zeiss) was used for the experiments. Briefly, mouse with cranial window was head fixed and anaesthetized with isoflurane (1% in 95% O₂, 5% CO₂). Body temperature was maintained by a self-regulating heating pad (Fine Science Tools GmbH) and each image session lasted less than 90 mins. Microscope was equipped a water-immersion objective (20x, NA=1.0; Carl Zeiss). Two photon Mai Tai DeepSee laser generator (Spectra Physics) was tuned at 920 nm wavelength (Spectra Physics). Overview images (351x351) and detailed dendritic images (70 × 97 μm) were acquired from each region of interested (Figure 8). Same dendrites were weekly acquired for a period of two months.

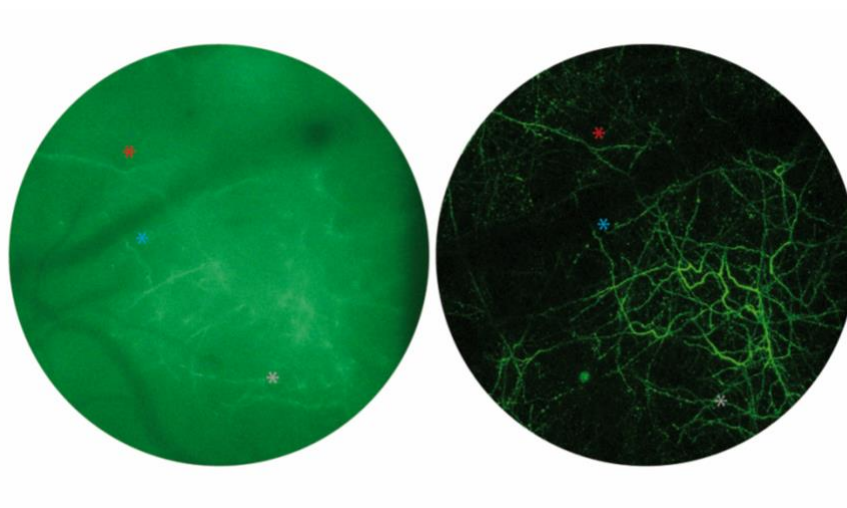


Figure 8: Cranial window and GFP positive dendrites.

*Photo of a cranial window were blood vessels and GFP positive dendrites are visible. Blood vessels are used during *in vivo* chronic imaging to repeatedly identify the regions to be imaged. On the right Z-stack of GFP positive dendrites acquired via two photon microscopy (LSM 7MP microscope Carl Zeiss, water immersion 20x objective, Leica). Each color of each asterisk identify a single dendrite visible in both the photos.*

5.6 IMAGES, DATA PROCESSING

Dendritic spines were counted manually, using a selfmade script on Zeiss blue software. For both confocal and *in vivo* micrographs, dendritic spines were counted in z-stacks by manually scrolling through the images. Because the z-plane resolution was low in two photon micrographs, the dendritic spines of cortical neurons were restricted to laterally protruding spines. As described before (Holtmaat et al., 2009), dendritic spines identified along the dendrite were marked as gained, lost, or stable.

The mean density of dendritic spines was estimated for each time point and expressed over the dendrite length. The stability of spines was calculated based on the amount of spines that remained unaltered for at least two subsequent imaging sessions. The spine turnover rate (TOR) was assessed based on gain and loss of spines over each day of imaging, calculated as follows: $TOR = (N_{gained} + N_{lost}) / (2 \times N_{present}) / I_t$, where N_{gained} , N_{lost} , and $N_{present}$ represent the number of gained, lost, or total spines at time points of interest, respectively, while I_t is the number of days between consecutive imaging sessions.

5.7 IN VIVO CALCIUM TWO PHOTON MICROSCOPY

Weekly imaging sessions started at earliest 4 weeks after surgery to allow mice to recover and cranial windows to become clear.

Mice were anesthetized by isoflurane inhalation (concentration: 1-1.5% mixed with oxygen), head fixed and placed under the microscope.

During every imaging session the body temperature was monitored and maintained at 37°C with a thermostat-controlled heating pad. To ensure mice were equally anesthetized during imaging breath rate, oxygen saturation and heart rate were monitored with the Oximeter probe (MouseOx; STARR Life Sciences, Oakmont, PA, USA) and kept constant (breath rate between 70 and 80; oxygen saturation between 98.8% and 99%, and heart rate between 450 and 500) as suggested in the monitoring protocol (Ewald et al., 2011) (Figure 9). In vivo time-lapse image series of GCaMP6f fluorescence were acquired in the layer 2/3 (120–200 μ m below the pial surface) of the somatosensory cortex.

Fluorescence images were collected by the LaVision Trim Scope equipped with tunable Ti:sapphire two photon lasers (Chameleon, Coherent, Santa Clara, CA, USA) tuned at 940nm and 25x 1.05NA water-immersion objective (Olympus, Hamburg, DE). The setup was controlled using LaVision Inspector software (LaVision BioTec GmbH, Bielefeld, DE).

Each image frame was acquired at the rate of 4.17 Hz and was approximately 75 x 75 μ m at 512 x 512 pixel resolution.

Laser intensity was always kept below 80mW. Mice were kept on the stage for a maximum of 1.30 hour and during this time period images from injected area of the somatosensory cortex were acquired (~8 min per area). Only images acquired under

same anesthesia condition were taken into consideration for astrocytic-calcium-activity analysis.

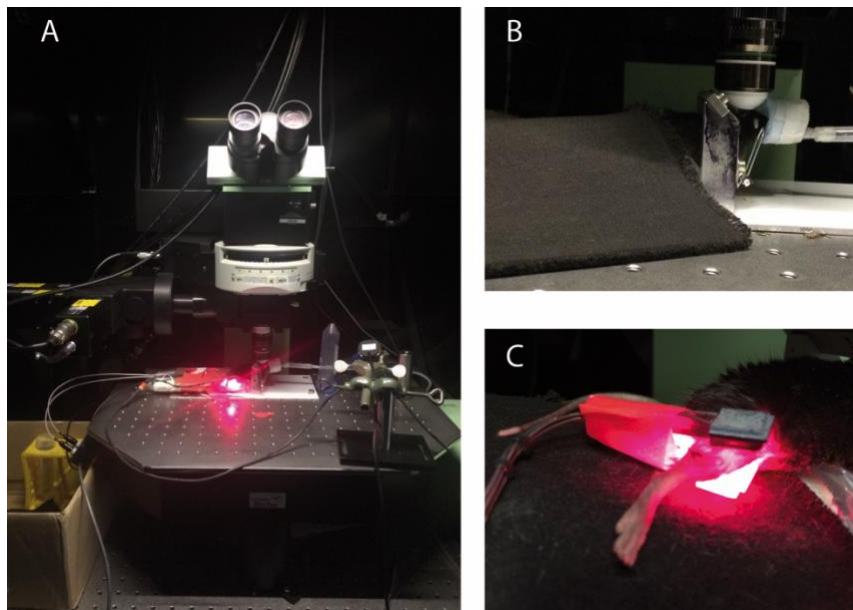


Figure 9: La vision setup.

Pictures taken before running imaging sessions. Briefly, Mouse is placed on an heating pad and under controlled anesthetic; the mouse is placed under the microscope and the cranial window aligned with the objective (A), the mouse is sleeping thanks to the anesthetic during the imaging sessions (B), a clamp of the Oximeter (MouseOx; STARR Life Sciences, Oakmont, PA, USA) is emitting a red light when actively recording the mouse parameters as reported in method session; the leg of the mouse needs to be shaved for a better recording of the vital parameters (C).

5.8 EXTRACTION AND ANALYSIS OF Ca^{2+} TRANSIENTS

After an image series was acquired, the x-y axis drift in the image stacks was stabilized using the software Igor 7 Pro (WaveMetrics Inc., Lake Oswego, OR, USA). The protocol used for astrocytic calcium investigation was adapted from the protocol “CASCADE” (Agarwal et al., 2017) (Protocol developed in collaboration with Dr. Carmelo Sgobio).

Calcium transient information from individual microdomains have been extracted by applying a combination of a custom written code in Fiji (Schindelin et al., 2012) and the MiniAnalysis Software (Synptosoft Inc., Decatur, GA, USA)

As first step background noise was subtracted by performing 3D convolutions (average and Gaussian filters of size 5x5x5 pixels (x,y,t)) on time-series image stacks (I(x,y,t)). By subtracting the products of average and gaussian filtering I

Methods

obtained a noise filtered image stack ($I(x,y,t)$). To identify those regions that exhibits frequent dynamic changes in fluorescence the mean intensity (AVG) and standard deviation (SD) of background pixels noise filtered stacks were calculated. The sum-intensity projected stacks were binarized using a threshold value of $AVG + 3 SD$. By summing the binarized sum- and SD-projected stacks of the noise filtered stack I generated a mask where the core of putative microdomains were detected. All domains with an area bigger than 25 pixels were taken into consideration. The binarized mask of the microdomain cores was used as template for ROIs detection. ROIs were finally applied on the raw time series image stack to plot the GCaMP intensity levels over time. Time traces of fluorescence intensity were extracted from the ROIs and converted to dF/F values. I analyzed spontaneous events that occurred in 300 seconds long recording session. Calcium transients were identified based on amplitudes that were at least 2-fold above the baseline noise of the dF/F value. Microdomains without any calcium transients were excluded from the defined “active microdomains”. Spontaneous events were tracked using MiniAnalysis software 6.0.07 (Synaptosoft), and event amplitudes, area under the curve, time to peak, decay time and event frequency per ROI per min were measured (Figure 10).

Methods

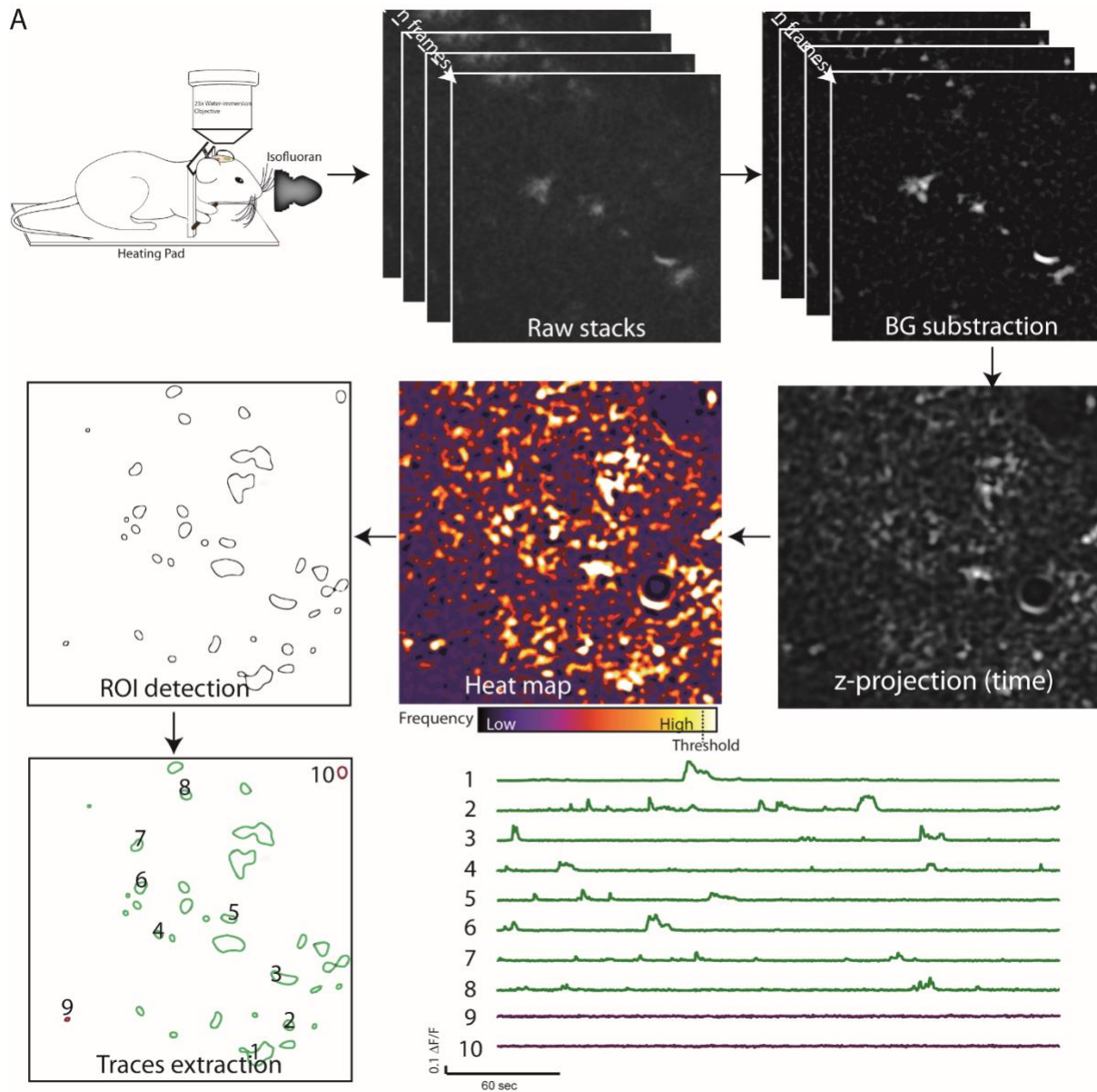


Figure 10: Representation of the protocol for the extraction and investigation of Ca^{2+} transients.

Briefly; for the movie acquisition mice were anesthetized and placed on the two photon microscopy set-up, parameters like breath, heart rate and oxygen saturation were constantly tracked while the mouse was imaged; 5 minutes image stacks were acquired in several regions of the somatosensory-cortex. The movie analysis was carried out adapting the protocol to "CASCADE" from Agarwal et al., 2017 (Agarwal et al., 2017). Filters on the raw movies were applied to subtract background from the original stacks. z-projected stack of averaged movies were thresholded and ROIs detected (as described in the method part). ROIs were finally applied on the raw data and traces were extracted via Fiji software. A low percentage of the traces from the detected ROIs were below the threshold (purple ROIs and traces) and therefore not included in the final statistical analysis

5.9 IMMUNOFLUORESCENCE

Mice were anesthetized with an intraperitoneal injection of ketamine/xylazine (0.14 mg / g body weight; WDT / Bayer Health Care) and transcardially perfused with phosphate buffered saline (PBS) followed by 4% paraformaldehyde in 0.12 M PBS, pH: 7.4. The brain was removed and post-fixed for 24 h at 4°C in the same fixative. The brains were washed in 1% PBS and coronal sections of 50 µm were obtained at room temperature by the vibratome Leica VT 1000S (Leica Mikrosysteme Vertrieb GmbH, Wetzlar, Germany). Immunofluorescence was performed on free floating sections. The study was focused on astrocytes of layer 2/3 of the somatosensory cortex (from Bregma 1.98mm to – 1.82mm). Sections were permeabilized (2% TritonX –PBS, Life Science, Darmstadt, De), gently shaken, overnight at 4°C. Blocking solution (10% normal goat or donkey serum - 1% PBS, Thermo Fisher Scientific Messtechnik GmbH, Munich, DE) was applied for 2 hours at room temperature (RT). Sections were incubated with primary antibody diluted in 3% normal goat/donkey serum, 0,03% Triton-X, 0,05% sodium azide – PBS overnight at 4°C, for a list of all the primary see table 4.

Secondary antibodies were all applied in a dilution of 1:500 in 3% normal goat/donkey serum, 0,03% Triton-X, 0,05% sodium azide – PBS for a minimum of 2 hours at room temperature. The secondary antibodies were raised in goat or donkey: Alexa 594, Alexa 488 and Alexa 647. Brain sections were mounted on polysine slides with Dako Fluorescent Mounting Medium (#S3023, Thermo Fisher Scientific Messtechnik GmbH, Munich, DE). Confocal images were acquired using a Zeiss LSM 780 with a Plan Aplanachromat 40x/ NA 1.4 Oil DIC M27 with a Pinhole set to 1 airy unit.

5.10 3D SHOLL ANALYSIS ON ASTROCYTES

High resolution confocal stacks of GFAP positive astrocytes of the somatosensory cortex (from 20 to 25 astrocytes per group, n= 4 mice/group) were acquired ($x=42$ µm, $y= 42$ µm, $z\sim 8$ µm) and deconvoluted using the software AutoQuantX3 (Media Cybernetics).

Custom written Fiji codes for Sholl analysis were applied to the image stacks (Schindelin et al., 2012, 2015; Theer et al., 2014). Sholl analysis is a method that

allows counting the number of intersections of GFAP positive leaflets, at circles of increasing radii from the center.

Shortly, stacks were thresholded and then the center of GFAP positive astrocytes was detected based on DAPI staining. First radius for the Sholl analysis was set at a distance of 50 radii (4 μm) from the center, and subsequently circles were placed every 5 radius (0,4 μm), till a maximum distance of 250 radii (20 μm).

5.11 MEASUREMENT OF THE VOLUME OF MOSSY FIBER IN APP FLOX X SLICK V MICE.

High resolution confocal stacks of YFP-VGluT positive mossy fibers (n=4 mice per control, 5 per tamoxifen treated) were acquired by confocal microscopy (x=212 μm , y= 212 μm , z= 32 μm)

For the quantification of the mossy fiber terminal volume, 3D image data stacks were analyzed using custom-written MATLAB software in combination with Imaris (Version 7.7.2). In detail, the surface detection algorithm of Imaris was applied using a smoothing value of 0.2 μm . Background subtraction was enabled by setting the diameter of the 'largest sphere that fits into the Object' to a value of 10 μm . Subsequently a manual threshold of 27000 and a minimal seed diameter of 4 μm were defined to detect individual terminals. The data was compiled in Matlab using ImarisXT interface. The MATLAB's script for the analysis of mossy fiber was developed in collaboration with Dr. Finn Peters.

5.12 CORTICAL ASTROCYTIC CULTURE

Primary cortical astrocyte cultures were prepared from P3 pups of APPKO and C57/Bl6 animals. The brain was isolated and placed in HBSS (Gibco, cat. 24020091, Thermo Fisher Scientific) at RT. Meninges were removed and the cortex was dissected. Cortices from 3 animals were pooled, cut into pieces, washed with HBSS, and digested in 5 ml Trypsin containing 0.05% EDTA (Gibco; cat. 25300062, Thermo Fisher Scientific) at 37°C for 15 min. The reaction was stopped by adding 5 ml of medium (MEM (Gibco cat. 31095029, Thermo Fisher Scientific), 0.6% Glucose (Merck # 1083371000, CAS 50-99-7), 5% heat-inactivated FBS (PAN Biotech P40-37500)). After washing with HBSS, cells were mechanically dissociated in culture medium to obtain a single-cell suspension and plated on a T-75 flask (Nunc EasY Flask cat. 156499, Thermo Fisher Scientific). The medium was changed the next day

in order to remove unattached cells. Cultures were grown in an incubator with humid environment at 37°C and 5% CO₂ (Hereaus, HERAcell 150i). Astrocytic cultures were split at 90% confluency by transferring the cells equally in T-175 flasks (Nunc EasY Flask cat.159910, Thermo Fisher Scientific). Primary cultures of astrocytes were prepared in collaboration with Sophie Crux.

5.13 IMMUNOFLUORESCENCE ON CULTURED CORTICAL ASTROCYTES

Cover glasses were placed into a humid chamber, quenched for 10 minutes with 50mM Ammonium Chloride and extracted with 0.1% Triton-X 1x PBS (Life Science, Darmstadt, De) for 3 minutes at RT.

To prevent unspecific binding, a 10 % blocking solution (2% FCS, 2%BSA, 0.2% fish Gelatin) diluted in 1x PBS was applied on the coverslips for 1 hour at room temperature.

For immunolabelling sections were incubated 1 hour at RT with primary antibody diluted in 10% blocking solution/ PBS (for a complete primary antibodies list see table). After rinsing the coverslips 3 times with 1x PBS I applied secondary antibodies diluted in 10% blocking solution/ PBS.

The secondary antibodies were raised in goat or donkey: Alexa 594, Alexa 488, and Alexa 647 diluted 1:500 in 10% blocking solution/PBS.

5.14 CONFOCAL CHARACTERIZATION OF MITOCHONDRIA MORPHOLOGY

Mitochondria from 22 different astrocytes were analyzed from 4 different cell cultures. Cultured astrocytes stably expressing Mito-GCaMP were stained with GFP-Alexa 488 (see table for protocol) and mounted with Dako Fluorescence Mounting Medium (S3023) on Polysine slides (Thermo Scientific, P4981).

Z-stacks confocal microscopy images were acquired (x: 106.07 µm, y: 106.07 µm, z: between 3-6 µm; Zeiss 40x/1.4, oil immersion) and 2-D deconvoluted (AutoQuantX3, Media Cybernetics). Projection on the z-axis was performed to obtain a single in-focus field projection.

Mitochondria were selected by thresholding the pictures and processing them using the software Fiji (Schindelin et al., 2012). Classification of mitochondria morphology

in network, rods and puncta was done accordingly to the following values: puncta area: 0,1 - 2,7 μm^2 ; rods area: 2,7 - 8.8 μm^2 and network area: from 8.9 μm^2 .

Based on the area covered by the mitochondria, a colour-coded image was generated to visualize puncta in red, rods in green and network in blue .

For the statistical analysis data are shown as percentage of the total area covered by each class of mitochondria divided by the sum of the area covered by the three different morphological classes.

5.15 EM CHARACTERIZATION OF MITOCHONDRIA MORPHOLOGY

During the second passaging, primary cortical astrocytes were plated on 15 mm glass coverslips (Marienfeld, pretreated overnight (o/n) with nitric acid (Merck) and sterilized) in a 12 well plate (Nunclon delta surface) at a density of 70 000 cells per well. After 5 days, astrocytes were rinsed with autoclaved phosphate buffered saline briefly and fixed with 2,5% glutardialdehyde in cacodylate-buffer (75 mM cacodylate, 75 mM NaCl, 2 mM MgCl_2) for 30 min, followed by 3 washing steps in cacodylate buffer. Thereafter, cells were post-fixed with 1% OsO_4 and 1% $\text{K}_4\text{Fe}(\text{CN})_6$ in cacodylate buffer for 30 min, washed 3 times in ddH₂O, incubated with 1% thiocarbohydrazide in ddH₂O for 30 minutes, washed with ddH₂O 3 times, followed by a second post-fixation with 1% OsO_4 in ddH₂O for 30 min. Samples were further rinsed 3 times with ddH₂O, dehydrated in a graded series of acetone (10%, 20%, 40%, 60%, 80%, 100%, 100%, 100%; 10 min each) including an incubation step in 1% uranyl acetate in 20 % acetone for 30 min. Subsequently, cells were infiltrated and embedded as described previously (Gaertner et al., 2017). Tomographic datasets were obtained by the 'slice and view' technique using a Zeiss Auriga 40 crossbeam workstation (Carl Zeiss Microscopy, Oberkochen, DE). For milling with the Ga-ion beam, the conditions were as follows: 0.5–1 nA milling current of the Ga-emitter; with each step 50 nm of the epoxy resin was removed. Scanning Electron Microscopy (SEM) images were recorded at 1.5 kV with an aperture of 60 μm operated in the high current mode with the in-lens EsB detector (EsB grid set to -1000 V). The voxel size was 5 nm in x/y and 50 in z. FIB/SEM image stacks were aligned, segmented and 3D reconstructed with Amira® (Thermo Fischer Scientific Messtechnik GmbH, Munich, DE). Manja Luckner provided EM imaging and 3D reconstructions of mitochondria.

5.16 IMMUNOHISTOCHEMICAL APPROACH TO QUANTIFY MCU PROTEIN

For quantitative image acquisition in astrocytic cell culture, images were acquired by confocal microscope Zeiss LSM 780 with a 40x/1.4 oil objective.

Single plane images (x: 53.09 μm , y: 53.09 μm) were further processed in Igor Pro to detect single MCU, based on published algorithms (Dorostkar et al., 2010). Briefly, the Laplace operator (which is the sum of the unmixed second partial derivatives in the Cartesian co-ordinates x and y), was calculated from an image. The result was thresholded at 2xstandard deviation of the pixel values to yield a binary image, from which centers of mass for each puncta were determined and counted. MCU densities were normalized to the area occupied by astrocytes (labeled with anti - Ezrin antibody, Sigma #E8897).

5.17 CONFOCAL MICROSCOPY AND DENDRITIC SPINE ACQUISITION

Brain sections of the somatosensory cortex from APP flox x Slick V mice were incubated with 0.1% Triton X-100, 5% normal goat serum (NGS) for 2 h at room temperature and stained with rabbit anti-GFP antibody tagged. The secondary antibody Alexa488 (1:200, Invitrogen) in PBS with 5% NGS for 2 h was used for incubate the sections at room temperature. After three washes with PBS, slices were mounted and covered with a glass coverslip for microscopic analysis. Images of apical dendrites of layer V pyramidal cells were acquired in slices through 40x oil immersion objective (NA 1.3; Carl Zeiss), using the LSM780 confocal microscope (Carl Zeiss).

5.18 *IN VIVO* AND *EX VIVO* DENDRITIC SPINE ANALYSIS

Dendritic spine density was determined using ZEN 2012 Light Edition software (version 8.0, Carl Zeiss MicroImaging GmbH) as previously described (Filser et al., 2015; Ochs et al., 2015; Zou et al., 2015). Images were corrected with a gamma of 0.45 and spines were counted manually by scrolling through the z-stacks. For *in vivo* study on APP Δ CT15 mice from 8 to 10 dendrites per mouse were investigated. For *ex vivo* study on APP flox x Slick V mice, 6 to 8 dendrites per mouse from somatosensory cortex, and 8-10 basal and 8-10 apical dendrites from CA1 hippocampal subregion were analyzed.

Methods

As previously described (Holtmaat et al., 2009) in time-series, a dendritic spine was defined as the same if its location did not change within a range of 1 μm along the dendrite. Since z-scaling was limited to 1 μm , only lateral protrusions of the dendritic shaft were analyzed.

Ex vivo image analysis measurements were performed manually from maximal projection images of deconvoluted (AutoQuantX3, Media Cybernetics) confocal stacks. As previously described all spines along the dendrite were marked and categorized into three morphologically different classes, according to established criteria (Jung et al, 2011). Morphological subtypes of dendritic spines were identified with the following criteria: mushroom spines: $\text{max_width}(\text{head})/\text{min_width}(\text{neck}) > 1.4 \mu\text{m}$ and $\text{max_width}(\text{head}) > 0.2 \mu\text{m}$ and $\text{min_width}(\text{neck}) > 0 \mu\text{m}$; stubby spines: $\text{length}(\text{spine})/\text{mean_width}(\text{neck}) \leq 3 \mu\text{m}$ or $\text{min_width}(\text{neck}) = 0 \mu\text{m}$ or $\text{min_width}(\text{neck}) > 0.5 \mu\text{m}$; thin spines: $\text{length}(\text{spine})/\text{mean_width}(\text{neck}) > 3 \mu\text{m}$. For illustration purpose only, image stacks were deconvoluted (AutoQuant X3, Media Cybernetics) and adjusted for contrast and brightness.

5.19 PRIMARY ANTIBODY LIST FOR IMMUNOFLUORESCENCE

ANTIGEN	SOURCE	TYPE	DILUTION FACTOR	INCUBATION	SAMPLE
GFAP	Abcam (#53554)	goat	1:500	1 night / 4°C	Brain slice
EZRIN	Sigma (#E8897)	ms	1:100	2 nights/ 4°C	Brain slice
GFP-Alexa conjugated488	Thermo Fisher (#A21311)	rb	1:500	2 h /room temp.	Brain slice
TOMM20	Abcam (#186735)	rb	1:200	1 hour/ room temp.	<u>Astrocytic culture</u>
CYTOCHROME C	BD Pharmigen (#556432)	ms	1:200	1 hour/ room temp.	<u>Astrocytic culture</u>
MCU	SIGMA (#HPA016480)	rb	1:200	1 hour/ room temp.	<u>Astrocytic culture</u>

Methods

APPY188	Abcam (#32136)	rb	1:200	1 hour/ room temp.	<u>Astrocytic culture</u>
VGlut	Millipore (#AB5905)	gp	1:200	1 night/4°C	Brain slice

Table 4 : Primary antibody list.

5.20 NOVEL OBJECT RECOGNITION TEST

To evaluate cognition and memory of APP Δ CT15 and WT mice, a modified version of novel objective recognition test was used as described before (Leger et al., 2013; Zou et al., 2016). Mice explored an open-field arena (40 × 40 cm) freely in the absence of objects for 10 min having their locomotor activity recorded. One day later, mice were placed in the open-field arena with two identical sample objects (two identical plastic rectangular-shaped blue objects) with exploration period of 10 minutes. Mice were returned to their home cages. After 24 h, mice were put back to the arena with one of the sample objects changed into a novel one (a grey plastic cylindrical-shaped object). This test phase lasted 5 min. The index of recognition was then calculated as ratio of the time spent exploring each object on the total time spent exploring both of the items.

5.21 ENVIRONMENTAL ENRICHMENT

Environmental enrichment (EE) housing condition is a group (3-6) of mice in 48cm × 48cm × 48cm cage with running wheels, ladders, tunnels and multiple hanging toys which were replaced with new objects 3 times per week (Figure 11). Mice of the same gender from APP Δ CT15 and WT litters were placed into EE housing conditions from 2-month-old or 3-month-old for 6-7 weeks. Both genders were use in this treatment. Aggressive mice were removed from EE housing. Standard cages were 30 × 15 × 20 cm in size without any wheels or toys.



Figure 11: Environmental housing condition.

Photo of an example of environmental enriched housing cage. Food and water are given ad libitum.

5.22 STATISTICAL ANALYSIS

For statistical analysis and comparisons GraphPad Prism 5.04 (GraphPad Software, Inc., La Jolla, CA USA) was used. For each set of data, I determined whether they were normally distributed or not. If they were normally distributed, I used parametric tests; otherwise, I used non-parametric tests (unpaired two-tailed Student's t test and two-way ANOVA followed by Bonferroni post-hoc test or Mann Whitney test). In frequency distribution comparison, Kolmogorov-Smirnov test was applied. P-value < 0.05 was defined as statistically significant. Wilcoxon signed-rank test was used test whether the quotient of interaction time with the novel object divided by interaction time with the familial object significantly differed from a hypothetical value of 1 (equal interaction times). All the analysis was performed blinded with respect to mouse genotype.

6 RESULTS

6.1 *IN VIVO* Ca^{2+} IMAGING TO UNRAVEL THE CRITICAL ROLE OF APP ALONG THE FINE PROCESSES OF ASTROCYTES

6.1.1 EXPRESSION OF MEMBRANE-ANCHORED GCaMP6f IN ASTROCYTES OF APP KO MICE

The astrocytic optically-unresolved structure “gliapil” is formed by thin lamellar sheets that extend from the cell body to either the pial surface or the blood vessels, or in some cases to freely moving axons and dendritic spines (Magistretti and Ransom, 2002; Bindocci et al., 2017). These long branching processes have reduced cytoplasm, thus rendering the investigation on calcium dynamics difficult (Agarwal et al., 2017).

The AAV.Pzac2.1gfaABC1Dlck-GCaMP6f (AAV-GFAP-GCaMP6) is a membrane-anchored adeno-associated virus carrying an ultrasensitive Ca^{2+} indicator (GCaMP6f) driven by a GFAP promoter (Chen et al., 2013; Shigetomi et al., 2013). By injecting this virus into mice, it is possible to overcome the aforementioned limitation.

In order to investigate spontaneous Ca^{2+} fluctuations along the fine astrocytic processes, I injected AAV.Pzac2.1gfaABC1Dlck-GCaMP6f (AAV-lck-GCaMP6f) encoding the membrane-associated Ca^{2+} indicator GCaMP6 under the control of the GFAP promoter into the somatosensory cortex of three months old WT and APP KO mice (Figure 12). With the same injection, mice were co-transduced with AAV.GfaABC1DcytotdTomato.SV40 (AAV.Gfacyto.tdtomato) encoding a cytosolic tdTomato fluorescent protein under the control of the GFAP promoter (Figure 12) to confirm the astrocyte-specific expression of the Ca^{2+} indicator AAV-lck-GCaMP6f. Due to its lck-membrane anchor, the AAV-lck-GCaMP6f expression is detectable within fine protrusions of astrocytes, and thus it is perfectly suitable for the investigation of astrocytic Ca^{2+} transients (ASCaTs).

Results

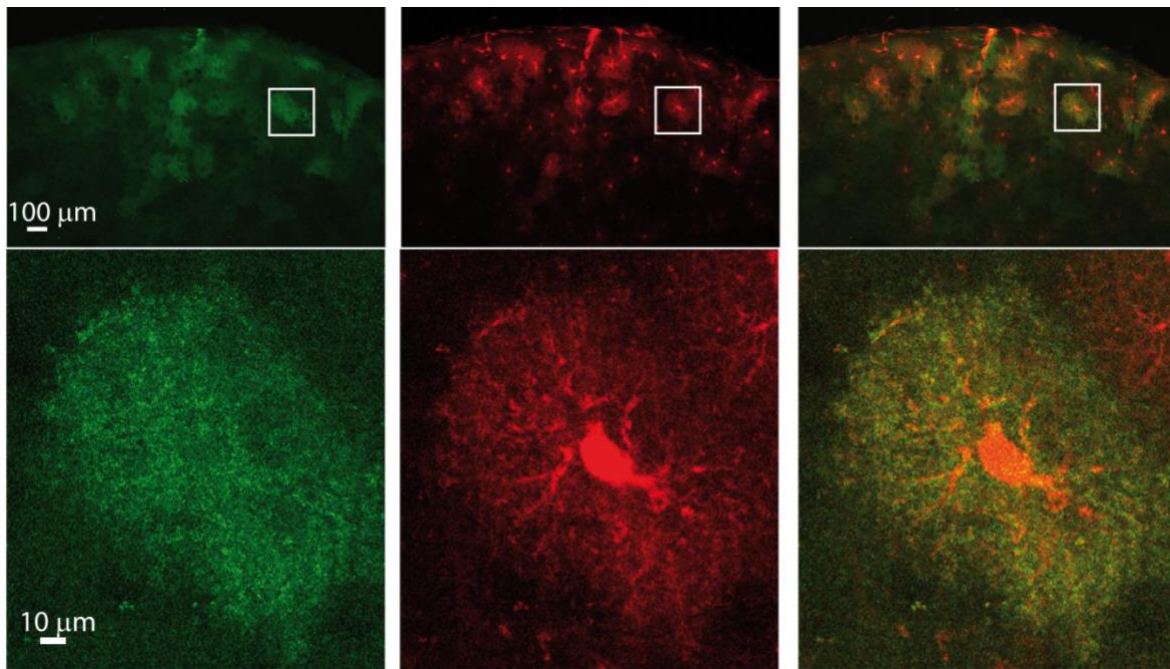


Figure 12: Expression pattern of GCaMP *in vivo* within astrocytes.

Confocal-tile scan of GCaMP respectively GFAP-cyto-tdTomato injected area, and merge (Zeiss 40X lens oil immersion). In the line below zoom in of single transfected astrocytes (GCaMP and cyto-TdTomato). The white rectangle in A is given in higher magnification below.

6.1.2 APP KO MICE SHOW IMPAIRED ASTROCYTIC CALCIUM TRANSIENTS ALONG THE FINE PROCESSES OF ASTROCYTES

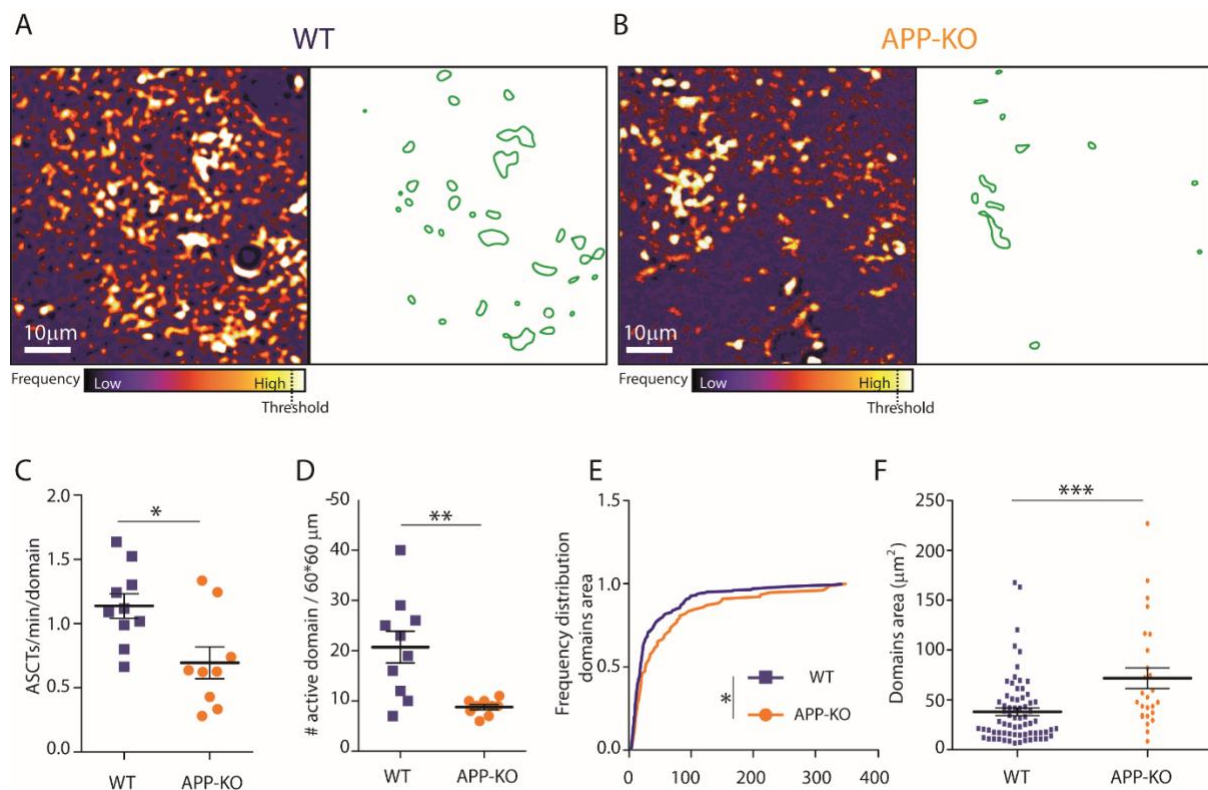
In order to investigate spontaneous Ca^{2+} fluctuations along the fine astrocytic processes, two-photon *in vivo* Ca^{2+} microscopy was conducted in the somatosensory cortex of mice kept under isoflurane anesthesia. Respiratory rate, temperature and oxygen levels in the blood were constantly monitored and isoflurane concentration was modified accordingly to guarantee equal depth of anesthesia between mice (Figure 13). Imaging series of 5 min were acquired with a sampling rate of 4.17 Hz. For the identification of active microdomains and their calcium transient activity analysis, I applied a protocol adapted from Agarwal et al. (Agarwal et al., 2017). The analysis was performed on single focal $60 \times 60 \mu\text{m}$ images, as a time stack image series. As described in more details in the method section, this involved low-pass filtering of the time stack for background noise. Then, a 2D activity profile of ASCaTs activity was generated and an arbitrary threshold (average of the overall activity plus three standard deviations) was used to identify active microdomains (Figure 13).

Results

With the analysis procedure I identified a mask of ROIs as active microdomains that could be further analyzed for time dependent properties. Subsequently, the traces of single ROIs were extracted and single ASCaTs were isolated and analyzed in terms of frequency, event size and kinetics. All ROIs with 1.5-fold fluorescence intensity above the baseline noise were considered as active domains.

From the analysis of active ROI/microdomain distribution (Figure 13A,B), I detected that active microdomain density was reduced by ~50% in APP KO compared to WT astrocytes (Figure 13C). This was accompanied by a substantial increase in the average area of individual active microdomains in APP KO astrocytes (~25% compared to WT) (Figure 13D). Likewise, the frequency distribution of the microdomain size (Figure 13E) was significantly shifted in APP KO mice, suggesting that APP KO astrocytes have fewer small microdomains. Finally, Ca²⁺ activity analysis based on the traces extracted from active microdomains showed a reduction of ~45% in ASCaTs frequency in APP KO astrocytes compared to WT (Figure 13F).

Taken together, these results indicate that lack of APP leads to a reduction in the number of active microdomains and a reduction in the frequency of spontaneous and locally restricted Ca²⁺ transients occurring in the fine processes of astrocytes *in vivo*.



Results

Figure 13: Altered astrocytic microdomain size and occurrence in the cortex of APP KO mice.

*Color-coded heat map of astrocyte activity showing ASCaTs frequency from WT (A) and APP KO (B) somatosensory cortex area extracted active microdomains (right, green encircled). Scale bar = 10 μ m. (C) Active microdomain density was decreased in APP KO mice (Student's *t* test: $t_{(17)}=3.53$, $p<0.005$). (D) APP KO microdomain areas were increased, as shown their averaged size ($t_{(94)}=3.723$, $p<0.001$) and (E) in their frequency distribution (KS test; $D=0.1955$, $p<0.05$). (F) The frequency (ASCaTs/min/domain) was reduced in APP KO mice ($t_{(17)}=2.878$, $p<0,05$). * $p<0.05$, ** $p<0.01$, *** $p<0.001$.*

6.1.3 MICRODOMAIN KINETICS ALONG THE FINE PROCESSES OF ASTROCYTES ARE ALTERED IN APP KO MICE

After confirming that the population of microdomains was not only smaller but also displayed less ASCaTs in APP KO, I analyzed spontaneous Ca^{2+} transients in terms of event amplitude, rise and decay time (Srinivasan et al., 2015). The Ca^{2+} transients typically occurred as single peaks and also as bursts, as shown in traces extracted from active microdomains (Figure 14A).

The total amount of single peak Ca^{2+} increase generated in each ASCaTs was examined as area under the curve (Figure 14B) and peak amplitude (Figure 14C). Statistical comparison revealed no significant difference between WT and APP KO mice. However, ASCaTs in APP KO mice displayed a longer rise time (~22%, Figure 14D) and a longer decay time (~20%, Figure 14E), implying slower kinetics of calcium regulation compared to WT controls. Next, the consecutive peaks from burst-like transients were grouped in categories depending on the order in which they appeared. Consistently, both area under the curve and amplitude were comparable to WT (Figure 14F,G). Again, ASCaTs of APP KO mice displayed significantly slower kinetics regardless of the order of appearance as a part of a burst activity (Figure 14H,I).

Taken together my results suggest that in the absence of APP the spontaneous increase of Ca^{2+} in microdomains is still able to reach calcium levels comparable to physiological conditions, but at a significant slower rate. As mentioned before, microdomain activity is often driven by mitochondrial Ca^{2+} buffering (Grosche et al., 1999; Srinivasan et al., 2015; Agarwal et al., 2017) that is responsible for the fine tuning of Ca^{2+} homeostasis in the cytosol. For this reason, I decided to focus on the effect of APP depletion on astrocytic mitochondria, considering it as a potential actor in the observed dysregulated ASCaTs.

Results

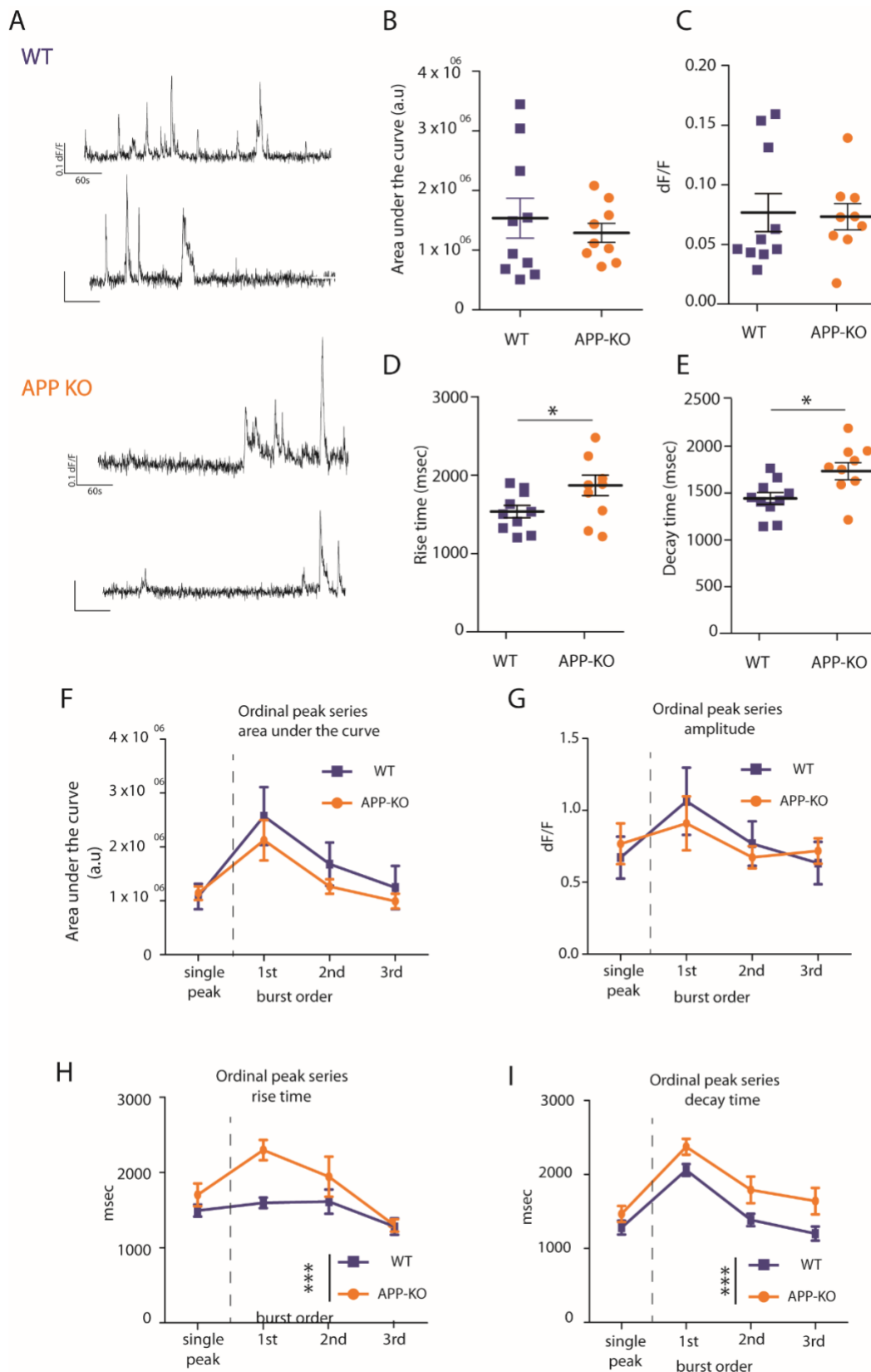


Figure 14: APP KO microdomains have impaired kinetics.

Representative traces from active microdomains of WT (above) and APP KO (below)(A). The area under the curve (B) and peak amplitudes (C) values were comparable between genotypes. The rise time (D)(Student's *t* test: $t(17)=2.24$, $p<0.05$) and decay times (E)($t(17)=2.118$, $p<0.05$) were significantly increased in APP KO ASCaTs. When considered as isolated (single peak) or ordered by occurrence along burst transients, both area

Results

(F) and amplitude (G) values showed no significant difference between KO and WT. More than a specific peak category, there was a general increase of the rise (H)(two-way ANOVA, genotype main factor, $F(1,65)=9.92$, $p<0.01$) and the decay time (I) (genotype main factor, $F(1,65)= 17.26$, $p<0.001$) in the kinetics of the ASCaTs of KO mice. * $p<0.05$, ** $p<0.01$, *** $p<0.001$.

6.1.4 GFAP SIGNAL INCREASES IN APP KO ASTROCYTES SHOWING A MORE COMPLEX BRANCHING COMPARED TO WT

Before investigating the effects of APP depletion on mitochondria I determined whether the lack of APP might influence the activation status of astrocytes through the investigation of their morphology and branching processes. To determine the complexity of astrocytes in the somatosensory cortex, brain sections of WT and APP KO mice were stained with the anti-GFAP antibody using the Sholl analysis approach; a method often used to quantify the complexity of neuronal processes and, more recently, of astrocytic processes (Sholl, 1953) (Figure 15A-D). Z-stacks containing entire cell ramifications (Figure 15A) and the 3D reconstructions of the GFAP-positive structures were acquired, revealing a compact and well defined architecture (Figure 15B).

The custom written FIJI Sholl scripts (Schindelin et al., 2015), used for the analysis, generates color coded images, based on the frequency of intersections (Figure 15C). As a result, a significant increase in the number of intersections with increasing distance from the cell soma was observed in APP KO compared to WT astrocytes (~10% increase in the farthest radii) (data shown as mean \pm SEM, two-way ANOVA, interaction $F_{(40,246)} = 3.16$, $p < 0.0001$) (Figure 15A,D).

These findings show that the lack of APP leads to an increase in the level of GFAP expression and to an enhanced branching, thus suggesting a role for APP in modulating the activation state of astrocytes.

Results

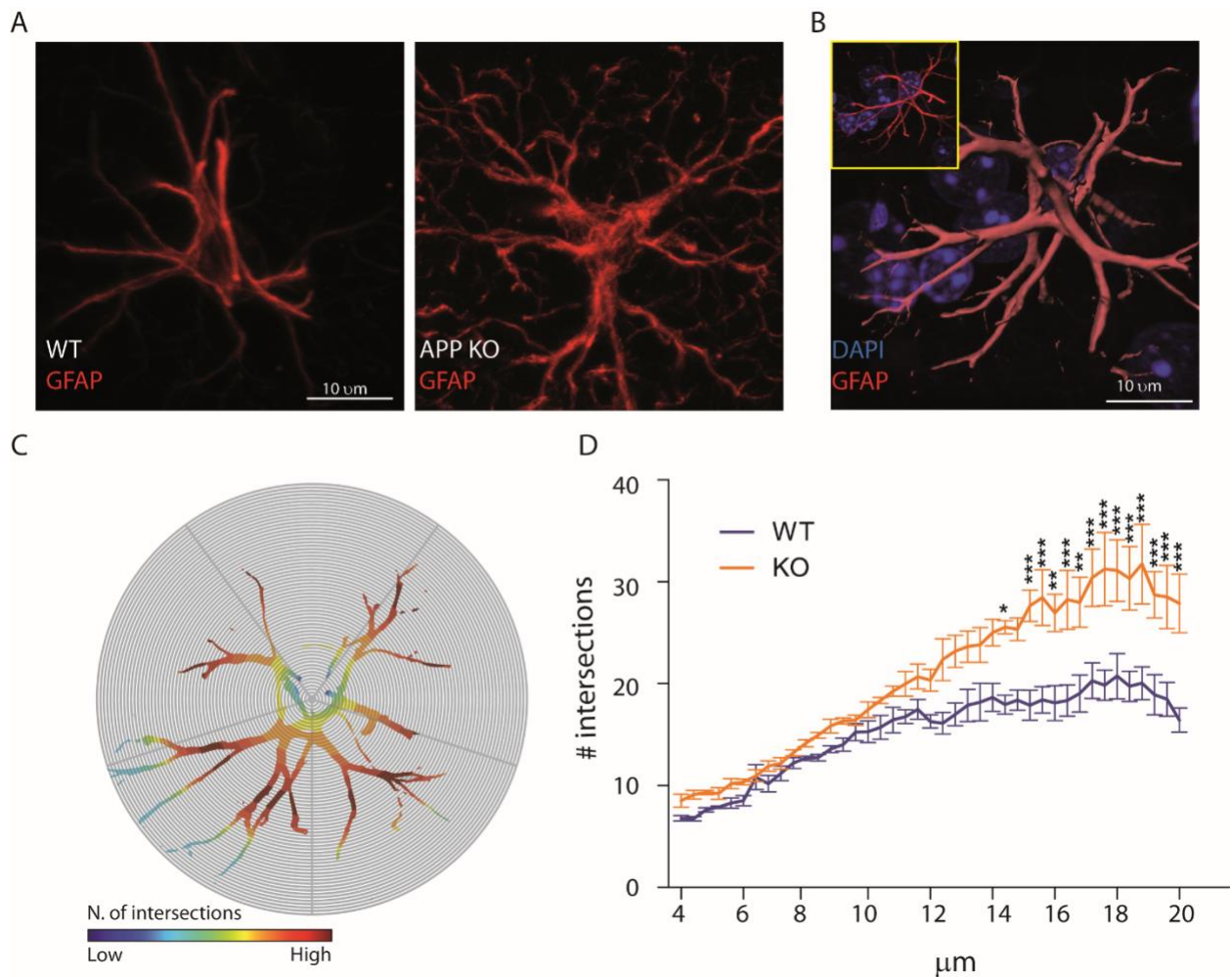


Figure 15: Sholl analysis on astrocytes.

Confocal images of GFAP positive astrocyte from somatosensory cortex of WT and APP KO (A); 3D reconstruction of somatosensory astrocyte (in red), DAPI staining showing nuclei (in blue) (B); Sholl analysis was applied for investigating complexity of astrocytes. As readout of Sholl analysis the number of intersections between GFAP positive branches and concentric circles is automatically extrapolated by custom written codes on Fiji (C); Number of intersections and distance from the center of the astrocytes were plotted. APP KO astrocytes showed significance increase in the number of intersections located farther from the soma (two-way ANOVA, interaction $F(40,246) = 3.16$, $p < 0.0001$) (D).

6.1.5 MITOCHONDRIA OF APP KO ASTROCYTES ARE FRAGMENTED AND DISTORTED

Prompted by my results of the lack of APP on calcium transients in astrocytic microdomains and the observed enhanced activation state of astrocytes I next aimed to identifying the underlying mechanisms.

The handling and buffering of Ca^{2+} by mitochondria has been shown to be a key feature for astrocytic microdomain activity (Srinivasan et al., 2016; Agarwal et al.,

Results

2017). Mitochondria are extremely dynamic organelles (Detmer and Chan, 2007), which are actively transported within any given cell and that actively modify their shape and size. The notion that their dynamics impact on cellular functionality is widely endorsed (Chang and Reynolds, 2006; Detmer and Chan, 2007; Picard et al., 2013).

To further address the questions why microdomains and ASCaTs are altered in astrocytes of APP KO mice, I analyzed the morphology of mitochondria. Thus, primary astrocyte cultures were prepared from WT and APP KO pups (postnatal day 3) and confirmed the lack of APP in astrocytes from APP KO animals by immunohistology (Figure 16A,B). Primary cultures of WT and APP KO astrocytes were next subjected to electron microscopy (EM) in order to obtain high-resolution micrographs of mitochondria and evaluate the effects of APP depletion in isolated astrocytes. 3D-reconstruction of EM image z-stacks revealed shorter and more fragmented, roundish-shaped mitochondria in APP KO astrocytes compared to WT (Figure 16C,D). This result is in line with previous evidence that the lack of APP results in Ca^{2+} and ATP dysregulations (Hamid et al., 2007; Linde et al., 2011; Pera et al., 2017) and morphological alterations of mitochondria (Wang et al., 2016) suggesting that APP regulates mitochondrial homeostasis.

Results

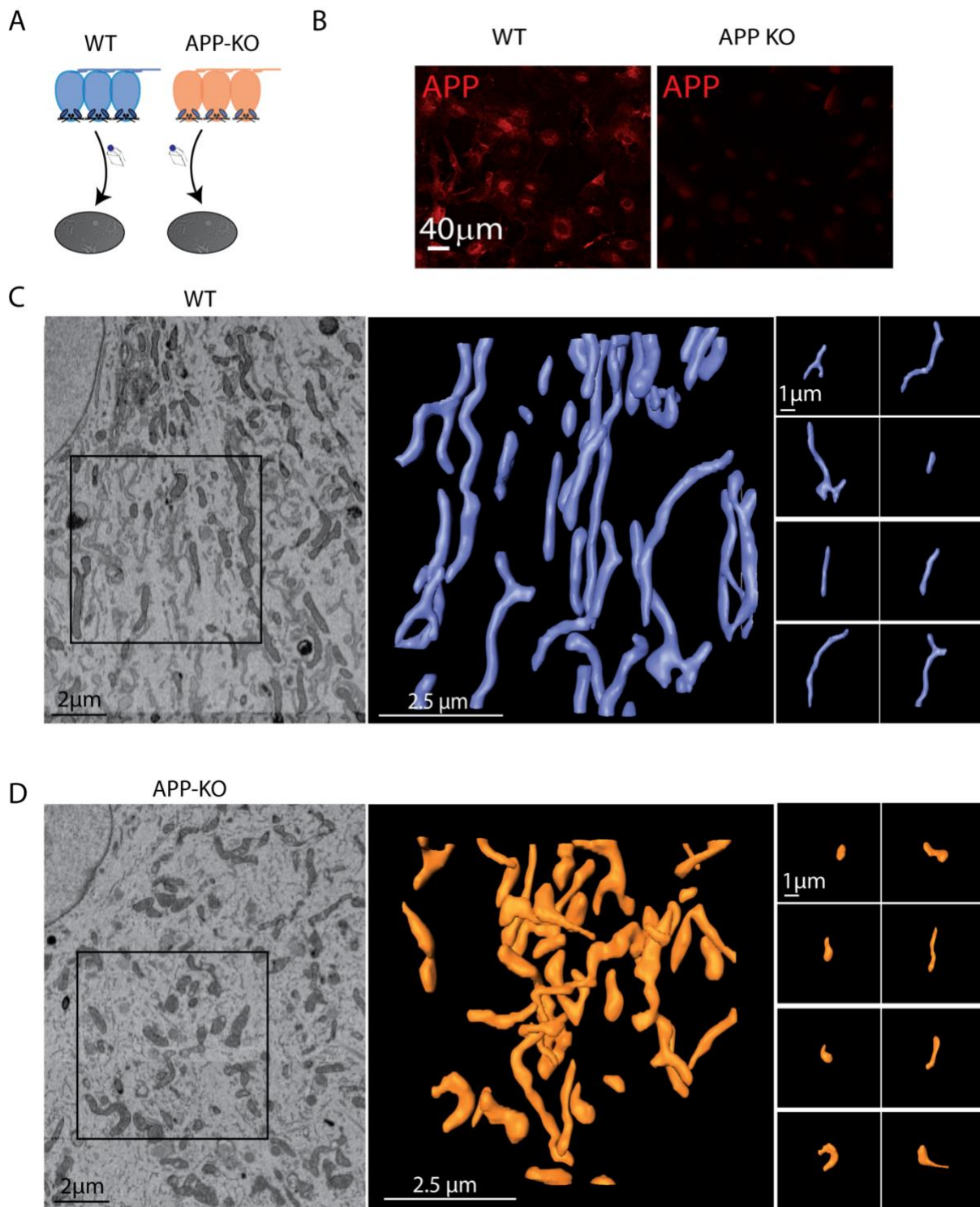


Figure 16: Primary cultured astrocytes lacking APP display fragmented mitochondrial morphology.

Each astrocytic cell culture was obtained from 3 P3 pups per group (A); Immunohistochemical analysis with C-terminus targeted APP antibody on WT (left) and APP KO (right) primary astrocytes shows exclusive expression of APP in WT. Scale bar = 40 μm . (B). Representative FIB/SEM microscopy of WT (C) and APP KO (D) cultured astrocytes with detailed images of 3D-reconstructions (right) illustrate the fragmentation of mitochondria in APP

Results

KO astrocytes. Original FIB/SEM image, scale bar = 2 μm ; overview reconstruction (middle), scale bar = 2.5 μm , single mitochondria fragments, scale bar = 1 μm .

To confirm the presence of shorter and more fragmented mitochondria in isolated astrocytes of APP KO mice, both WT and APP KO astrocytic cultures were transfected with the plasmid pZac2.1-gfaABC1D-mito-GCaMP5G and stained against GFP (mito-GCaMP) (Hailong Li, Xiaowan Wang Nannan Zhanga, Manoj K. Gottipati, Vladimir Parpura, 2005) (Figure 17). Additional markers commonly used for the investigation of mitochondria structures, such as Cytochrome C and TOMM 20 antibodies, were applied on astrocytic cultures (Figure 17). While Cyto C is a small hemeprotein on the inner membrane of mitochondria, TOMM 20 is a component of the receptor complex expressed on the outer membrane (Figure 17). Independently from the antibody applied on isolated astrocytes and from the approach used to visualize mitochondria, that is, either EM or confocal microscopy, I observed the presence of fragmented mitochondria along astrocytes of APP KO mice, thus providing us further confirmation on the fragmentation of mitochondria, independently from the kind of staining applied.

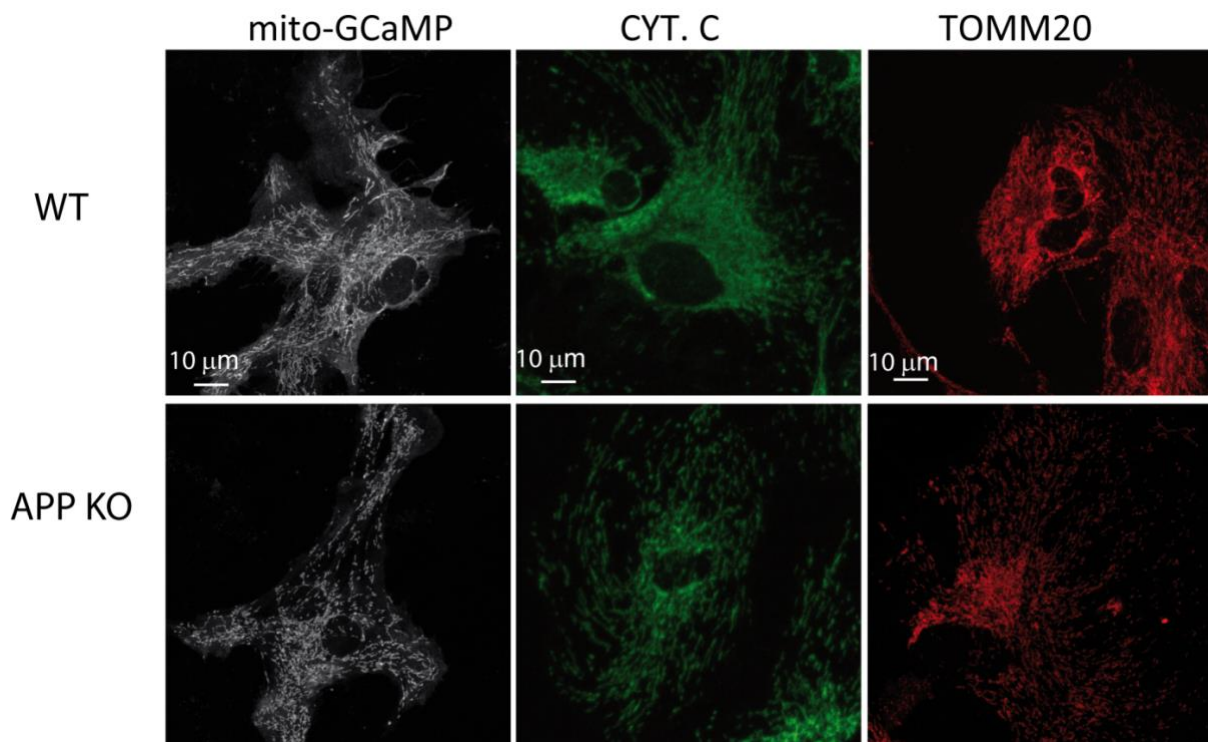


Figure 17: Different mitochondrial markers show mitochondria fragmentation in APP KO astrocytic cultures.

Results

Z stack from confocal microscopy (353 μm x 353 μm) images of mitochondria from WT and APP KO cultured astrocytes transfected with pZac2.1-gfaABC1D-mito-GCaMP5G (mito-GCaMP). Anti-GFP antibody was applied to strengthen the fluorescent signal (in grey); confocal images of WT and APP KO mitochondria stained with mouse anti-Cytochrome C antibody followed by anti-mouse Alexa-488 (in green); confocal images of WT and APP KO mitochondria stained with rabbit anti-TOMM 20 antibody followed by anti-rabbit Alexa-647 (in red).

6.1.6 EXPRESSION OF APP ECTODOMAIN ALONE IN APP Δ CT15 MICE IS NOT SUFFICIENT TO RESTORE MITOCHONDRIA MORPHOLOGY

Next I assessed if the staining of TOMM 20 (mitochondrial import receptor located at the surface of mitochondria outer membrane) co-localizes with the signal from anti-mito-GCaMP staining (Figure 18). I further investigated mitochondria morphology based on the staining of the GCaMP plasmid; with the benefit of being able to isolate single cell mitochondria, not possible by using TOMM20 antibody.

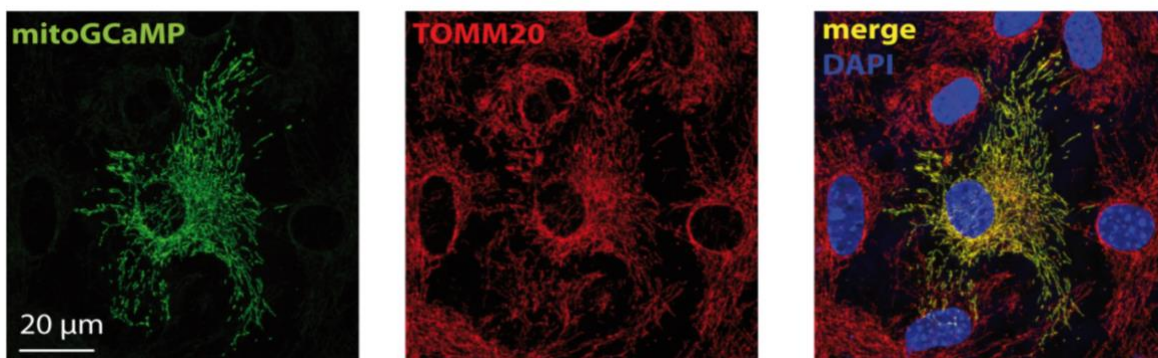


Figure 18: mitoGCaMP colocalize with TOMM20.

Single plane confocal images of astrocytes (353 μm x 353 μm) stained with anti GFP (green), anti TOMM20 (red) and DAPI (blue). The overlapping of mito-GCaMP and TOMM20 is visible as yellow colour in the merge image. .

Based on their morphology, mitochondria were subsequently classified into networks, rods and puncta (Figure 19A,B) (Leonard et al., 2015). Interestingly, the analysis revealed a ~25% decrease of the area covered by network-shaped mitochondria, together with a ~12% increase of puncta and 12% increase of rod types in APP KO astrocytes compared to WT (Figure 19B). By classifying mitochondria in network, rods and puncta, as described in the methods, I could quantify the presence of more fragmented mitochondria, as outlined through EM, as

Results

the result of a reduction of networked mitochondria in favor of more rods and puncta mitochondria (Figure 19 B).

Considering that the multidomain structure of APP gives to the protein multi functional properties (De Strooper and Annaert, 2000; Andrew et al., 2016; Müller et al., 2017), I asked whether the presence of the APP ectodomain in its physiological location could rescue the mitochondrial morphology. The APP ectodomain extrudes into the extracellular space and is needed for trans- and homo- dimerizations and it is important as main source of sAPP α and A β (Ring et al., 2007). I investigated the influence of APP ectodomain on mitochondria morphology by applying the same approach, mitochondria morphology in APP Δ CT15 astrocytic cultures. These mice are KI animals that express a truncated form of APP, which lacks the 15 C-terminal amino-acids and with improved hippocampal spine plasticity and LTP compared to APP KO mice (Ring et al., 2007). Surprisingly, once performing the same procedure on mitochondria of APP Δ CT15 astrocytic culture I observed a significant reduction of ~7% of networked mitochondria compare to WT, whereas investigation on the percentage of rod and puncta mitochondria did not reveal any significant difference neither from WT nor from APP KO (Figure 19A,B). Thus my results firstly show that the GCaMP-plasmid efficiently allowed a quantitative definition of mitochondria, confirming the presence of fragmented mitochondria in APP KO astrocytes as revealed by the EM investigation (figure 17). Moreover I could prove that the presence of APP ectodomain alone does not efficiently restore the mitochondrial network and therefore mitochondria of APP Δ CT15 still show an increase in fragmentation.

Results

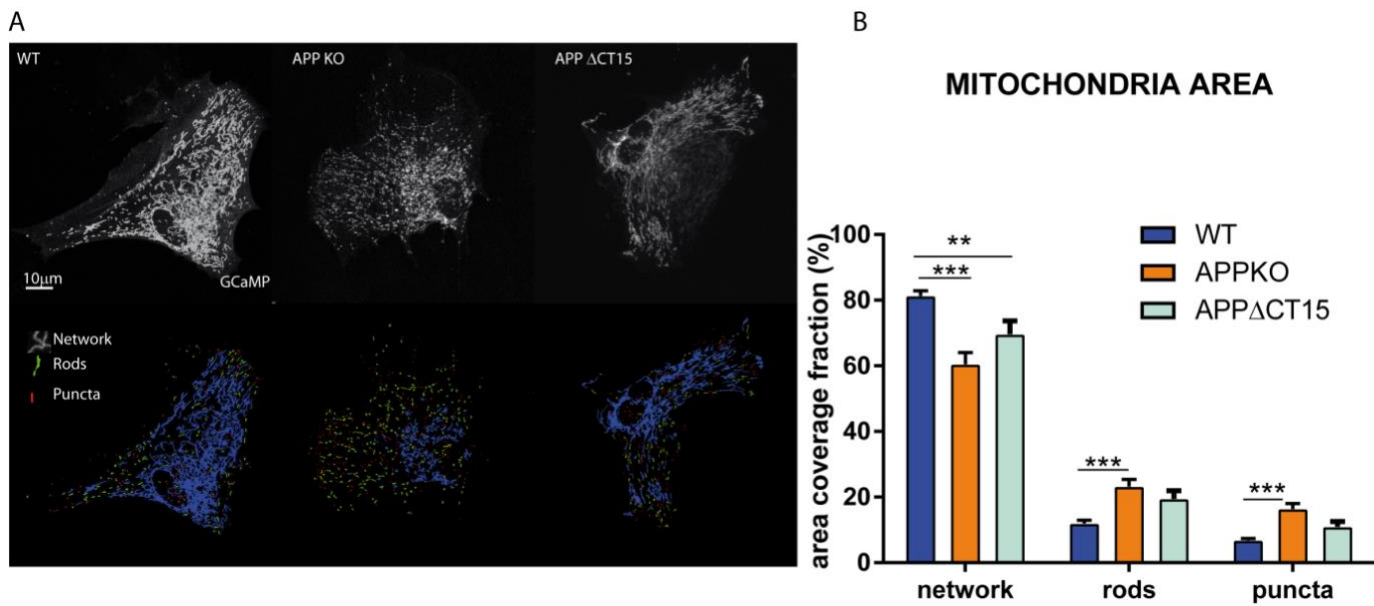


Figure 19: APP KO mitochondria show fragmented mitochondria and APP ectodomain cannot recover completely to a normal phenotype.

Mitochondrial morphology analysis in WT, APP KO and APP Δ CT15 astrocytic cultures. Confocal pictures of GFP-positive mitochondria and relative classification in network (blue), rods (green) and puncta (red) (A), Area covered by APP KO and APP Δ CT15 mitochondria is more fragmented compared to mitochondria area in WT astrocytes (2-way anova followed by Bonferroni, $p < 0,001$, $dF(4,53) = 18.08$).

6.1.7 APP KO FRAGMENTED MITOCHONDRIA COLOCALIZE WITH CYTOCHROME C

Apoptosis is a process of programmed cell death, necessary for the development and homeostasis of living organisms (Parsons and Green, 2010). Although mitochondria provide the cell with energy needed in form of ATP, paradoxically, they also play an important role in the apoptotic pathway of cell death. The release of various mitochondrial intermembrane proteins, like Cyto C, activates numerous caspases that lead to apoptosis (Tait and Green, 2013). The mitochondrial CytoC is also a component of the mitochondrial electron transport chain that, after the increase of mitochondrial Ca^{2+} , is released in the cytosol, where it executes its apoptotic function (Tait and Green, 2013).

Dysfunctional mitochondria present alterations in their morphology showing enlarged structures often call “mito-bulb structures” (Ban-Ishihara et al., 2013). Within these structures Cyto C accumulates. Such accumulation does not simply reflect an increase in the mitochondrial respiratory activity, but it is often the result of a delay in Cyto C release into the cytoplasm (Ban-Ishihara et al., 2013). However, while it is

Results

known that the accumulation of Cyto C in the mitochondria does not enhance the mitochondrial respiration activity the reasons behind such accumulation are not clear yet (Ban-Ishihara et al., 2013). My confocal data clearly indicate mito-bulbs-like structures in the mitochondria of APP KO astrocytes (Figure 20A). I further characterized the mito-bulbs by looking at Cyto C using confocal microscopy (Figure 20B) and I observed that Cyto C clustered in the bulbs-like regions of APP KO mitochondria. As dysfunctional mitochondria are often presenting mito bulb structures enriched with Cyto C (Ban-Ishihara et al., 2013), I combined together the observed fragmentation of mitochondria and the accumulation of Cyto C in the mito-bulb structures to delineate an “unhealthy “ status for mitochondria of astrocytes lacking APP. The “unhealthy” status of mitochondria could be most likely affecting the buffering of Ca^{2+} all over the astrocytes, thus resulting in altered Ca^{2+} transients as shown by the in vivo data.

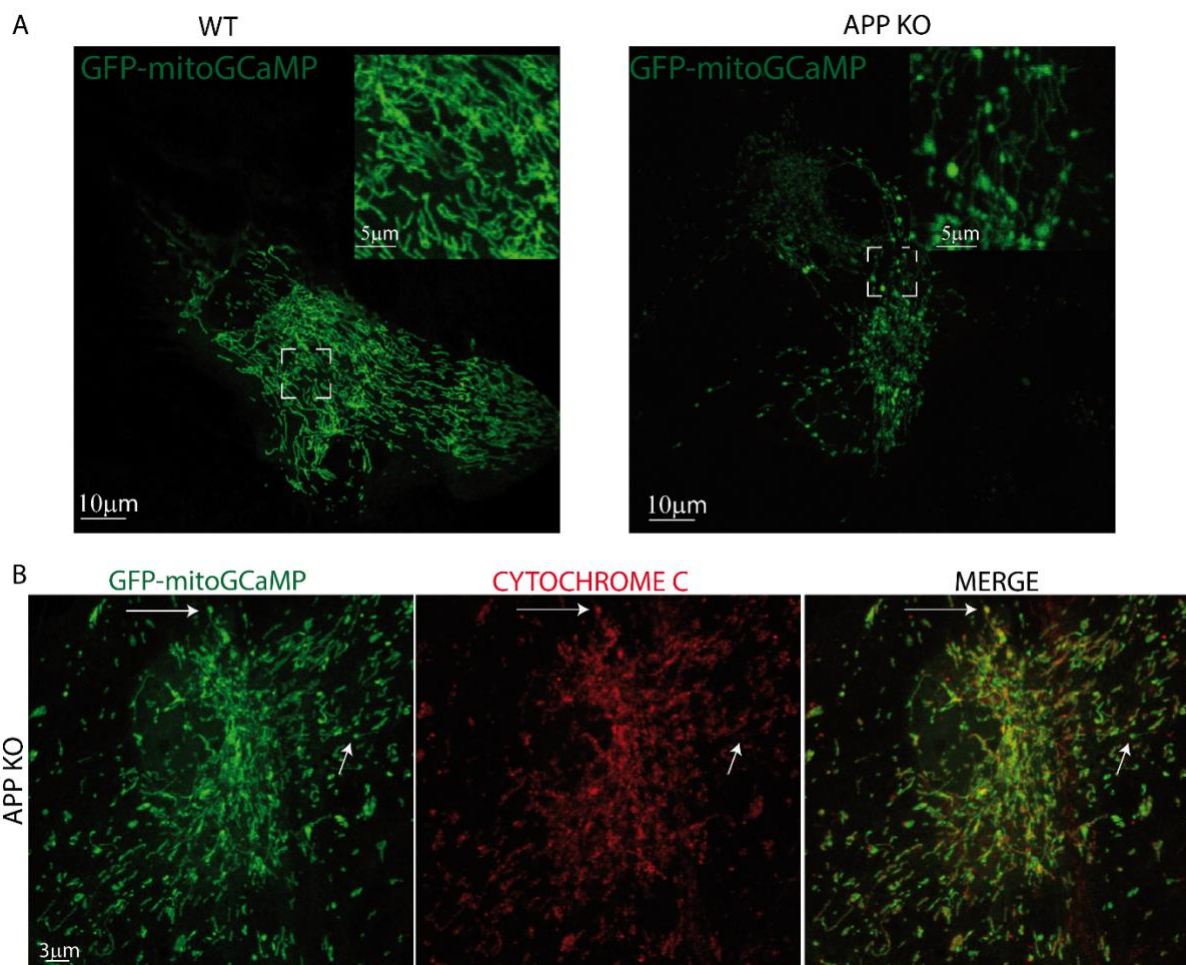


Figure 20: APP KO mitochondria show "teardrop" like structures enriched with Cytochrome C.

Results

Mitochondria of WT astrocytic cultures show a tubular, interconnected shape; APP KO mitochondria instead present enlarged regions named as “mito-bulbs”, on the right upper corner magnification of the white square delimited areas (A); staining of GFP positive mitochondria (green) and Cyto C (red) on APP KO astrocytic cultures show clustering of Cyto C in the mito-bulb structures. In insets, magnification of “mito-bulbs” structure colocalizing with Cyto C (B).

6.1.8 MITOCHONDRIAL CALCIUM UNIPORTER EXPRESSION IS INCREASED IN ASTROCYTIC CULTURES OF APP KO MICE

To better understand if the mitochondria machinery that modulates Ca^{2+} buffering along the astrocytes of APP KO mice is affected, I further investigated the expression pattern of MCU, the mitochondrial calcium uniporter. Mitochondrial Ca^{2+} uptake regulates the cellular energy production, influences the intracellular free Ca^{2+} concentration and modulates the release of Cyto C (Bianchi et al., 2004; Kirichok et al., 2004; Patterson et al., 2004) (Figure 21A). The close apposition between ER IP_3 -gated receptors (IP_3Rs) and mitochondria, as well as the close proximity of mitochondria with transmembrane Ca^{2+} channels, allows mitochondria to modulate shape and amplitude of cytosolic Ca^{2+} transients (Gunter and Gunter, 2002; Rizzuto et al., 2004). The MCU, is responsible for the electrophoretic Ca^{2+} uptake across the inner mitochondrial membrane (IMM), and is able to bind Ca^{2+} with extremely high affinity and then release it into mitochondria (Kirichok et al., 2004).

Astrocytic cultures of WT and APP KO mice were stained with an anti-MCU antibody (Figure 21B), and counterstained with an anti-EZRIN antibody to identify the borders of the astrocytic area. The quantification of MCU positive spots, on the EZRIN-positive covered area, revealed an increase in MCU distribution of around 15% in APP KO astrocytes compared to WT (Figure 21C,D). Increased levels of MCU seem to correlate with the accumulation of Cyto C as previously reported (Figure 21).

In conclusion, an increased number of MCU positive spots might be the consequence of an enhanced internalization of MCU into the mitochondrial membrane of APP KO astrocytes, resulting in a subsequent reduction of free cytosolic Ca^{2+} , which in turn influences astrocytic Ca^{2+} dynamics.

Results

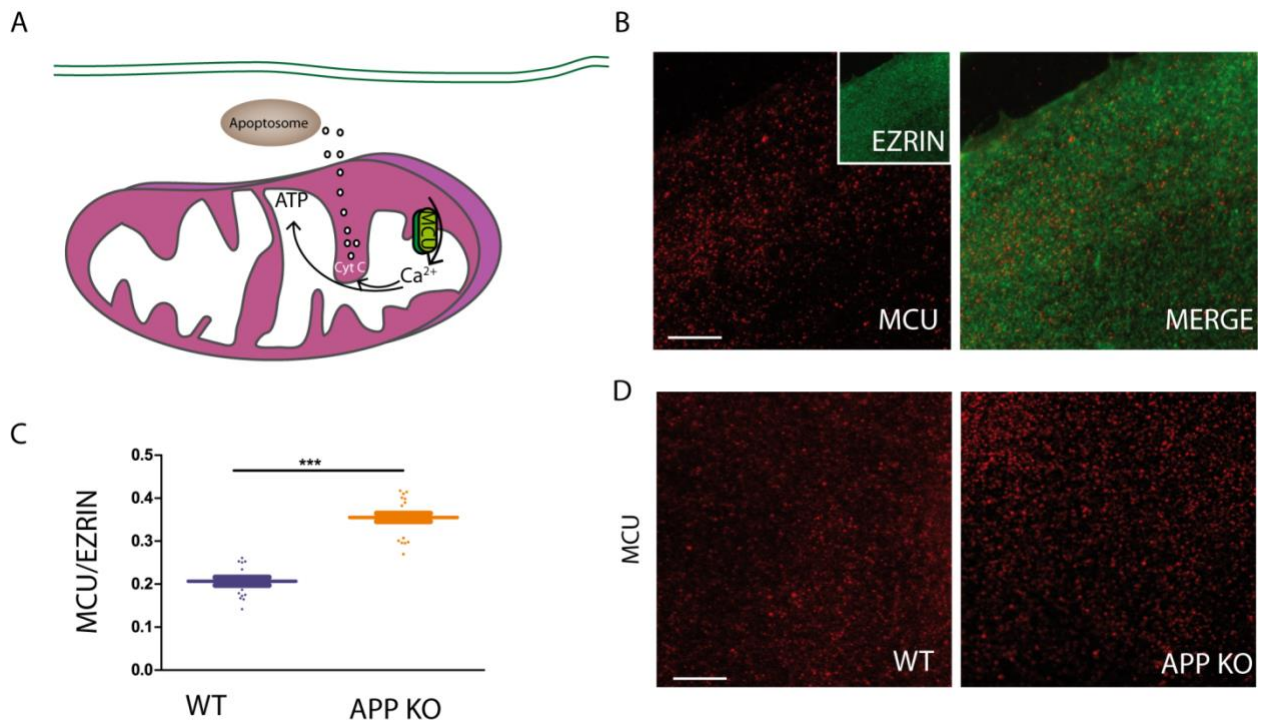


Figure 21: Immunofluorescence of MCU shows enhanced number of MU-positive spots in APP KO astrocytic culture.

The mitochondrial calcium uniporter (MCU) is a transmembrane protein. It is one of the primary sources of mitochondrial Ca²⁺ uptake. If one hand Ca²⁺ is necessary for the production of ATP, on the other hand accumulation of Ca²⁺ into mitochondria activates the apoptotic machinery via released of cyto C into the cytosol (A); astrocytic culture were stained for MCU and EZRIN (B); MCU-positive spots were increased in APP KO compare to WT Mann Whitney test, U=285, p<0,005(C,D).

6.1.9 SUMMARY OF THE FUNCTIONAL ROLE OF APP IN ASTROCYTES

Here, I established a protocol for the *in vivo* investigation of Ca²⁺ activity in the small microdomains of astrocytes. I show for the first time that the Ca²⁺ activity in astrocytic microdomains is severely compromised in the absence of APP. However, the molecular mechanism by which the lack of APP mediates this alteration needs to be further investigated. In response to the lack of APP I observed enhanced mitochondrial fragmentation, the presence of bulb structures containing Cyto C and an overexpression of MCU, all clear hallmarks of malfunctioning mitochondria. Interestingly I could also demonstrate that the expression of a truncated form of APP is not sufficient to restore the morphological alterations of mitochondria. Since morphology of mitochondria and their functionality are strongly connected, I

Results

speculate on the need of full length APP for an efficient functioning of mitochondria and for the consequent astrocytic Ca^{2+} activity along the fine processes of astrocytes.

6.2 POST SYNAPTIC APP AND APP ECTODOMAIN ARE NECESSARY FOR THE MAINTENANCE OF DENDRITIC SPINE PLASTICITY

6.2.1 FIVE DAYS TAMOXIFEN-TREATMENT DEPLETED APP FROM THY-1 YFP POSITIVE NEURONS IN APP-FLOX/SLICK V MICE

In order to investigate the role of APP in modulating dendritic spine plasticity, I used a mouse model co-expressing tamoxifen-inducible Cre recombinase and the fluorophore YFP (SlickV) (Young et al., 2008) to specifically delete APP in a small subset of pyramidal neurons in the somatosensory cortex as well as in the region CA1 region of the hippocampus (Figure 22). APP KO was achieved in 10 weeks old mice by 5 days of application of tamoxifen, which caused almost complete loss of APP immunoreactivity in YFP positive neurons (Figure 22E). As control group, APPflox mice crossed with Slick V received a solution of peanut oil instead of Tamoxifen for a period of 5 days which did not cause any loss of APP (Figure 22E). Treatment with tamoxifen allows translocation of the complex CreERT2 into the nucleus where it exerts its recombinase functions on APP lox P sites (Figure 22B,C).

Results

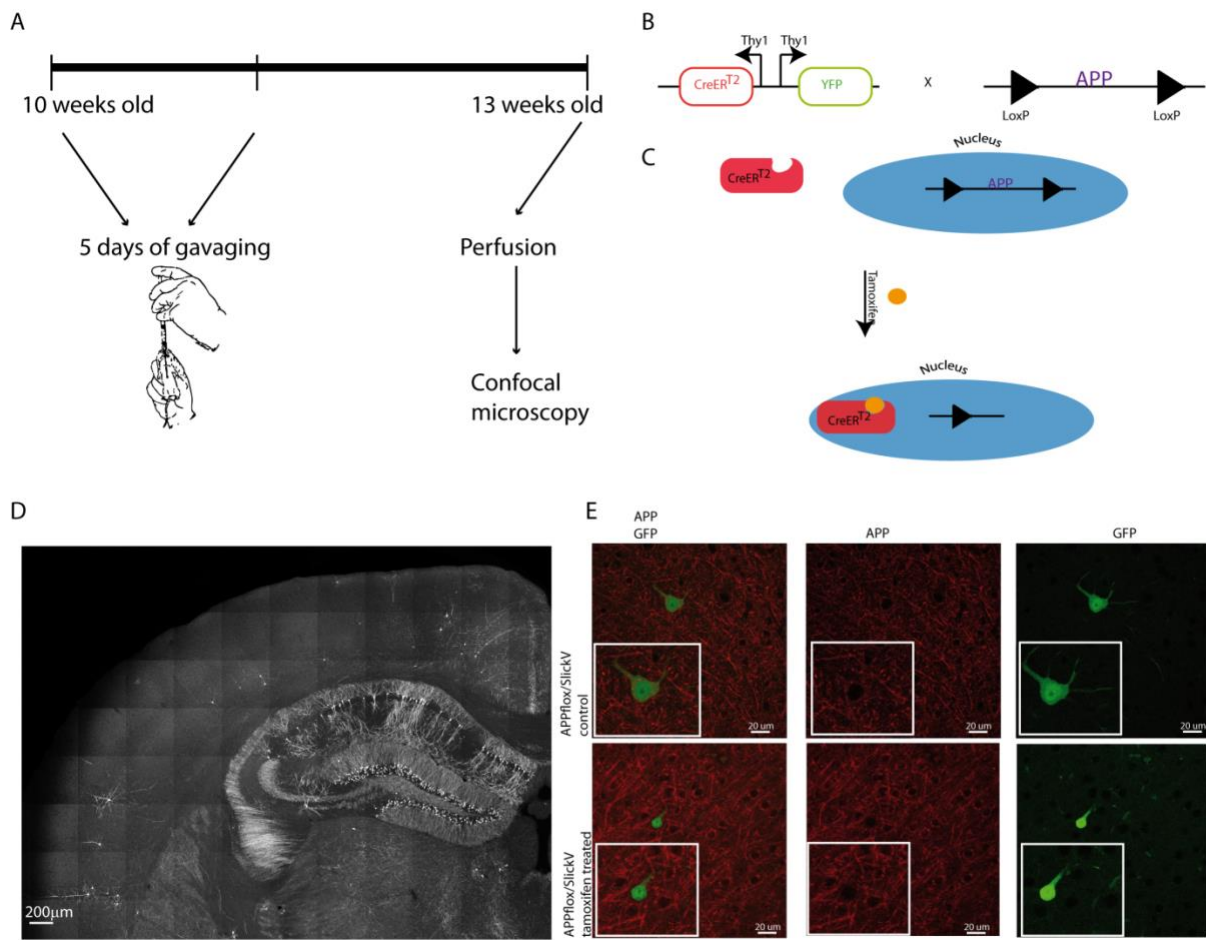


Figure 22: Knockout of APP in a sparse subset of hippocampal and cortical neurons

10 weeks old APP flox(tg/tg) SlickV(tg/-) were administered tamoxifen or peanut oil for 5 days and post-mortem fixed brains were used for spine density and morphology investigations (A); Breeding scheme to obtain inducible APP knockout. *SlickV* mice co-express tamoxifen-inducible cre recombinase ($CreER^{T2}$) with YFP under the *Thy-1* promoter. These were crossed with *APPLoxP/LoxP* mice, in which APP is flanked by LoxP sites. Administration of tamoxifen irreversibly excises APP in YFP-expressing neurons (B,C). Sagittal section through the brain of a *SlickV* mouse, YFP stain. Note the sparse labelling in the cortex and CA1 region. (D). Immunofluorescence stain against APP reveals selective loss in YFP-expressing cortical neurons. Scale bar, 20 μm (E).

6.2.2 CONDITIONAL POST SYNAPTIC KO OF APP AFFECTS DENDRITIC SPINE DENSITY AND MORPHOLOGY

As the fraction of somatosensory as well as hippocampal YFP-positive neurons is very low, they are not expected to provide a substantive fraction of presynaptic input into any given neuron (Figure 23D).

Therefore, I assumed that any of the observed effects are exclusively due to the loss of cell autonomous APP and to the subsequent lack of APP-APP trans dimerization

Results

at the synapses, known to play a role in the maintenance of spine stability (Müller and Zheng, 2012; Andrew et al., 2016; Montagna et al., 2017).

To pin down the effect of a post synaptic KO of APP, spine density and morphology were investigated from apical dendrites of layer V somatosensory neurons and from apical and basal dendrites of the region CA1 of the hippocampus (Figure 23 and Figure 24).

Spine density of layer V somatosensory apical dendrites was significantly decreased in tamoxifen treated APP flox/Slick V mice to around 35% compared with control animals (*t test* $dF_9= 3.22p<0,05$) (Figure 23A,B,C). Morphologically, three basic types of dendritic spines were distinguished: stubby, mushroom-shaped and thin spines. The affected spine density was driven by a significant decrease of the more stable mushroom spines, with around 30% fewer mushroom spines in tamoxifen treated mice compared to control group (*2 way anova*, $dF_{2,27}=12.94$, $p<0,05$) (Figure 23D). Density of thin and stubby were not significantly affected by the lack of APP (Figure 23D).

Pyramidal dendritic spine density of CA1 region of the hippocampus was also considered in our study (Figure 23). It has been shown that dendritic spines of CA1 hippocampal pyramidal neurons are more motile than their cortical partners, and their plasticity correlates with LTP, therefore with learning and memory formation processes (Woolfrey and Srivastava, 2016). However it has been also reported that apical and basal dendrites do not respond equally to LTP stimuli: basal dendritic potentiation is quicker than potentiation of apical dendrites (Kaibara and Leung, 1993), thereby I decided to analyze the apical and basal dendrites independently (Figure 24). This investigation revealed that dendritic spine reduction was more evident in apical (around 42% less spines in tamoxifen treated mice compared to control group) (*t test* $dF_8=5.519$, $p<0,001$) than in basal dendrites (around 40% less spines in tamoxifen treated mice compared to control group) (*t test* $dF_7=2.633$, $p<0,05$) (Figure 24G,K).

Moreover, the morphology was differently affected in the two dendritic populations. Apical dendrites of tamoxifen treated mice show a significant reduction of around 30% of mushroom spines and of almost 50% of stubby spines compared to control mice (*2 way anova*, $dF_{2,24}=6.25$, $p<0,05$) (Figure 21H). In basal dendrite a reduction of around 40% of mushroom spines was observed and is the driving factor for the decreased density of spines in tamoxifen treated mice (*2 way anova* $dF_{2,21}=3.79$,

Results

$p < 0,05$). Overall, these data show that post synaptic conditional KO of APP strongly affects dendritic spines.

As I was interested in understanding the effects of post-synaptical KO of APP on the pre-synapses, I investigated whether the sphericity of the presynaptic terminals of mossy fibers was altered in tamoxifen treated mice (Figure 25). The morphology of mossy fibers boutons is a parameter used to investigate the number of established synapses (Blaabjerg and Zimmer, 2007). Interestingly, no detectable differences in the sphericity of the mossy fibers were identified (Figure 25).

Taken together these results show that APP is important for dendritic spine stability and morphology not only during the developmental phase of the mouse (De Strooper and Annaert, 2000; Laßek et al., 2013) but also during its adulthood. Additionally, using this approach I could demonstrate that while post-synaptic dendritic spines are very sensitive to conditional KO of APP, the presynaptic terminal did not undergo any substantial change when sphericity was investigated.

Results

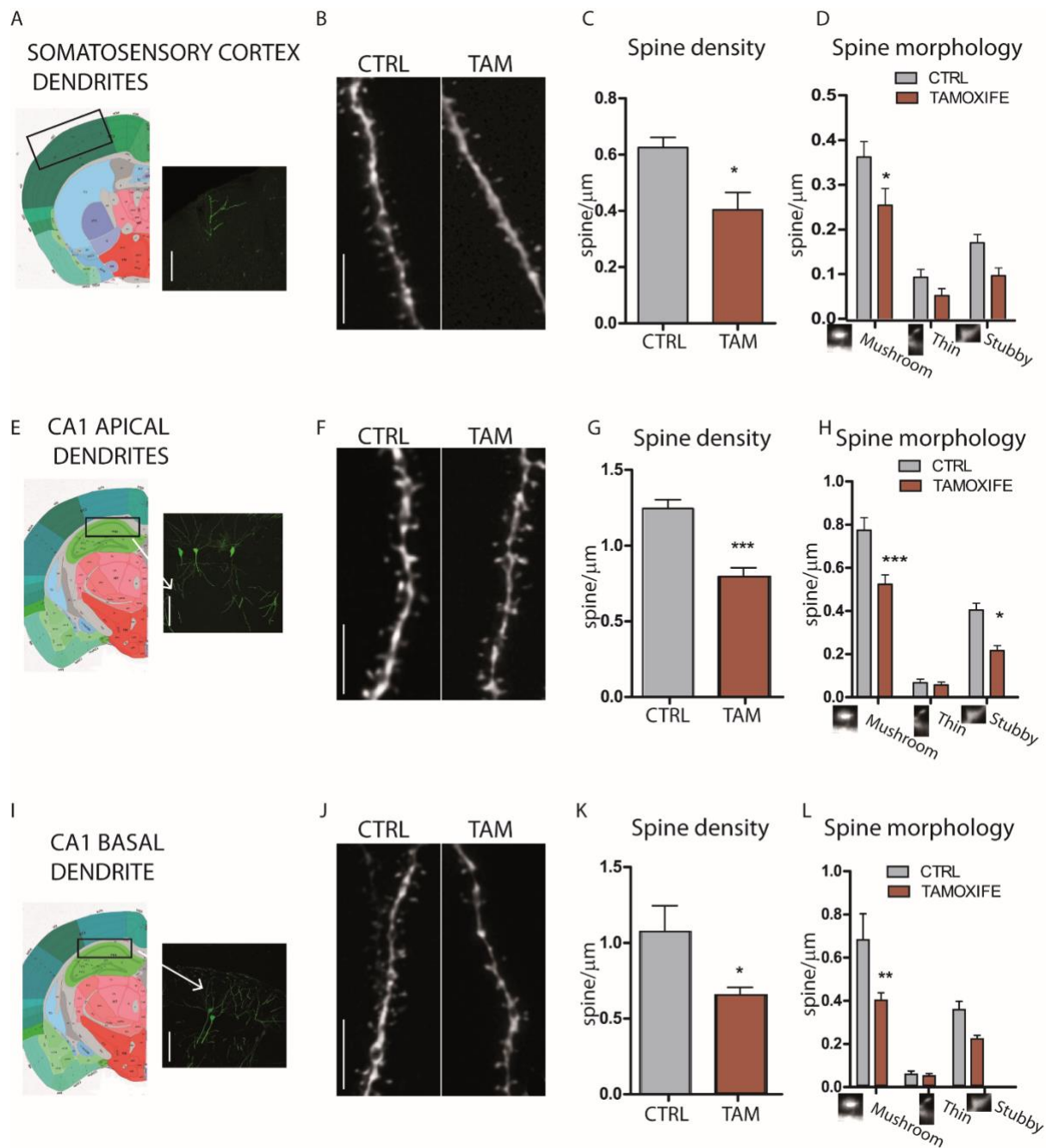


Figure 23: Conditional post synaptic KO of APP affects dendritic spines of the somatosensory cortex and of hippocampal CA1 pyramidal neurons.

Coronal section of mouse brain showing the somatosensory cortex (black rectangular) where YFP-positive dendrites were depicted and confocal picture of somatosensory dendrites used for dendritic spine analysis, scale bar= 100 μm (A) ; two representative dendrites of control (CTRL) and tamoxifen (TAM) treated mice, scale bar=10 μm (B); spine density quantification (t test $dF_9= 3.22p<0,05$) (C); morphological quantification of dendritic spines (2 way anova, $dF_{2,27}=12.94, p<0,05$) (D); Coronal section of mouse brain showing the CA1 hippocampal region (black rectangular) where apical YFP-positive dendrites were depicted (white arrow) and confocal picture of apical CA1 dendrite used for dendritic spine analysis, scale bar=100 μm (E) ; two representative dendrites of control (CTRL) and tamoxifen (TAM) treated mice, scale bar= 10 μm (F); spine density quantification (t test $dF_8=5.519, p<0,001$) (G); morphological quantification of dendritic spines (2 way anova, $dF_{2,24}=6.25, p<0,05$) (H); Coronal section of mouse brain showing the CA1 hippocampal region (black rectangular) where basal YFP-positive dendrites were depicted (white arrow), confocal picture of basal CA1 dendrite used for dendritic spine

Results

analysis, scale bar=100 μ m (I) ; two representative dendrites of control (CTRL) and tamoxifen (TAM) treated mice, scale bar= 10 μ m (J); spine density quantification (t test $dF_7=2.633$, $p<0,05$) (K); morphological quantification of dendritic spines (2 way anova $dF_{2,21}=3.79$, $p<0,05$) (L).

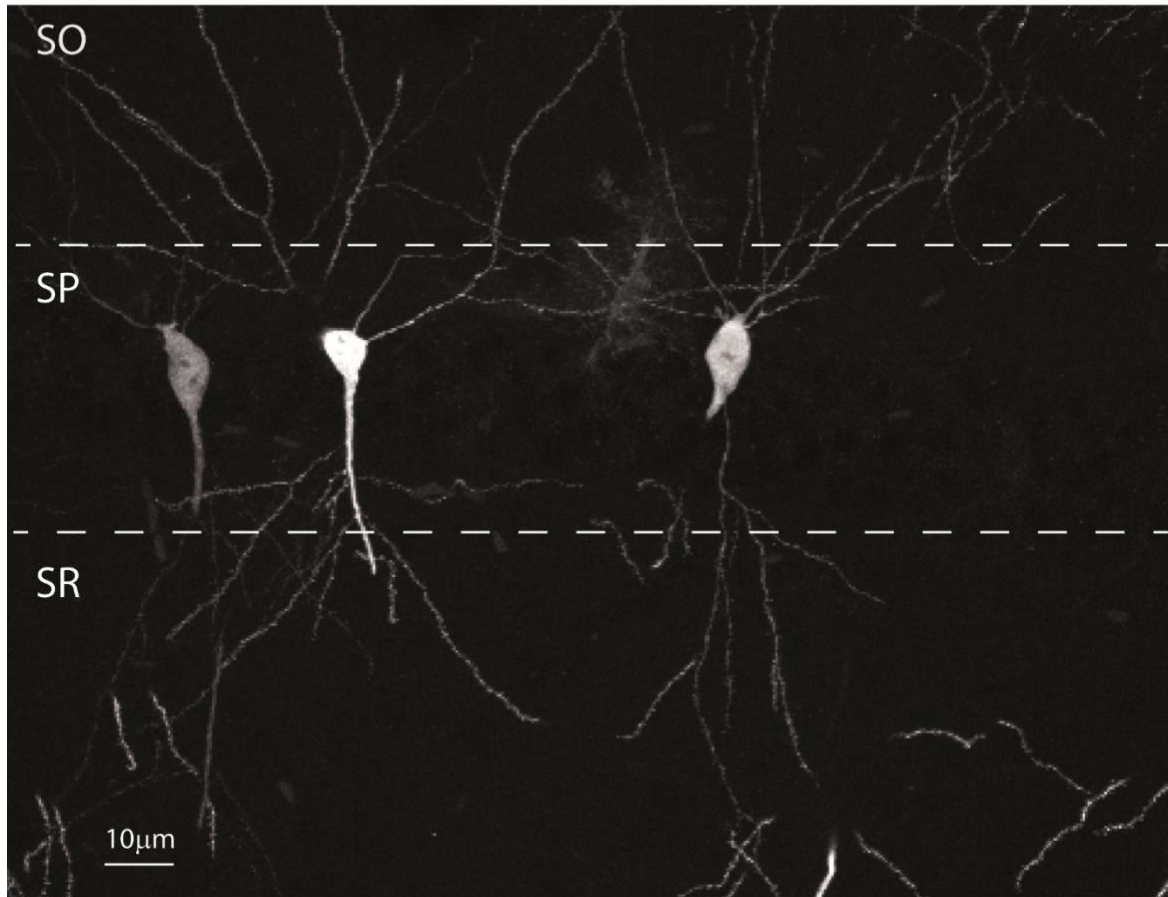


Figure 24: Hippocampal pyramidal neurons: apical and basal dendrites.

Confocal picture of YFP positive pyramidal CA1 neurons. Basal dendrites in the Stratum Oriens (SO) were independently analyzed from apical dendrites in the Stratum Radiatum. Soma of CA1 pyramidal neuron is located in the Stratum Pyramidale (SP). Scale bar=10 μ m.

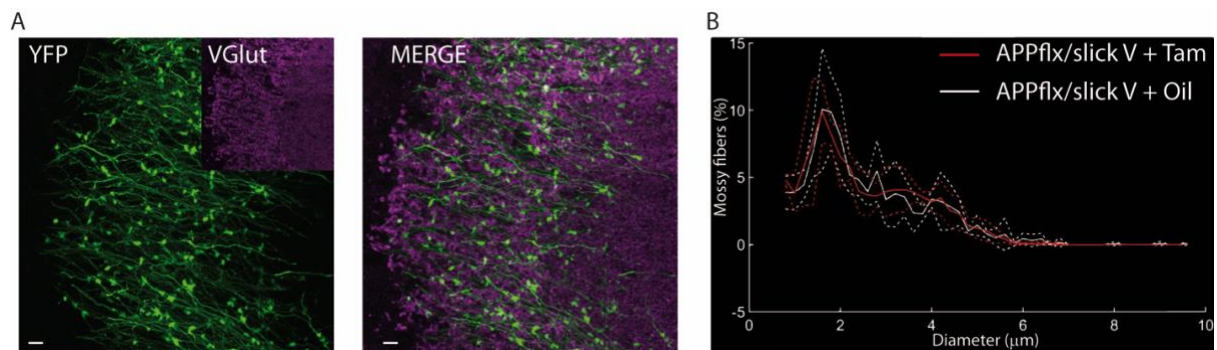


Figure 25: Mossy fiber' s terminals of conditional APP KO mice do not show any alteration compare to control group.

Results

Z-stack of confocal pictures of YFP positive mossyfibers (green) co-expressing VGlut (purple) as marker of pre-synaptic terminal (A) Scale bar =10um; analysis of sphericity of mossy fibers terminal in APP-flox SLick V mice treated with tamoxifen or peanut oil did not reveal evident differences between the two groups (B).

6.2.3 APP ECTODOMAIN IS CRUCIAL FOR SPINE DYNAMICS UPON EE STIMULATION

Given that the conditional KO of full length APP strongly affects spine density and morphology, and given that APP KO mice show impaired spine plasticity if exposed to EE (Zou et al., 2016), I decided to further explore the role of the APP ectodomain in regulating spine dynamics. Under the correct experimental conditions, *in vivo* imaging approaches can simultaneously allow imaging of spines and monitoring of specific populations of dendrites in a living organism in real time (Jung and Herms, 2012), hence being an advantageous tool to investigate the effects of environmental stimulation on a subpopulation of neurons. Therefore I decided to apply two photon *in vivo* microscopy to APP Δ CT15 mice (Ring et al., 2007) and monitor the dynamics of apical dendritic spines of layer V somatosensory neurons. Studies conducted so far on APP Δ CT15 mice reported an overall improvement of LTP, brain weight and body growth compared to APP KO mice, thus suggesting APP ectodomain as crucial for the establishment and maintenance of the brain network (Ring et al., 2007).

Three months olds APP Δ CT15 and WT mice were exposed to EE for a period of 4 weeks and dendritic spines were monitored weekly (Figure 26A,B), as previously described (Zou et al., 2016). EE is known to provide a spectrum of synaptic inputs, which lead to adaptive synaptic alterations within the adult brain (Nithianantharajah and Hannan, 2006). In agreement with previous observations (Jung and Herms, 2014; Zou et al., 2016) exposure to EE induced a steady increase of spine density in the WT mice (Figure 26 D).

Interestingly my results clearly indicate that, in contrast to APP KO mice (Zou et al., 2016), spine density of layer V pyramidal neurons in the somatosensory cortex of APP Δ CT15 mice increases after exposure to EE by ~5%, similar to dendritic spines of WT mice (*2 way anova, $dF_{7,49} = 0.16, p < 0.001$*) (Figure 26CD). Moreover, the spine density of WT and APP Δ CT15 mice showed no significant difference (*t test $p > 0,05$*) (Figure 26D). Taken together I observations reveal a crucial role of APP ectodomain to maintain an efficient and functional spine plasticity. APP ectodomain at its physiological location is needed to preserve the capability of dendritic spines to

Results

adaptively remodel their location, thus determining the whole brain network in the adult brain.

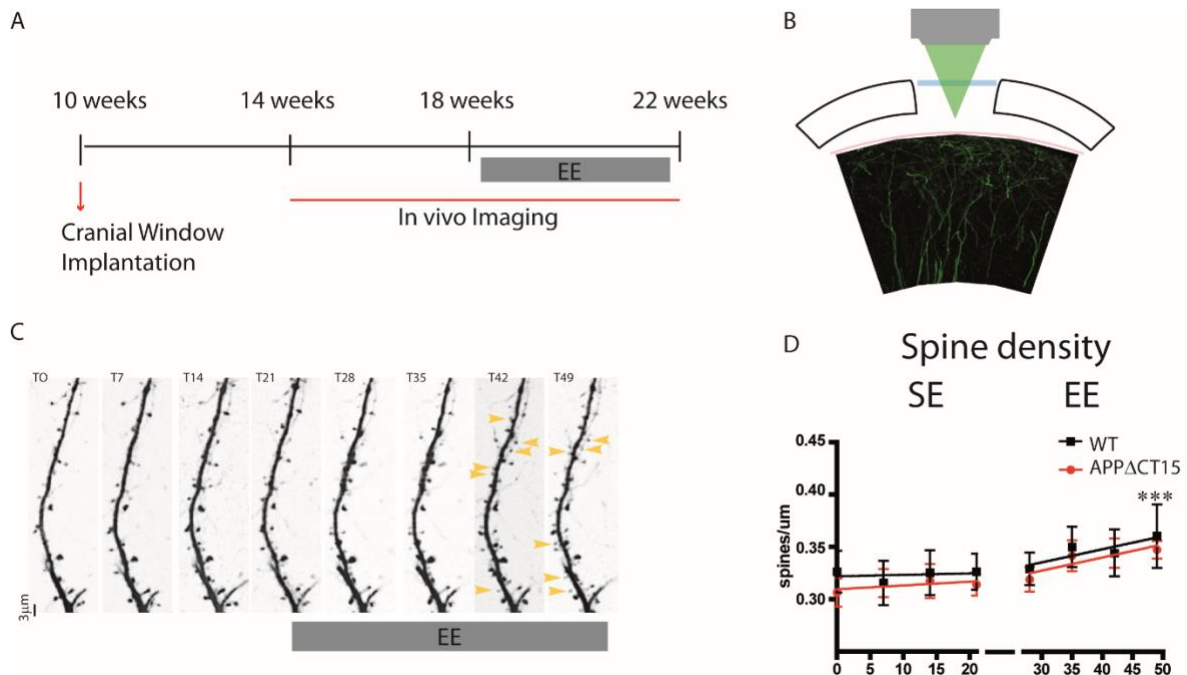


Figure 26: APP ectodomain is necessary for spine plasticity upon EE stimulation.

10 weeks old mice underwent cranial window implantation. 4 weeks later mice were anesthetized (mixture of isoflurane and oxygen) and placed under two photon microscopy where somatosensory dendritic spines were imaged weekly for a period of 8 weeks. For 4 weeks, before and after the imaging session the mice were housed in single caged conditions, whereas for the last 4 weeks of imaging the mice were housed in EE conditions (A); Representation of apical dendrites imaged through a two photon in vivo microscopy setup; a thin glass allows imaging of apical dendrites in vivo (B); typical somatosensory dendrite whose spines have been counted for 49 days, before and after exposure to EE (C); dendritic spine density of WT and APP Δ CT15 mice kept in single cage environment (SE) and in enriched environment (EE) condition; no significant differences of spine density was detected between the two groups (t test $p > 0.05$), both groups showed significant increase of spine density after exposure to EE of ~5% (2 way anova, $dF_{7,49} = 0.16$, $p < 0.001$).

6.3 APP Δ CT15 MICE CAN DISCRIMINATE BETWEEN FAMILIAR AND NOVEL OBJECTS DURING A NOVEL OBJECT RECOGNITION TEST

Dendritic spine plasticity strongly affects cognition and memory (Lai and Ip, 2013; Zou et al., 2016)

To understand whether the dendritic spines in APP Δ CT15 mice impact and ameliorate the cognition performances, shown to be impaired in mice with full KO of

Results

APP (Ring et al., 2007; Zou et al., 2016), I performed novel object recognition (NOR). Following the previously established protocol on APP KO mice (Zou et al., 2016) I could demonstrate that APP Δ CT15 mice can discriminate between novel and familiar objects, in a similar manner as WT mice (Wilcoxon signed rank test was performed to compare data to the hypothetical value 1. $*p < 0,05$). (Figure 27 A,B). This means that, during the test phase, the mice spent the majority of the time next to the new object, which draws their curiosity.

Overall, these data show that cognition and memory tasks are not affected by the lack of the 15 C-terminal aminoacids of APP. Hence, the APP ectodomain alone at its physiological expression at the cell membrane allows mice to perform the NOR paradigm similar to control WT mice, and therefore ameliorates behavioral deficits observed in condition of full APP KO mice (Ring et al., 2007; Zou et al., 2016).

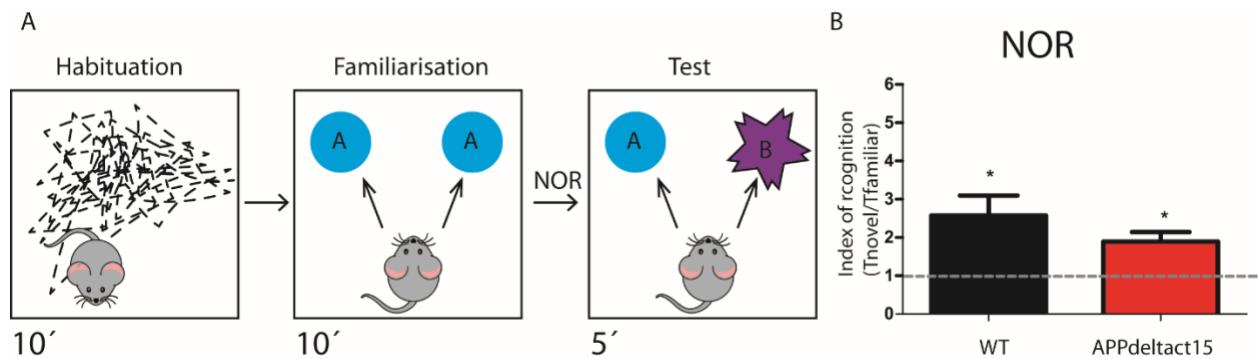


Figure 27: APP Δ CT15 mice can discriminate between novel and familiar object during a NOR test.

*Schematic representation of NOR paradigm applied to WT and APP Δ CT15 mice. Briefly mice spent 10 minutes in an open field arena where they could familiarize with the environment (Habituation phase), 24 hours later mice were placed back in the arena with two identical object for a period of 10 minutes (Familiarization phase), after placing back the mice in their cage they were re-locate in the arena, this time with a familiar object and with a new one (Test phase); the time spent exploring each object was calculated (A); Both WT and APP Δ CT15 were able to discriminate between a novel and familiar object spending more time next to the novel object compare to the old one (Wilcoxon signed rank test was performed to compare data to the hypothetical value 1. $*p < 0,05$ (B)).*

6.3.1 SUMMARY OF THE FUNCTIONAL ROLE OF APP IN MODULATING DENDRITIC SPINE PLASTICITY

I applied *ex vivo* as well as *in vivo* approaches to unravel the role of APP in spine dynamics, stability and structure in different conditions and upon environmental stimulation. Density as well as dynamics of dendritic spine correlates with the plasticity and the structure of the brain network and its ability to adapt in response to

Results

external stimuli. Through the *ex-vivo* investigation I could demonstrate that the conditional KO of APP in adult mice induces a clear reduction of dendritic spines and alters spine morphology, in the hippocampal CA1 neurons as well as layer 5 pyramidal neurons of the somatosensory cortex. Additionally I confirmed that neurons undergo rearrangement of dendritic spines also during mouse adulthood, ascribing to APP a pivotal role in this function. In fact I demonstrated how conditional APP KO negatively impacts on spine density and structure. Due to the low fraction of YFP positive neurons I also assumed that the observed alterations were induced by the loss of the cell autonomous APP, whose role at the synapses, among the others, is to govern spine stability through APP-APP dimerization and/or through the activation of intracellular pathways (Müller et al., 2008b; Baumkötter et al., 2012; Baumkötter et al., 2014; Hoefgen et al., 2014; Klevanski et al., 2015). Moreover, thanks to the *in vivo* results on spine dynamics in APP Δ CT15 mice I could prove the necessity for the expression of the APP ectodomain at its physiological location, in order to have a constitutive and adaptive spine plasticity comparable to the one observed in the control mice. Furthermore, the lack of the 15 intracellular amino acids of APP in these mice did not affect the performances during the NOR test.

7 DISCUSSION

In the past, astrocytes have been considered as passive elements involved in the modulation of neuronal functions. Today their active role in regulating brain network, refining synapses, modulating the concentration of neuro- and glio- transmitters in the extracellular space is widely accepted in the field of neuroscience (Perea et al., 2009; Perez-Alvarez et al., 2014). Although the role of APP has been widely investigated in neurons (Müller et al., 2017), it has been for too long overlooked in astrocytes.

Therefore, I decided to focus this study on the role of APP in astrocytes, as active partners in synaptic function (Perea et al., 2009). Namely, astrocytes conduct a great number of functions, which often require increased levels of intracellular Ca^{2+} , and are partners of neurons in modulating synaptic networks (Perea et al., 2009). As we recently demonstrated, the lack of APP affects glio-transmission of D-serine, a co-agonist of NMDA receptors. This alteration, in turn, leads to defects in dendritic spines plasticity of adult APP KO mice (Zou et al., 2016). Considering that the D-serine release from astrocytes is mediated by intracellular Ca^{2+} -dependent mechanisms, I hypothesized that Ca^{2+} activity in the fine astrocytic processes of APP KO mice is altered. Hamid et al. showed alterations in both resting free cytosolic Ca^{2+} and in the Ca^{2+} release from ER in primary astrocytic cultures from APP KO mice (Hamid et al., 2007). Additionally, in 2011 Linde and colleagues showed altered Ca^{2+} homeostasis in astrocytic cultures of APP KO mice, suggesting a strong correlation between APP and Ca^{2+} modulation in astrocytes.

In this study I considered the effects of APP depletion on spontaneous *in vivo* Ca^{2+} dynamics within microdomains of astrocytic fine processes known to be closely associated with synapses. It is fundamental to understand the local function of these microdomains in order to decode the contribution of APP to the communication between astrocytes and neurons (Perea et al., 2009).

Thus, I used a membrane-tagged genetically encoded Ca^{2+} indicator for the investigation of astrocytic Ca^{2+} transients in astrocytic fine processes (Shigetomi et al., 2013).

The challenging *in vivo* investigation of Ca^{2+} transients in the distal part of the astrocytes has been recently resolved by the development of the AAV-GCaMP6f carrying a GFAP promoter and a plasma membrane localization signal. This tool

Discussion

allowed me to establish a new protocol for the analysis of *in vivo* Ca²⁺ transients in APP KO astrocytic fine processes. My data show that lack of APP significantly affects *in vivo* spontaneous Ca²⁺ activity along the fine processes defined as microdomains. These autonomous, functional units are able to modulate dendritic spine plasticity (Perea et al., 2009). My *in vivo* two-photon imaging results clearly demonstrate that lack of APP affects the density of microdomains, with a significant loss of small active domains compared to control animals. Moreover, frequency and kinetics of Ca²⁺ transients along the fine processes were reduced as well, without any substantial change in amplitude.

These results provide new insights on the *in vivo* role of APP in the modulation of Ca²⁺ transients in astrocytes. Given that Ca²⁺ transients along the fine processes of astrocytes are defined by mitochondria-mediated ion homeostasis (Jackson and Robinson, 2015; Agarwal et al., 2017), I hypothesized and investigated possible mitochondria dysfunctions. The KPI domain of APP is expressed in the 751-770 amino acids long APP isoforms, predominantly expressed in astrocytes (Rohan de Silva et al., 1997). In 2016 Wang and colleagues generated KPI-APP mutants, lacking the 12 C-terminal amino-acids in HeLa cells. Wang observed that the mutated KPI-APPs exhibited decreased mitochondrial localization. In addition, mitochondrial morphology was altered, resulting in an increase in spherical mitochondria in the mutant cells through the disruption of the balance between fission and fusion (Wang et al., 2016). These data are in strong agreement with my assumptions of an astrocytic-specific phenotype of mitochondria in this context. Indeed, I observed that mitochondria from APP KO astrocytic cultures are fragmented, in accordance with the observations of Wang in HeLa cells (Wang et al., 2016). Moreover, my findings indicate that the expression of the APP ectdomain alone is not sufficient to rescue this fragmentation. Mitochondria fragmentation correlates with unhealthy mitochondria, present in many neurological diseases, as AD (Spuch et al., 2012). Intriguingly, mitochondria ability of buffering Ca²⁺ over a big area is strongly linked to their physiological tubular morphology (Chang and Reynolds, 2006). In the case of fragmented and more sparse mitochondria, instead, Ca²⁺ will be buffered over a smaller cytoplasmic area. Therefore, as a result of the observed mitochondria fragmentation, microdomains may get deprived of their main energetic sources and cannot sufficiently support surrounding neuronal activity. Therefore I hypothesize that the highly ramified protrusions of astrocytes, where microdomains are located,

Discussion

are not fully functional in APP KO mice, thus explaining the impairments in synaptic plasticity and gliotransmitter release observed in APP KO animals (Zou et al., 2016). It has previously been shown that APP harbors a mitochondrial targeting signal and forms complexes with the translocase of the outer mitochondrial membrane 40 (TOMM40) and the inner mitochondrial membrane 23 (TIMM23) (also known as TOM complex), regulating the translocation of nuclear-encoded proteins into the mitochondria (Devi et al., 2006; Pagani and Eckert, 2011). I therefore reasoned that depletion of APP may compromise mitochondrial protein translocation affecting mitochondria functions and leading to imbalanced intracellular Ca^{2+} homeostasis. In fact, the mitochondria-associated ER membranes (MAMs) are sites where the APP cleavage product C99 accumulates and interferes with the mitochondrial respiratory chain (Pera et al., 2017). Hence, I speculate that full-length APP or any of its cleavage products at physiological levels have a function in ensuring ER-mitochondria proximity and thus permitting proper mitochondria integrity

Notably, I also observed an augmented level of the nuclear-encoded protein MCU. MCUs are Ca^{2+} uniporter, responsible for the uptake of Ca^{2+} from the cytosolic space into the mitochondria, where it is used for the production of ATP or it is simply stored and then released again in the cytoplasm (Gunter and Gunter, 2002). The more spread distribution of MCU observed in APP KO astrocytes could be a consequence of either a mis-regulation of APP-TOM dependent protein translocation or the result of the fragmented mitochondria network.

In summary, the alteration of ASCTs in APP KO may be either due to a higher expression of MCUs and as a consequence an enhanced uptake of Ca^{2+} from ER/cytoplasm or due to an impaired buffering of Ca^{2+} resulting from the alteration in the morphology or functionality of mitochondria. Thus, the malfunctioning of mitochondria could cause a reduction of free cytosolic Ca^{2+} , hence explaining my *in vivo* observations (Figure 28).

In conclusion, I introduced a new protocol for the investigation of Ca^{2+} dynamics along the fine processes of astrocytes. Thanks to this approach I could provide novel insights into the role of APP as a regulator of mitochondrial network and Ca^{2+} homeostasis in astrocytes. My data represent a valuable resource for further investigations on APP functions in astrocytes that have been neglected for too long.

Discussion

LEGEND

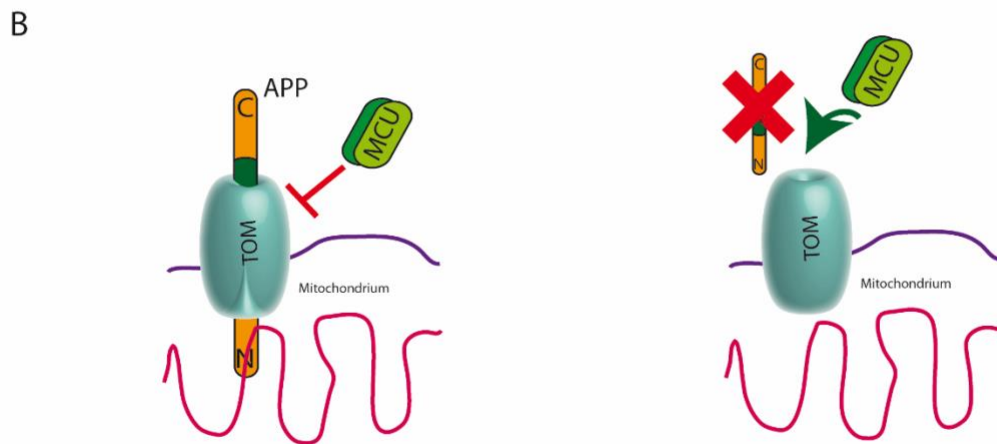
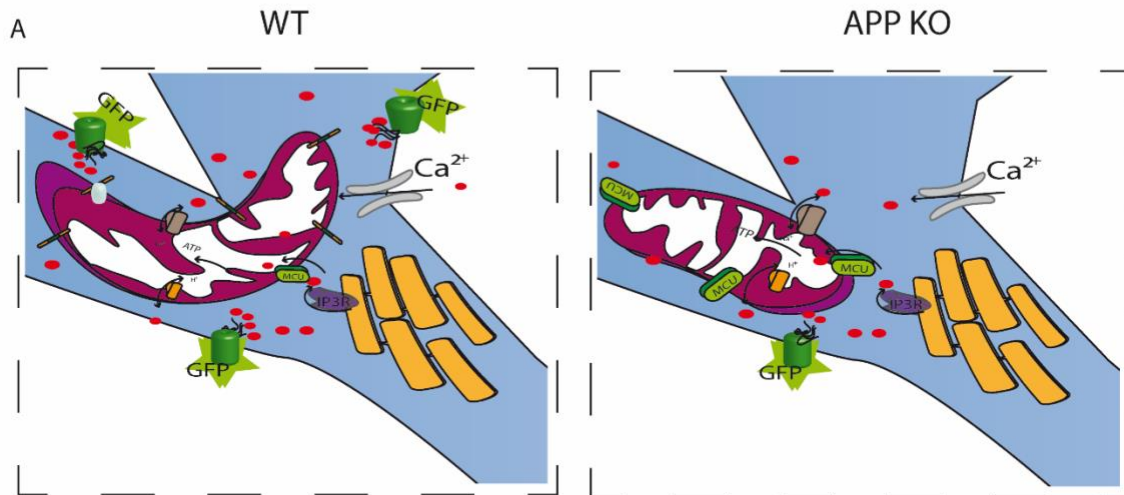
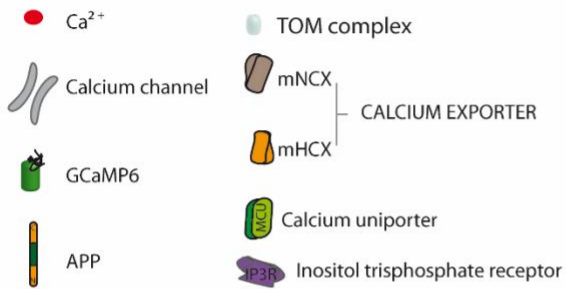


Figure 28: Schematic representation of the interplay between APP –mitochondria and calcium transients in fine processes of astrocytes.

WT astrocytes show more elongate mitochondria with a typical tubular shape, that allow them to cover a bigger area compared to the fragmented mitochondria present in APP KO astrocytes. As WT mitochondria cover a bigger area within an astrocyte they can buffer Ca^{2+} over a larger cytoplasmic area than APP KO, thus influencing the decrease number and slower kinetics of active microdomains of APP KO astrocytes, as our *in vivo* observations show. Influx of Ca^{2+} into mitochondria is modulated by the uniporter MCU. Its proximity to IP3R2 and of other Ca^{2+} channels modulate the concentration of free cytosolic Ca^{2+} . Increased number of MCU let us

Discussion

hypothesize that correlate to less free cytosolic Ca^{2+} (A). The link between APP and TOM complexes regulates the entrance of nuclear encoded mitochondria protein, like MCU for instance. The lack of APP might affect the TOM-dependent protein translocation into the mitochondria, determining an overexpression of protein, like MCU, involved in the uptaken of Ca^{2+} affecting the concentration of free cytosolic Ca^{2+} (B).

Next, I provided new insights on the role of APP in modulating dendritic spine plasticity by using both *in vivo* and *ex vivo* approaches. To understand the role of full length APP and of APP functional domains, I pursued two different strategies: 1) APP was conditionally KO in adult mice and spine density and morphology was investigated; 2) dendritic spine plasticity of APP Δ CT15 mice was investigated to unravel the specific role of the APP ectodomain in spine dynamics. It has been shown that APP can form dimers, through the interaction of APP-APP ectodomains and with other APP family members, both in *cis* as in *trans* orientations (Figure 29A) (Soba et al., 2005; Dahms et al., 2010; Xue et al., 2011). The formation of *trans*-dimers allows APPs to act as synaptic adhesion molecules (Wang et al., 2009; Müller and Zheng, 2012; Baumkötter et al., 2014). This study demonstrated that conditional APP KO in a small subset of cortical and hippocampal neurons allowed us to analyze the effects of the KO at the postsynaptic plasmamembrane. Under such conditions the APP expressed in the presynaptic terminals is very likely unable to dimerize with the post-synaptic APP, hence affecting dendritic spine stability. Moreover, due to the low percentage of conditional KO neurons I assumed that the observed outcome is the result of a cell autonomous lost of APP. The conditionally APP KO in adult mouse brain revealed its utility to understand how adult neurons are sensitive to a sudden KO of APP, without being able to take any advantage from possible compensatory mechanisms that occur during brain development (El-Brolosy and Stainier, 2017). Data obtained within my study indicates that post synaptic KO of APP leads to a reduction of spine density in regions like the somatosensory cortex and in the more plastic CA1 region of the hippocampus. Moreover the observed altered spine density seems to be induced from a loss of the stable mushroom spines. Spine density and plasticity correlates with experience dependent plasticity and with memory and learning processes (Ring et al., 2007; Knott and Holtmaat, 2008; Ochs et al., 2015; Zou et al., 2016). The effects observed by the conditional KO of APP show how even during adulthood the brain maintains its plasticity and dendritic spines lose their stability in response to the conditional APP

Discussion

KO. However, I cannot assess the contribution of the transcriptional role played by the intracellular domain of APP (Müller and Zheng, 2012) or by the dimerization driven by APP ectodomains in this model (Figure 29B). Thereby, I decided to investigate spine plasticity in the APP Δ CT15 mouse models (Ring et al., 2007), where the intracellular domain of APP is missing and therefore its transcriptional role.

My study is based on our recent findings. I demonstrated through an *in vivo* study in the somatosensory cortex of adult APP KO mice that lack of APP does not affect spine density in standard housing condition. However, the exposure of mice to EE stimulates formation of new spines in WT mice (Nithianantharajah and Hannan, 2006), but not in APP KO mice (Zou et al., 2016). The mutated APP in the APP Δ CT15 is expressed under its endogenous promoter, but it lacks the C-terminal 15 aminoacids (Ring et al., 2007). Nevertheless it still expresses its transmembrane domain, thus allowing the protein to be located in the membrane and form dimers at the synapses (Figure 29C). Previous data already reported a rescue in behavioural deficits, weight loss and reduced dimension of the brain in these mice (Ring et al., 2007). On the same line, my data clearly indicate that there are no deficits in the spine density of apical dendrites of layer V somatosensory neurons of APP Δ CT15 mice compared to WT. Moreover, the presence of this truncated form of APP is enough to observe a physiological increase in the spine density of the mice after exposure to EE. Following the protocol performed on the APP KO mice, I also observed no behavioral deficits in the NOR test, thus suggesting that the expression of APP ectodomain is enough for maintaining a functional brain network, in accordance with previous studies on this mouse line (Ring et al., 2007).

Overall, I show that APP is indeed fundamental for the regulation of spine stability, plasticity and morphology in adult mice. I additionally claim that APP ectodomain, at his physiological location, is strongly required for functional brain network and for spine plasticity. Thus, my study gives an overview of the role of APP in defining the brain network and the formation/stabilization of new synapses through the modulation of both astrocytes and neuronal dendritic spines.

In conclusion, my study on APP physiological functions identifies astrocytes as new partners involved in the APP-dependent regulation of the brain network. I additionally

Discussion

provided new information regarding the interplay between APP and mitochondria, although the molecular mechanisms of this interaction need to be further investigated. I contributed to the understanding of APP role in governing spine dynamics, a topic that is still being explored. I showed that dendritic spines reduce their stability upon KO of APP, and I hypothesize a pivotal role of the APP ectodomain in the regulation of this process. Taken together, my results give an overview of the role of APP in defining the brain network and the formation/stabilization of new synapses through the modulation of both astrocytes and neuronal dendritic spines. To more deeply understand the way APP influences brain network, future studies should take into consideration the relationship of astrocytes and neurons as part of one single process and investigate the effect of the lack of APP as the result of altered communication among different cell types, shifting the neurocentric view that has been driving neuro scientists for too long.

.

Discussion

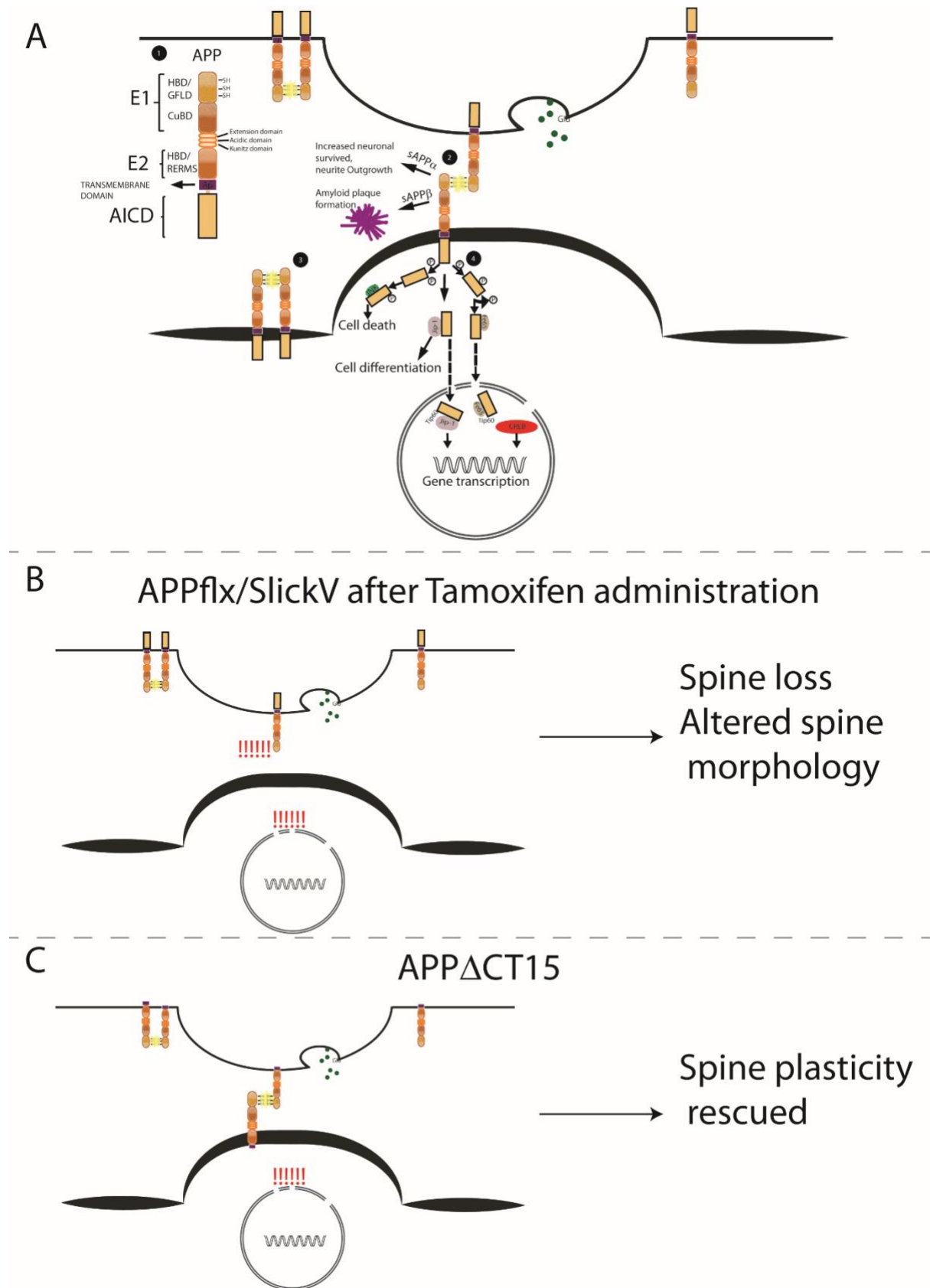


Figure 29: Schematic representation on how APP can influence spine dynamics in WT mice, in mice where APP has been conditional KO and in APP Δ CT15 KI mice.

Discussion

(Previous page) APP dimerization as well as APP intracellular signaling cascade are important for dendritic spine plasticity.

1. Schematic representation of APP domain structure. From the N-terminal region; the E1 domain formed by: heparin binding domain (HBD), growth factor like domain (GFLD) and copper binding domain (CuBD). The E2 domain that includes the heparin binding domain and the pentapeptide sequence (RERMS). A β region and transmembrane region precede the AICD intracellular domain. 2,3. Example of APP dimerization occurring at the synapses and between two molecules of APP on the same neuron. The dimerization is stabilized by the formation of disulfide bridges (SH-SH) highlighted in yellow. 4. Schematic representation of AICD intracellular pathway. Phosphorylated AICD interacts with

JNK triggering cell death, with JIP stimulating cell differentiation and with Fe65 or JIP to get transport into the nucleus and modulate gene transcription (A); Schematic representation of readouts from APP flox- tamoxifen treated mice. Lack of post synaptic, therefore of the trans-dimerization and of the intracellular signaling cascade, lead to a reduction in spine density and altered spine morphology (B); Schematic representation of APP Δ CT15 experiments, expression of APP ectodomain allows still the formation of trans dimers, while the intracellular cascade activated by the AICD domain is still missing. However mice show dynamic and functional spine plasticity (C).

8 ACKNOWLEDGEMENTS

I firstly would like to thank my supervisor Prof. Jochen Herms, for the guidance and the advices he provided throughout my time as a PhD student. At many stages in the course of this research I could benefit of his advices and support.

I would like to thank all my colleagues, with whom I could spend valuable time at work and enjoyed the life outside, sharing beers and nice chats. Thanks to Carmelo for his scientific support, for his energy and enthusiasm and for being a good Italian companion during my time in the lab. Big thank goes the first people I had the chance to meet during my first period as Ph.D. student: Susy, Ana, my good friends Lidia and Eva. I can't forget how important it has been for me having you all around during my first time in Munich. Special thanks goes to Hazal with whom I feel sharing a long path of our lives, professional and not.

Thanks to my EXTRABRAIN colleagues and friends, particularly to Maura. All together we shared great experiences and you all are amazing people. Despite the fact our lives were conducted in different countries, every time with you there was a great connection and amazing exchange of scientific ideas that helped me a lot to find new energy for my Ph.D studies.

A big thanks goes to all my Munich friends, my strength in this foreign city, thanks to you. Thanks to Maria, the first person I really got to know here, with you is always like been at home, and this is amazing. Thanks to Elena and Silvia, our Italian roots, a lot to talk, a lot to share, connected us like sisters and without you this city wouldn't be the same.

Thanks to all the people I met during these years, Alessandra, Angelica, Veronica, Larissa, Anita, Alessandro, Andrea, Alessio and many others.

Sharing our different backgrounds, our point of view, our hobbies, dream and hopes, our experiences as people living abroad made me a different person, more complete, more open, more curious, more flexible, a better person.

Ora veniamo a chi mi conosce da sempre, alla mia famiglia. Grazie a mia madre e mio padre per avermi insegnato ad affrontare la vita e le sue sfide, insegnandomi il rispetto, l'onestà e l'amore. Grazie a mia sorella, per essere parte di me, per essere come un libro aperto, per essere le mie radici e il mio sostegno in ogni momento

Acknowledgement

della mia vita. E Grazie a lei e Davide per aver portato la dolcissima Eleonora nelle nostre vite. E quindi grazie alla piccoletta.

Grazie alle mie amiche di sempre. A Chiara, la mia maghetta, sempre vicina nonostante la distanza, la mia porta verso un mondo diverso, fatto di piante e folletti, la mia amica di sempre, unica e insostituibile, l'amica che ti capisce senza bisogno di parole. Grazie a Jacopo, parte importante di ciò che sono e sarò. Grazie alla mia squadra di sempre, a Gnappa, per essere un compagna di squadra e di vita, per essere lì, sempre e incondizionatamente, a Lavina e Cicci, compagne di una squadra che non ha confini. Grazie per non avermi mai fatto sentire sola durante questi anni. E quindi grazie a te, per amarmi, spronarmi, stimarmi, conoscermi e rispettarci. Non un grazie ma mille per tutto ciò che abbiamo costruito in questi anni, insieme, grazie per tutte le tue parole, i tuoi sguardi, i tuoi baci e abbracci che sono oggi, così come ieri e come lo saranno domani, parte vitale della mia forza, del mio coraggio, dei miei sorrisi e dei miei pensieri. Grazie per tutto ciò e per tanto altro ancora.

9 LIST OF ABBREVIATIONS

AD	Alzheimer's disease
APLP	Amyloid Precursor Like Protein
APP	Amyloid Precursor Protein
AICD	APP intracellular domain
A β	Beta-amyloid
CTF	C-terminal fragment
Ca ²⁺	Calcium
CuBD	Copper binding domain
Cyto C	Cytochrome C
°C	Degree Celsius
EE	Enriched Environment
ECS	Extra-Cellular Space
GECI	Genetically encoded calcium indicators
GCaMP	GFP, Calmodulin, peptide sequence from myosin light chain
GFAP	Glial fibrillar acid
GFP	Green fluorescent protein
GFLD	Growth factor like domain
Gp	Guinea pig
HBD	Heparin binding domain
IMM	Inner Mitochondria Membrane
TIMM23	Inner Mitochondrial Membrane 23
KI	Knock In
KO	Knock Out
KPI	Kunitz Protase inhibitor
μ g	Microgram
μ l	Microliter
μ m	Micrometer
MitoGCaMP	Mitochondria targeted GCaMP
MCU	Mitochondrial Ca ²⁺ uniporter
Ms	Mouse
NOR	Novel Object Recognition Test
OMM	Outer Mitochondria Membrane
PM	Plasma membrane
Rb	Rabbit
ER	Reticulum Endoplasmaticum
sAPP α	Soluble APP alpha
TGN	Trans-Golgi Network
TOMM40	Translocase of the Outer Mitochondrial Membrane 40
VGLUT1	Vesicular glutamate transporter 1

10 REFERENCES

- Abbott NJ (2002) Astrocyte-endothelial interactions and blood-brain barrier permeability. *J Anat* 200:629–638 Available at: <http://www.ncbi.nlm.nih.gov/pubmed/12162730>.
- Agarwal A, Wu P-H, Hughes EG, Fukaya M, Tischfield MA, Langseth AJ, Wirtz D, Bergles DE (2017) Transient Opening of the Mitochondrial Permeability Transition Pore Induces Microdomain Calcium Transients in Astrocyte Processes. *Neuron* 93:1–19 Available at: <http://linkinghub.elsevier.com/retrieve/pii/S0896627316310078>.
- Agulhon C, Boyt KM, Xie AX, Friocourt F, Roth BL, Mccarthy KD (2013) Modulation of the autonomic nervous system and behaviour by acute glial cell Gq protein-coupled receptor activation in vivo. *J Physiol* 591:5599–5609 Available at: <http://www.ncbi.nlm.nih.gov/pubmed/24042499>.
- Agulhon C, Fiacco TA, McCarthy KD (2010) Hippocampal Short- and Long-Term Plasticity Are Not Modulated by Astrocyte Ca²⁺ Signaling. *Science* (80-) 327:1250–1254 Available at: <http://www.ncbi.nlm.nih.gov/pubmed/20203048>.
- Alvarez VA, Sabatini BL (2007) Anatomical and physiological plasticity of dendritic spines. *Annu Rev Neurosci* 30:79–97 Available at: <http://www.ncbi.nlm.nih.gov/pubmed/17280523>.
- Anandatheerthavarada HK, Biswas G, Robin MA, Avadhani NG (2003) Mitochondrial targeting and a novel transmembrane arrest of Alzheimer's amyloid precursor protein impairs mitochondrial function in neuronal cells. *J Cell Biol* 161:41–54 Available at: <http://www.ncbi.nlm.nih.gov/pubmed/12695498>.
- Ando K, Oishi M, Takeda S, Iijima K, Isohara T, Nairn AC, Kirino Y, Greengard P, Suzuki T (1999) Role of phosphorylation of Alzheimer's amyloid precursor protein during neuronal differentiation. *J Neurosci* 19:4421–4427 Available at: <http://www.ncbi.nlm.nih.gov/pubmed/10341243>.
- Andrew RJ, Kellett KAB, Thinakaran G, Hooper NM (2016) A Greek Tragedy: The Growing Complexity of Alzheimer Amyloid Precursor Protein Proteolysis. *J Biol Chem* 291:19235–19244 Available at: <http://www.jbc.org/lookup/doi/10.1074/jbc.R116.746032>.
- Araque A, Martín ED, Perea G, Arellano JI, Buño W (2002) Synaptically released acetylcholine evokes Ca²⁺ elevations in astrocytes in hippocampal slices. *J Neurosci*

References

- 22:2443–2450 Available at: <http://www.ncbi.nlm.nih.gov/pubmed/11923408> [Accessed May 15, 2017].
- Araque A, Parpura V, Sanzgiri RP, Haydon PG (1999) Tripartite synapses: glia, the unacknowledged partner. *Trends Neurosci* 22:208–215 Available at: <http://www.ncbi.nlm.nih.gov/pubmed/10322493> [Accessed May 15, 2017].
- Ban-Ishihara R, Ishihara T, Sasaki N, Mihara K, Ishihara N (2013) Dynamics of nucleoid structure regulated by mitochondrial fission contributes to cristae reformation and release of cytochrome c. *Proc Natl Acad Sci U S A* 110:11863–11868 Available at: <http://www.pubmedcentral.nih.gov/articlerender.fcgi?artid=3718159&tool=pmcentrez&rendertype=abstract>.
- Baranger K, Marchalant Y, Bonnet AE, Crouzin N, Carrete A, Paumier J-M, Py NA, Bernard A, Bauer C, Charrat E, Moschke K, Seiki M, Vignes M, Lichtenthaler SF, Checler F, Khrestchatsky M, Rivera S (2016) MT5-MMP is a new pro-amyloidogenic proteinase that promotes amyloid pathology and cognitive decline in a transgenic mouse model of Alzheimer's disease. *Cell Mol Life Sci* 73:217–236 Available at: <http://link.springer.com/10.1007/s00018-015-1992-1>.
- Basso E, Fante L, Fowlkes J, Petronilli V, Forte MA, Bernardi P (2005) Properties of the permeability transition pore in mitochondria devoid of cyclophilin D. *J Biol Chem* 280:18558–18561 Available at: <http://www.ncbi.nlm.nih.gov/pubmed/15792954>.
- Baumkötter F, Schmidt N, Vargas C, Schilling S, Weber R, Wagner K, Fiedler S, Klug W, Radzimanowski J, Nickolaus S, Keller S, Eggert S, Wild K, Kins S (2014) Amyloid Precursor Protein Dimerization and Synaptogenic Function Depend on Copper Binding to the Growth Factor-Like Domain. *J Neurosci* 34:11159–11172 Available at: <http://www.ncbi.nlm.nih.gov/pubmed/25122912>.
- Baumkötter F, Wagner K, Eggert S, Wild K, Kins S (2012) Structural aspects and physiological consequences of APP/APLP trans-dimerization. *Exp Brain Res* 217:389–395 Available at: <http://www.ncbi.nlm.nih.gov/pubmed/21952790>.
- Bazargani N, Attwell D (2016) Astrocyte calcium signaling: the third wave. *Nat Neurosci* 19:182–189 Available at: <http://www.ncbi.nlm.nih.gov/pubmed/26814587>.
- Beck A, Nieden R Zur, Schneider H-P, Deitmer JW (2004) Calcium release from intracellular stores in rodent astrocytes and neurons in situ. *Cell Calcium* 35:47–58 Available at: <http://www.ncbi.nlm.nih.gov/pubmed/14670371>.
- Berman RF, Hannigan JH, Sperry MA, Zajac CS (1996) Prenatal alcohol exposure and the effects of environmental enrichment on hippocampal dendritic spine density. *Alcohol*

References

- 13:209–216 Available at: <http://www.ncbi.nlm.nih.gov/pubmed/8814658>.
- Bezprozvanny I (2005) The inositol 1,4,5-trisphosphate receptors. *Cell Calcium* 38:261–272 Available at: <http://www.ncbi.nlm.nih.gov/pubmed/16102823>.
- Bianchi K, Rimessi A, Prandini A, Szabadkai G, Rizzuto R (2004) Calcium and mitochondria: Mechanisms and functions of a troubled relationship. *Biochim Biophys Acta - Mol Cell Res* 1742:119–131.
- Bindocci E, Savtchouk I, Liaudet N, Becker D, Carriero G, Volterra A (2017) Three-dimensional Ca²⁺-imaging advances understanding of astrocyte biology. *Science* (80-) 356:eaai8185 Available at: <http://www.sciencemag.org/lookup/doi/10.1126/science.aai8185%5Cnpapers3://publication/doi/10.1126/science.aai8185>.
- Bittner T, Fuhrmann M, Burgold S, Jung CKE, Volbracht C, Steiner H, Mitteregger G, Kretschmar HA, Haass C, Herms J (2009) -Secretase Inhibition Reduces Spine Density In Vivo via an Amyloid Precursor Protein-Dependent Pathway. *J Neurosci* 29:10405–10409 Available at: <http://www.ncbi.nlm.nih.gov/pubmed/19692615>.
- Blaabjerg M, Zimmer J (2007) The dentate mossy fibers: structural organization, development and plasticity. *Prog Brain Res* 163:85–803 Available at: <https://www.sciencedirect.com/science/article/pii/S0079612307630052?via%3Dihub> [Accessed May 26, 2018].
- Cai Q, Tammineni P (2016) Alterations in Mitochondrial Quality Control in Alzheimer's Disease. *Front Cell Neurosci* 10:1–17 Available at: <http://journal.frontiersin.org/Article/10.3389/fncel.2016.00024/abstract>.
- Calabrese B (2006) Development and Regulation of Dendritic Spine Synapses. *Physiology* 21:38–47 Available at: <http://www.ncbi.nlm.nih.gov/pubmed/16443821>.
- Camello C, Lomax R, Petersen OH, Tepikin A V. (2002) Calcium leak from intracellular store - The enigma of calcium signalling. *Cell Calcium* 32:355–361 Available at: <http://www.ncbi.nlm.nih.gov/pubmed/12543095>.
- Cao X, Südhof TC (2001) A transcriptionally active complex of APP with Fe65 and histone acetyltransferase Tip60. *Science* (80-) 293:115–120 Available at: <http://www.ncbi.nlm.nih.gov/pubmed/11441186>.
- Cao X, Südhof TC (2004) Dissection of amyloid- β precursor protein-dependent transcriptional transactivation. *J Biol Chem* 279:24601–24611 Available at: <http://www.ncbi.nlm.nih.gov/pubmed/15044485>.
- Cataldo AM, Broadwell RD (1986) Cytochemical identification of cerebral glycogen and

References

- glucose-6-phosphatase activity under normal and experimental conditions: I. Neurons and glia. *J Electron Microsc Tech* 3:413–437 Available at: <http://www.ncbi.nlm.nih.gov/pubmed/3018177>.
- Celis-Muñoz T, Silva-Grecchi T, A Godoy P, Panes-Fernández J, Barra K, Guzmán L, Fuentealba J (2016) Impact of mitochondrial dysfunction on neurodegenerative diseases: a key step on Alzheimer's disease. *J Syst Integr Neurosci* 2:166–173 Available at: <https://oatext.com/Impact-of-mitochondrial-dysfunction-on-neurodegenerative-diseases-a-key-step-on-Alzheimers-disease.php>.
- Chang DTW, Reynolds IJ (2006) Mitochondrial trafficking and morphology in healthy and injured neurons. *Prog Neurobiol* 80:241–268 Available at: <http://www.ncbi.nlm.nih.gov/pubmed/17188795>.
- Charles AC, Merrill JE, Dirksen ER, Sanderson MJ (1991) Intercellular signaling in glial cells: calcium waves and oscillations in response to mechanical stimulation and glutamate. *Neuron* 6:983–992 Available at: <http://www.ncbi.nlm.nih.gov/pubmed/1675864> [Accessed May 15, 2017].
- Chasseigneaux S, Allinquant B (2012) Functions of A β , sAPP α and sAPP β : Similarities and differences. *J Neurochem* 120:99–108 Available at: <http://www.ncbi.nlm.nih.gov/pubmed/22150401>.
- Chen TW, Wardill TJ, Sun Y, Pulver SR, Renninger SL, Baohan A, Schreiter ER, Kerr RA, Orger MB, Jayaraman V, Looger LL, Svoboda K, Kim DS (2013) Ultrasensitive fluorescent proteins for imaging neuronal activity. *Nature* 499:295–300 Available at: <http://www.ncbi.nlm.nih.gov/pubmed/23868258>.
- Coburger I, Hoefgen S, Than ME (2014) The structural biology of the amyloid precursor protein APP - A complex puzzle reveals its multi-domain architecture. *Biol Chem* 395:485–498 Available at: <http://www.ncbi.nlm.nih.gov/pubmed/24516000>.
- Collins TJ, Berridge MJ, Lipp P, Bootman MD (2002) Mitochondria are morphologically and functionally heterogeneous within cells. *EMBO J* 21:1616–1627.
- Copenhaver PF, Kögel D (2017) Role of APP Interactions with Heterotrimeric G Proteins: Physiological Functions and Pathological Consequences. *Front Mol Neurosci* 10:3 Available at: <http://journal.frontiersin.org/article/10.3389/fnmol.2017.00003/full>.
- Cornell-Bell AH, Finkbeiner SM, Cooper MS, Smith SJ (1990) Glutamate induces calcium waves in cultured astrocytes: long-range glial signaling. *Science* 247:470–473 Available at: <http://www.ncbi.nlm.nih.gov/pubmed/1967852> [Accessed May 15, 2017].

References

- Dahms SO, Hoefgen S, Roeser D, Schlott B, Guhrs K-H, Than ME (2010) Structure and biochemical analysis of the heparin-induced E1 dimer of the amyloid precursor protein. *Proc Natl Acad Sci* 107:5381–5386 Available at: <http://www.ncbi.nlm.nih.gov/pubmed/20212142>.
- Dahms SO, Könnig I, Roeser D, Gührs K-H, Mayer MC, Kaden D, Multhaup G, Than ME (2012) Metal Binding Dictates Conformation and Function of the Amyloid Precursor Protein (APP) E2 Domain. *J Mol Biol* 416:438–452.
- Dawkins E, Small DH (2014) Insights into the physiological function of the β -amyloid precursor protein: Beyond Alzheimer's disease. *J Neurochem* 129:756–769 Available at: <http://www.ncbi.nlm.nih.gov/pubmed/24517464>.
- Dawson G., Seabrook G., Zheng H, Smith D., Graham S, O'Dowd G, Bowery B., Boyce S, Trumbauer M., Chen H., Van der Ploeg LH., Sirinathsinghji DJ. (1999) Age-related cognitive deficits, impaired long-term potentiation and reduction in synaptic marker density in mice lacking the β -amyloid precursor protein. *Neuroscience* 90:1–13 Available at: <http://www.ncbi.nlm.nih.gov/pubmed/10188929>.
- de Brito OM, Scorrano L (2010) An intimate liaison: spatial organization of the endoplasmic reticulum-mitochondria relationship. *EMBO J* 29:2715–2723 Available at: <http://www.ncbi.nlm.nih.gov/pubmed/20717141> [Accessed January 24, 2018].
- De Strooper B, Annaert W (2000) Proteolytic processing and cell biological functions of the amyloid precursor protein. *J Cell Sci*:1857–1870 Available at: <http://www.ncbi.nlm.nih.gov/pubmed/10806097>.
- Del Prete D, Suski JM, Oulès B, Debayle D, Gay AS, Lacas-Gervais S, Bussiere R, Bauer C, Pinton P, Paterlini-Bréchet P, Wieckowski MR, Checler F, Chami M (2017) Localization and Processing of the Amyloid- β Protein Precursor in Mitochondria-Associated Membranes. *J Alzheimer's Dis* 55:1549–1570.
- DeLuca HF, Engstrom GW (1961) CALCIUM UPTAKE BY RAT KIDNEY MITOCHONDRIA. *Proc Natl Acad Sci* 47:1744–1750 Available at: <http://www.ncbi.nlm.nih.gov/pubmed/13885269> [Accessed January 24, 2018].
- Detmer S a, Chan DC (2007) Functions and dysfunctions of mitochondrial dynamics. *Nat Rev Mol Cell Biol* 8:870–879.
- Devi L, Prabhu BM, Galati DF, Avadhani NG, Anandatheerthavarada HK (2006) Accumulation of amyloid precursor protein in the mitochondrial import channels of human Alzheimer's disease brain is associated with mitochondrial dysfunction. *J Neurosci* 26:9057–9068 Available at: <http://www.ncbi.nlm.nih.gov/pubmed/16943564>.

References

- Deys C, Thinakaran G, Parent AT (2016) APP Receptor? To Be or Not To Be. *Trends Pharmacol Sci* 37:390–411 Available at:
<http://www.ncbi.nlm.nih.gov/pubmed/26837733>.
- Deys C, Vetrivel KS, Das S, Shepherd YM, Dupré DJ, Thinakaran G, Parent AT (2012) Novel GαS-protein signaling associated with membrane-tethered amyloid precursor protein intracellular domain. *J Neurosci* 32:1714–1729 Available at:
<http://www.ncbi.nlm.nih.gov/pubmed/22302812>.
- Dieckmann M, Dietrich MF, Herz J (2010) Lipoprotein receptors--an evolutionarily ancient multifunctional receptor family. *Biol Chem* 391:1341–1363 Available at:
<http://www.ncbi.nlm.nih.gov/pubmed/20868222> [Accessed June 23, 2017].
- Du H, Guo L, Yan S, Sosunov AA, McKhann GM, ShiDu Yan S (2010) Early deficits in synaptic mitochondria in an Alzheimer's disease mouse model. *Proc Natl Acad Sci* 107:18670–18675 Available at: <http://www.ncbi.nlm.nih.gov/pubmed/20937894>.
- Dulubova I, Ho A, Huryeva I, Südhof TC, Rizo J (2004) Three-Dimensional Structure of an Independently Folded Extracellular Domain of Human Amyloid-β Precursor Protein † , ‡. *Biochemistry* 43:9583–9588 Available at:
<http://www.ncbi.nlm.nih.gov/pubmed/15274612>.
- Dunn KW, Sutton TA (2008) Functional studies in living animals using multiphoton microscopy. *ILAR J* 49:66–77 Available at:
<http://www.ncbi.nlm.nih.gov/pubmed/18172334>.
- Ebrahimi S, Okabe S (2014) Structural dynamics of dendritic spines: Molecular composition, geometry and functional regulation. *Biochim Biophys Acta - Biomembr* 1838:2391–2398 Available at: <http://dx.doi.org/10.1016/j.bbamem.2014.06.002>.
- El-Brolosy MA, Stainier DYR (2017) Genetic compensation: A phenomenon in search of mechanisms. *PLoS Genet* 13:e1006780 Available at:
<http://www.ncbi.nlm.nih.gov/pubmed/28704371> [Accessed June 2, 2018].
- Emsley JG, Macklis JD (2006) Astroglial heterogeneity closely reflects the neuronal-defined anatomy of the adult murine CNS. *Neuron Glia Biol* 2:175 Available at:
<http://www.ncbi.nlm.nih.gov/pubmed/17356684>.
- Ermak G, Davies KJ. (2002) Calcium and oxidative stress: from cell signaling to cell death. *Mol Immunol* 38:713–721 Available at:
<https://www.sciencedirect.com/science/article/pii/S0161589001001080> [Accessed January 24, 2018].
- Ewald AJ, Werb Z, Egeblad M (2011) Monitoring of vital signs for long-term survival of

References

- mice under anesthesia. *Cold Spring Harb Protoc* 2011:pdb.prot5563 Available at: <http://www.cshprotocols.org/cgi/doi/10.1101/pdb.prot5563>.
- Feng G, Mellor RH, Bernstein M, Keller-Peck C, Nguyen QT, Wallace M, Nerbonne JM, Lichtman JW, Sanes JR (2000) Imaging Neuronal Subsets in Transgenic Mice Expressing Multiple Spectral Variants of GFP. *Neuron* 28:41–51 Available at: <http://www.ncbi.nlm.nih.gov/pubmed/11086982>.
- Filadi R, Greotti E, Turacchio G, Luini A, Pozzan T, Pizzo P (2017) On the role of Mitofusin 2 in endoplasmic reticulum–mitochondria tethering. *Proc Natl Acad Sci* 114:E2266–E2267 Available at: <http://www.ncbi.nlm.nih.gov/pubmed/28289206> [Accessed January 24, 2018].
- Filser S, Ovsepian S V., Masana M, Blazquez-Llorca L, Brandt Elvang A, Volbracht C, Müller MB, Jung CKE, Herms J (2015) Pharmacological Inhibition of BACE1 Impairs Synaptic Plasticity and Cognitive Functions. *Biol Psychiatry* 77:729–739 Available at: <http://www.ncbi.nlm.nih.gov/pubmed/25599931> [Accessed April 21, 2018].
- Foster M, Sherrington CS (1897) *Text book of physiology*, Volume 3. London: London Macmillan. Available at: <https://archive.org/details/b21271458>.
- Frey TG, Renken CW, Perkins GA (2002) Insight into mitochondrial structure and function from electron tomography. *Biochim Biophys Acta* 1555:196–203 Available at: <http://www.ncbi.nlm.nih.gov/pubmed/12206915> [Accessed July 24, 2017].
- Fuhrmann M, Mitteregger G, Kretschmar H, Herms J (2007) Dendritic Pathology in Prion Disease Starts at the Synaptic Spine. *J Neurosci* 27:6224–6233 Available at: <http://www.ncbi.nlm.nih.gov/pubmed/17553995>.
- Gaertner F et al. (2017) Migrating Platelets Are Mechano-scavengers that Collect and Bundle Bacteria. *Cell* 171:1368–1382.e23 Available at: <http://www.ncbi.nlm.nih.gov/pubmed/29195076>.
- Galione A (2011) NAADP receptors. *Cold Spring Harb Perspect Biol* 3:a004036 Available at: <http://www.ncbi.nlm.nih.gov/pubmed/21047915>.
- García-López P, García-Marín V, Freire M (2007) The discovery of dendritic spines by Cajal in 1888 and its relevance in the present neuroscience. *Prog Neurobiol* 83:110–130 Available at: <http://www.ncbi.nlm.nih.gov/pubmed/17681416>.
- Gee JM, Gibbons MB, Taheri M, Palumbos S, Morris SC, Smeal RM, Flynn KF, Economo MN, Cizek CG, Capecchi MR, Tvrdik P, Wilcox KS, White JA (2015) Imaging activity in astrocytes and neurons with genetically encoded calcium indicators following in utero

References

- electroporation. *Front Mol Neurosci* 8:10 Available at:
<http://www.ncbi.nlm.nih.gov/pubmed/25926768>.
- Gincel D, Zaid H, Shoshan-Barmatz V (2001) Calcium binding and translocation by the voltage-dependent anion channel: a possible regulatory mechanism in mitochondrial function. *Biochem J* 358:147–155 Available at:
<http://www.ncbi.nlm.nih.gov/pubmed/11485562> [Accessed July 24, 2017].
- Goldgaber D, Lerman MI, McBride OW, Saffiotti U, Gajdusek DC (1987) Characterization and chromosomal localization of a cDNA encoding brain amyloid of Alzheimer's disease. *Science* 235:877–880 Available at:
<http://www.ncbi.nlm.nih.gov/pubmed/3810169> [Accessed April 21, 2017].
- Golpich M, Amini E, Mohamed Z, Azman Ali R, Mohamed Ibrahim N, Ahmadiani A (2017) Mitochondrial Dysfunction and Biogenesis in Neurodegenerative diseases: Pathogenesis and Treatment. *CNS Neurosci Ther* 23:5–22 Available at:
<http://doi.wiley.com/10.1111/cns.12655>.
- Grienberger C, Konnerth A (2012) Imaging Calcium in Neurons. *Neuron* 73:862–885 Available at: <http://www.ncbi.nlm.nih.gov/pubmed/22405199>.
- Grosche J, Matyash V, Möller T, Verkhratsky A, Reichenbach A, Kettenmann H (1999) Microdomains for neuron-glia interaction: parallel fiber signaling to Bergmann glial cells. *Nat Neurosci* 2:139–143 Available at:
<http://www.ncbi.nlm.nih.gov/pubmed/10195197>.
- Gunter TE, Gunter KK (2002) Uptake of calcium by mitochondria: Transport and possible function. *IUBMB Life* 52:197–204 Available at:
<http://www.ncbi.nlm.nih.gov/pubmed/11798033>.
- Haass C, Hung a Y, Selkoe DJ (1991) Processing of beta-amyloid precursor protein in microglia and astrocytes favors an internal localization over constitutive secretion. *J Neurosci* 11:3783–3793.
- Haass C, Kaether C, Thinakaran G, Sisodia S (2012) Trafficking and Proteolytic Processing of APP. *Cold Spring Harb Perspect Med* 2:a006270–a006270 Available at:
<http://www.ncbi.nlm.nih.gov/pubmed/22553493>.
- Hailong Li, Xiaowan Wang Nannan Zhanga, Manoj K. Gottipatic, Vladimir Parpura and SD (2005) Imaging of mitochondrial Ca²⁺ dynamics in astrocytes using cell-specific mitochondria-targeted GCaMP5G/6s: Mitochondrial Ca²⁺ uptake and cytosolic Ca²⁺ availability via the endoplasmic reticulum store. *Biophys Chem* 257:2432–2437.
- Hamid R, Kilger E, Willem M, Vassallo N, Kostka M, Bornhövd C, Reichert AS,

References

- Kretschmar HA, Haass C, Herms J (2007) Amyloid precursor protein intracellular domain modulates cellular calcium homeostasis and ATP content. *J Neurochem* 102:1264–1275 Available at: <http://www.ncbi.nlm.nih.gov/pubmed/17763532>.
- Hamilton NB, Attwell D (2010) Do astrocytes really exocytose neurotransmitters? *Nat Rev Neurosci* 11:227–238 Available at: <http://dx.doi.org/10.1038/nrn2803>.
- Hamilton SL (2005) Ryanodine receptors. *Cell Calcium* 38:253–260 Available at: <http://www.ncbi.nlm.nih.gov/pubmed/16115682>.
- Hayashi T, Rizzuto R, Hajnoczky G, Su T-P (2009) MAM: more than just a housekeeper. *Trends Cell Biol* 19:81–88 Available at: <http://www.ncbi.nlm.nih.gov/pubmed/19144519> [Accessed January 24, 2018].
- Henneberger C, Papouin T, Olier SHR, Rusakov DA (2010) Long-term potentiation depends on release of D-serine from astrocytes. *Nature* 463:232–236 Available at: <http://www.ncbi.nlm.nih.gov/pubmed/20075918>.
- Hering H, Sheng M (2001) Dendritic spines: structure, dynamics and regulation. *Nat Rev Neurosci* 2:880–888 Available at: <http://www.ncbi.nlm.nih.gov/pubmed/11733795>.
- Herms J, Anliker B, Heber S, Ring S, Fuhrmann M, Kretschmar H, Sisodia S, Müller U (2004) Cortical dysplasia resembling human type 2 lissencephaly in mice lacking all three APP family members. *EMBO J* 23:4106–4115 Available at: <http://www.ncbi.nlm.nih.gov/pubmed/15385965>.
- Hick M, Herrmann U, Weyer SW, Mallm J-P, Tschäpe J-A, Borgers M, Mercken M, Roth FC, Draguhn A, Slomianka L, Wolfer DP, Korte M, Müller UC (2015) Acute function of secreted amyloid precursor protein fragment APPs α in synaptic plasticity. *Acta Neuropathol* 129:21–37 Available at: <http://www.ncbi.nlm.nih.gov/pubmed/25432317> [Accessed October 27, 2016].
- Hoe H-S, Lee H-K, Pak DTS (2012) The upside of APP at synapses. *CNS Neurosci Ther* 18:47–56 Available at: <http://www.ncbi.nlm.nih.gov/pubmed/21199446> [Accessed October 26, 2016].
- Hoe HS, Fu Z, Makarova A, Lee JY, Lu C, Feng L, Pajoohesh-Ganji A, Matsuoka Y, Hyman BT, Ehlers MD, Vicini S, Pak DTS, Rebeck GW (2009) The effects of amyloid precursor protein on postsynaptic composition and activity. *J Biol Chem* 284:8495–8506 Available at: <http://www.ncbi.nlm.nih.gov/pubmed/19164281>.
- Hoefgen S, Coburger I, Roeser D, Schaub Y, Dahms SO, Than ME (2014) Heparin induced dimerization of APP is primarily mediated by E1 and regulated by its acidic domain. *J Struct Biol* 187:30–37 Available at: <http://www.ncbi.nlm.nih.gov/pubmed/24859793>.

References

- Holtmaat A, Bonhoeffer T, Chow DK, Chuckowree J, De Paola V, Hofer SB, Hübener M, Keck T, Knott G, Lee W-CA, Mostany R, Mrcic-Flogel TD, Nedivi E, Portera-Cailliau C, Svoboda K, Trachtenberg JT, Wilbrecht L (2009) Long-term, high-resolution imaging in the mouse neocortex through a chronic cranial window. *Nat Protoc* 4:1128–1144 Available at: <http://www.ncbi.nlm.nih.gov/pubmed/19617885>.
- Jackson JG, Robinson MB (2015) Reciprocal Regulation of Mitochondrial Dynamics and Calcium Signaling in Astrocyte Processes. *J Neurosci* 35:15199–15213 Available at: <http://www.ncbi.nlm.nih.gov/pubmed/26558789>.
- Jacobson J, Duchen MR (2002) Mitochondrial oxidative stress and cell death in astrocytes-- requirement for stored Ca²⁺ and sustained opening of the permeability transition pore. *J Cell Sci* 115:1175–1188 Available at: <http://www.ncbi.nlm.nih.gov/pubmed/11884517> [Accessed January 24, 2018].
- Johansson BB, Belichenko P V. (2002) Neuronal Plasticity and Dendritic Spines: Effect of Environmental Enrichment on Intact and Postischemic Rat Brain. *J Cereb Blood Flow Metab* 22:89–96 Available at: <http://www.ncbi.nlm.nih.gov/pubmed/11807398> [Accessed September 1, 2017].
- Jouaville LS, Pinton P, Bastianutto C, Rutter GA, Rizzuto R (1999) Regulation of mitochondrial ATP synthesis by calcium: evidence for a long-term metabolic priming. *Proc Natl Acad Sci U S A* 96:13807–13812 Available at: <http://www.ncbi.nlm.nih.gov/pubmed/10570154>.
- Jung CKE, Herms J (2012) Role of APP for dendritic spine formation and stability. *Exp Brain Res* 217:463–470 Available at: <http://www.ncbi.nlm.nih.gov/pubmed/22094714>.
- Jung CKEE, Herms J (2014) Structural Dynamics of Dendritic Spines are Influenced by an Environmental Enrichment: An In Vivo Imaging Study. *Cereb Cortex* 24:377–384 Available at: <http://www.ncbi.nlm.nih.gov/pubmed/23081882> [Accessed October 27, 2016].
- Kaibara T, Leung LS (1993) Basal versus apical dendritic long-term potentiation of commissural afferents to hippocampal CA1: a current-source density study. *J Neurosci* 13:2391–2404 Available at: <http://www.ncbi.nlm.nih.gov/pubmed/8501513> [Accessed January 4, 2018].
- Kanemaru K, Sekiya H, Xu M, Satoh K, Kitajima N, Yoshida K, Okubo Y, Sasaki T, Moritoh S, Hasuwa H, Mimura M, Horikawa K, Matsui K, Nagai T, Iino M, Tanaka KF (2014) In Vivo Visualization of Subtle, Transient, and Local Activity of Astrocytes Using an Ultrasensitive Ca²⁺ Indicator. *CellReports* 8:311–318 Available at:

References

- <http://dx.doi.org/10.1016/j.celrep.2014.05.056> [Accessed December 5, 2017].
- Kang J, Lemaire H-G, Unterbeck A, Salbaum JM, Masters CL, Grzeschik K-H, Multhaup G, Beyreuther K, Müller-Hill B (1987) The precursor of Alzheimer's disease amyloid A4 protein resembles a cell-surface receptor. *Nature* 325:733–736 Available at: <http://www.ncbi.nlm.nih.gov/pubmed/2881207> [Accessed April 21, 2017].
- Keil C, Huber R, Bode W, Than ME (2004) Cloning, expression, crystallization and initial crystallographic analysis of the C-terminal domain of the amyloid precursor protein APP. *Acta Crystallogr D Biol Crystallogr* 60:1614–1617 Available at: <http://www.ncbi.nlm.nih.gov/pubmed/15333934> [Accessed October 26, 2016].
- Kettenmann H, Ransom BR (2005) Neuroglia.
- Kettenmann H, Verkhratsky A (2013) Glial Cells. In: *Neuroscience in the 21st Century*, pp 475–506. New York, NY: Springer New York. Available at: http://link.springer.com/10.1007/978-1-4614-1997-6_19 [Accessed October 6, 2017].
- Kimelberg HK, Nedergaard M (2010) Functions of Astrocytes and their Potential As Therapeutic Targets. *Neurotherapeutics* 7:338–353.
- Kirichok Y, Krapivinsky G, Clapham DE (2004) The mitochondrial calcium uniporter is a highly selective ion channel. *Nature* 427:360–364 Available at: <http://www.nature.com/doi/10.1038/nature02246>.
- Klevanski M, Herrmann U, Weyer SW, Fol R, Cartier N, Wolfer DP, Caldwell JH, Korte M, Müller UC (2015) The APP Intracellular Domain Is Required for Normal Synaptic Morphology, Synaptic Plasticity, and Hippocampus-Dependent Behavior. *J Neurosci* 35:16018–16033 Available at: <http://www.jneurosci.org/cgi/doi/10.1523/JNEUROSCI.2009-15.2015> [Accessed January 27, 2017].
- Knott G, Holtmaat A (2008) Dendritic spine plasticity—Current understanding from in vivo studies. *Brain Res Rev* 58:282–289 Available at: <http://www.ncbi.nlm.nih.gov/pubmed/18353441> [Accessed November 1, 2017].
- Kofuji P, Newman EA (2004) Potassium buffering in the central nervous system. *Neuroscience* 129:1045–1056 Available at: <http://www.ncbi.nlm.nih.gov/pubmed/15561419> [Accessed July 25, 2017].
- Kozorovitskiy Y, Gross CG, Kopil C, Battaglia L, McBreen M, Stranahan AM, Gould E (2005) Experience induces structural and biochemical changes in the adult primate brain. *Proc Natl Acad Sci* 102:17478–17482 Available at: <http://www.pnas.org/cgi/doi/10.1073/pnas.0508817102> [Accessed October 25, 2016].

References

- Kroenke CD, Ziemnicka-Kotula D, Xu J, Kotula L, Palmer AG (1997) Solution conformations of a peptide containing the cytoplasmic domain sequence of the beta amyloid precursor protein. *Biochemistry* 36:8145–8152 Available at: <http://www.ncbi.nlm.nih.gov/pubmed/9201963> [Accessed October 26, 2016].
- Kuffler SW, Nicholls JG (1966) The physiology of neuroglial cells. *Ergeb Physiol* 57:1–90 Available at: <http://www.ncbi.nlm.nih.gov/pubmed/5330861> [Accessed July 25, 2017].
- Kukkonen JP, Lund P-E, Åkerman KEO (2001) 2-aminoethoxydiphenyl borate reveals heterogeneity in receptor-activated Ca²⁺ discharge and store-operated Ca²⁺ influx. *Cell Calcium* 30:117–129 Available at: <http://www.ncbi.nlm.nih.gov/pubmed/11440469> [Accessed July 28, 2017].
- Lai K-O, Ip NY (2013) Structural plasticity of dendritic spines: the underlying mechanisms and its dysregulation in brain disorders. *Biochim Biophys Acta* 1832:2257–2263 Available at: <http://www.ncbi.nlm.nih.gov/pubmed/24012719> [Accessed October 27, 2016].
- Lai K-O, Jordan BA, Ma X-M, Srivastava DP, Tolias KF (2016) Molecular Mechanisms of Dendritic Spine Development and Plasticity. *Neural Plast* 2016:2078121 Available at: <http://www.ncbi.nlm.nih.gov/pubmed/27127656> [Accessed September 1, 2017].
- Lamb BT, Sisodia SS, Lawler AM, Slunt HH, Kitt CA, Kearns WG, Pearson PL, Price DL, Gearhart JD (1993) Introduction and expression of the 400 kilobase precursor amyloid protein gene in transgenic mice. *Nat Genet* 5:22–30 Available at: <http://www.ncbi.nlm.nih.gov/pubmed/8220418> [Accessed April 25, 2017].
- Lang BF, Burger G, O’Kelly CJ, Cedergren R, Golding GB, Lemieux C, Sankoff D, Turmel M, Gray MW (1997) An ancestral mitochondrial DNA resembling a eubacterial genome in miniature. *Nature* 387:493–497 Available at: <http://www.ncbi.nlm.nih.gov/pubmed/9168110> [Accessed May 11, 2017].
- Laßek M, Weingarten J, Einsfelder U, Brendel P, Müller U, Volkandt W (2013) Amyloid precursor proteins are constituents of the presynaptic active zone. *J Neurochem* 127:n/a-n/a Available at: <http://www.ncbi.nlm.nih.gov/pubmed/23815291> [Accessed April 21, 2017].
- LeBlanc AC, Papadopoulos M, Bélair C, Chu W, Crosato M, Powell J, Goodyer CG (1997) Processing of amyloid precursor protein in human primary neuron and astrocyte cultures. *J Neurochem* 68:1183–1190 Available at: <http://www.ncbi.nlm.nih.gov/pubmed/9048765> [Accessed October 5, 2017].
- Lee KJ, Moussa CEH, Lee Y, Sung Y, Howell BW, Turner RS, Pak DTS, Hoe HS (2010)

References

- Beta amyloid-independent role of amyloid precursor protein in generation and maintenance of dendritic spines. *Neuroscience* 169:344–356 Available at: <http://www.ncbi.nlm.nih.gov/pubmed/20451588> [Accessed February 9, 2017].
- Leger M, Quiedeville A, Bouet V, Haelewyn B, Boulouard M, Schumann-Bard P, Freret T (2013) Object recognition test in mice. *Nat Protoc* 8:2531–2537 Available at: <http://www.nature.com/doi/10.1038/nprot.2013.155> [Accessed November 3, 2017].
- Leonard AP, Cameron RB, Speiser JL, Wolf BJ, Peterson YK, Schnellmann RG, Beeson CC, Rohrer B (2015) Quantitative analysis of mitochondrial morphology and membrane potential in living cells using high-content imaging, machine learning, and morphological binning. *Biochim Biophys Acta - Mol Cell Res* 1853:348–360 Available at: <http://www.ncbi.nlm.nih.gov/pubmed/25447550> [Accessed September 27, 2017].
- Linde CI, Baryshnikov SG, Mazzocco-Spezia A, Golovina VA (2011) Dysregulation of Ca²⁺ signaling in astrocytes from mice lacking amyloid precursor protein. *AJP Cell Physiol* 300:C1502–C1512.
- Lorent K, Overbergh L, Moechars D, De Strooper B, Van Leuven F, Van den Berghe H (1995) Expression in mouse embryos and in adult mouse brain of three members of the amyloid precursor protein family, of the alpha-2-macroglobulin receptor/low density lipoprotein receptor-related protein and of its ligands apolipoprotein E, lipoprotein lipase, alpha-2-macroglobulin and the 40,000 molecular weight receptor-associated protein. *Neuroscience* 65:1009–1025 Available at: <http://www.ncbi.nlm.nih.gov/pubmed/7542371> [Accessed April 21, 2017].
- Magistretti PJ, Ransom BR (2002) Astrocytes. *Neuropsychopharmacol Fifth Gener Prog*:133–145.
- Magistretti J. P, Ransom R. B (n.d.) Astrocytes-magistretti | Astrocyte | Synaptic Plasticity. Available at: <https://www.scribd.com/document/151499356/Astrocytes-magistretti> [Accessed July 25, 2017].
- Mallm JP, Tschäpe JA, Hick M, Filippov MA, Müller UC (2010) Generation of conditional null alleles for APP and APLP2. *Genesis* 48:200–206.
- Mancuso JJ, Chen Y, Li X, Xue Z, Wong STC (2013) Methods of dendritic spine detection: From Golgi to high-resolution optical imaging. *Neuroscience* 251:129–140 Available at: <http://www.ncbi.nlm.nih.gov/pubmed/22522468> [Accessed October 3, 2017].
- Martineau M, Parpura V, Mothet JP (2014) Cell-type specific mechanisms of D-serine uptake and release in the brain. *Front Synaptic Neurosci* 6:1–9.

References

- Mathiisen TM, Lehre KP, Danbolt NC, Ottersen OP (2010) The perivascular astroglial sheath provides a complete covering of the brain microvessels: An electron microscopic 3D reconstruction. *Glia* 58:1094–1103 Available at: <http://www.ncbi.nlm.nih.gov/pubmed/20468051> [Accessed December 4, 2017].
- McCarron JG, Wilson C, Sandison ME, Olson ML, Girkin JM, Saunter C, Chalmers S (2013) From structure to function: mitochondrial morphology, motion and shaping in vascular smooth muscle. *J Vasc Res* 50:357–371 Available at: <http://www.ncbi.nlm.nih.gov/pubmed/23887139> [Accessed July 23, 2017].
- McLoughlin DM, Miller CCJ (2008) The FE65 proteins and Alzheimer's disease. *J Neurosci Res* 86:744–754 Available at: <http://www.ncbi.nlm.nih.gov/pubmed/17828772> [Accessed October 26, 2016].
- Montagna E, Dorostkar MM, Herms J (2017) The Role of APP in Structural Spine Plasticity. *Front Mol Neurosci* 10:136 Available at: <http://journal.frontiersin.org/article/10.3389/fnmol.2017.00136/full> [Accessed June 28, 2017].
- Mora F, Segovia G, del Arco A (2007) Aging, plasticity and environmental enrichment: structural changes and neurotransmitter dynamics in several areas of the brain. *Brain Res Rev* 55:78–88 Available at: <http://www.ncbi.nlm.nih.gov/pubmed/17561265> [Accessed October 27, 2016].
- Morales-Corraliza J, Mazzella MJ, Berger JD, Diaz NS, Choi JHK, Levy E, Matsuoka Y, Planel E, Mathews PM (2009) In Vivo Turnover of Tau and APP Metabolites in the Brains of Wild-Type and Tg2576 Mice: Greater Stability of sAPP in the β -Amyloid Depositing Mice Bush AI, ed. *PLoS One* 4:e7134 Available at: <http://dx.plos.org/10.1371/journal.pone.0007134> [Accessed April 21, 2017].
- Moser MB, Trommald M, Andersen P (1994) An increase in dendritic spine density on hippocampal CA1 pyramidal cells following spatial learning in adult rats suggests the formation of new synapses. *Proc Natl Acad Sci U S A* 91:12673–12675 Available at: <http://www.ncbi.nlm.nih.gov/pubmed/7809099> [Accessed October 3, 2017].
- Moya KL, Benowitz LI, Schneider GE, Allinquant B (1994) The amyloid precursor protein is developmentally regulated and correlated with synaptogenesis. *Dev Biol* 161:597–603 Available at: <http://www.ncbi.nlm.nih.gov/pubmed/8314003> [Accessed October 26, 2016].
- Müller T, Meyer HE, Egensperger R, Marcus K (2008a) The amyloid precursor protein intracellular domain (AICD) as modulator of gene expression, apoptosis, and

References

- cytoskeletal dynamics-relevance for Alzheimer's disease. *Prog Neurobiol* 85:393–406 Available at: <http://www.ncbi.nlm.nih.gov/pubmed/18603345> [Accessed October 26, 2016].
- Müller T, Meyer HE, Egensperger R, Marcus K (2008b) The amyloid precursor protein intracellular domain (AICD) as modulator of gene expression, apoptosis, and cytoskeletal dynamics-relevance for Alzheimer's disease. *Prog Neurobiol* 85:393–406 Available at: <http://www.ncbi.nlm.nih.gov/pubmed/18603345> [Accessed October 27, 2016].
- Müller UC, Deller T, Korte M (2017) Not just amyloid: physiological functions of the amyloid precursor protein family. *Nat Rev Neurosci* 18:281–298 Available at: <http://www.nature.com/doi/10.1038/nrn.2017.29>.
- Müller UC, Zheng H (2012) Physiological functions of APP family proteins. *Cold Spring Harb Perspect Med* 2:a006288 Available at: <http://www.ncbi.nlm.nih.gov/pubmed/22355794> [Accessed October 26, 2016].
- Munno DW, Syed NI (2003) Synaptogenesis in the CNS: An odyssey from wiring together to firing together. *J Physiol* 552:1–11 Available at: <http://www.ncbi.nlm.nih.gov/pubmed/12897180> [Accessed January 24, 2018].
- Nakai J, Ohkura M, Imoto K (2001) A high signal-to-noise Ca(2+) probe composed of a single green fluorescent protein. *Nat Biotechnol* 19:137–141 Available at: <http://www.ncbi.nlm.nih.gov/pubmed/11175727> [Accessed June 4, 2017].
- Newey SE, Velamoor V, Govek E-E, Van Aelst L (2005) Rho GTPases, dendritic structure, and mental retardation. *J Neurobiol* 64:58–74 Available at: <http://www.ncbi.nlm.nih.gov/pubmed/15884002> [Accessed September 1, 2017].
- Nhan HS, Chiang K, Koo EH (2015) The multifaceted nature of amyloid precursor protein and its proteolytic fragments: friends and foes. *Acta Neuropathol* 129:1–19 Available at: <http://www.ncbi.nlm.nih.gov/pubmed/25287911> [Accessed October 27, 2016].
- Ninomiya H, Roch JM, Sundsmo MP, Otero DA, Saitoh T (1993) Amino acid sequence RERMS represents the active domain of amyloid beta/A4 protein precursor that promotes fibroblast growth. *J Cell Biol* 121:879–886 Available at: <http://www.ncbi.nlm.nih.gov/pubmed/8491779> [Accessed April 27, 2017].
- Nithianantharajah J, Hannan AJ (2006) Enriched environments, experience-dependent plasticity and disorders of the nervous system. *Nat Rev Neurosci* 7:697–709 Available at: <http://www.nature.com/doi/10.1038/nrn1970> [Accessed October 27, 2016].
- O'Brien RJ, Wong PC (2011) Amyloid precursor protein processing and Alzheimer's

References

- disease. *Annu Rev Neurosci* 34:185–204 Available at:
<http://www.ncbi.nlm.nih.gov/pubmed/21456963> [Accessed October 5, 2017].
- Oberheim NA, Takano T, Han X, He W, Lin JHC, Wang F, Xu Q, Wyatt JD, Pilcher W, Ojemann JG, Ransom BR, Goldman SA, Nedergaard M (2009) Uniquely hominid features of adult human astrocytes. *J Neurosci* 29:3276–3287 Available at:
<http://www.ncbi.nlm.nih.gov/pubmed/19279265> [Accessed July 25, 2017].
- Oberheim NA, Wang X, Goldman S, Nedergaard M (2006) Astrocytic complexity distinguishes the human brain. Available at:
<https://www.urmc.rochester.edu/MediaLibraries/URMCMedia/labs/nedergaard-lab/documents/Astrocytic-Complexity.pdf> [Accessed July 25, 2017].
- Ochs SM, Dorostkar MM, Aramuni G, Schön C, Filser S, Pöschl J, Kremer A, Van Leuven F, Ovsepian S V., Herms J (2015) Loss of neuronal GSK3 β reduces dendritic spine stability and attenuates excitatory synaptic transmission via β -catenin. *Mol Psychiatry* 20:482–489.
- Okamoto T et al. (1990) A simple structure encodes G protein-activating function of the IGF-II/mannose 6-phosphate receptor. *Cell* 62:709–717 Available at:
<http://www.ncbi.nlm.nih.gov/pubmed/2167177> [Accessed October 27, 2016].
- Pagani L, Eckert A (2011) Amyloid-Beta interaction with mitochondria. *Int J Alzheimers Dis* 2011:925050 Available at:
<http://www.pubmedcentral.nih.gov/articlerender.fcgi?artid=3065051&tool=pmcentrez&rendertype=abstract>.
- Papa M, Bundman MC, Greenberger V, Segal M (1995) Morphological analysis of dendritic spine development in primary cultures of hippocampal neurons. *J Neurosci* 15:1–11 Available at: <http://www.ncbi.nlm.nih.gov/pubmed/7823120> [Accessed October 3, 2017].
- Pardossi-Piquard R, Checler F (2012) The physiology of the β -amyloid precursor protein intracellular domain AICD. *J Neurochem*:109–124 Available at:
<http://www.ncbi.nlm.nih.gov/pubmed/22122663> [Accessed October 27, 2016].
- Parri HR, Gould TM, Crunelli V (2001) Spontaneous astrocytic Ca²⁺ oscillations in situ drive NMDAR-mediated neuronal excitation. *Nat Neurosci* 4:803–812 Available at:
<http://www.ncbi.nlm.nih.gov/pubmed/11477426> [Accessed May 15, 2017].
- Parsons MJ, Green DR (2010) Mitochondria in cell death. *Essays Biochem* 47:99–114 Available at: <http://www.ncbi.nlm.nih.gov/pubmed/20533903> [Accessed January 8, 2018].

References

- Pasti L, Volterra A, Pozzan T, Carmignoto G (1997) Intracellular calcium oscillations in astrocytes: a highly plastic, bidirectional form of communication between neurons and astrocytes in situ. *J Neurosci* 17:7817–7830 Available at: <http://www.ncbi.nlm.nih.gov/pubmed/9315902> [Accessed December 11, 2017].
- Patterson RL, Boehning D, Snyder SH (2004) Inositol 1,4,5-Trisphosphate Receptors as Signal Integrators. *Annu Rev Biochem* 73:437–465 Available at: <http://www.ncbi.nlm.nih.gov/pubmed/14726673> [Accessed September 15, 2017].
- Pavlov PF, Wiehager B, Sakai J, Frykman S, Behbahani H, Winblad B, Ankarcrona M (2011) Mitochondrial γ -secretase participates in the metabolism of mitochondria-associated amyloid precursor protein. *FASEB J* 25:78–88 Available at: <http://www.ncbi.nlm.nih.gov/pubmed/20833873> [Accessed May 11, 2017].
- Pera M, Larrea D, Guardia-Laguarta C, Montesinos J, Velasco KR, Agrawal RR, Xu Y, Chan RB, Paolo G Di, Mehler MF, Perumal GS, Macaluso FP, Freyberg ZZ, Acin-Perez R, Enriquez JA, Schon EA, Area-Gomez E (2017) Increased localization of APP–C99 in mitochondria–associated ER membranes causes mitochondrial dysfunction in Alzheimer disease. *EMBO J* 36:3356–3371.
- Perea G, Araque A (2005) Glial calcium signaling and neuron–glia communication. *Cell Calcium* 38:375–382 Available at: <http://www.ncbi.nlm.nih.gov/pubmed/16105683> [Accessed May 15, 2017].
- Perea G, Navarrete M, Araque A (2009) Tripartite synapses: astrocytes process and control synaptic information. *Trends Neurosci* 32:421–431.
- Perez-Alvarez A, Navarrete M, Covelo A, Martin ED, Araque A (2014) Structural and functional plasticity of astrocyte processes and dendritic spine interactions. *J Neurosci* 34:12738–12744 Available at: <http://www.ncbi.nlm.nih.gov/pubmed/25232111> [Accessed October 27, 2016].
- Perez-Costas E, Melendez-Ferro M, Roberts RC (n.d.) Microscopy techniques and the study of synapses. Available at: <http://www.formatex.org/microscopy3/pdf/pp164-170.pdf> [Accessed October 3, 2017].
- Perez RG, Soriano S, Hayes JD, Ostaszewski B, Xia W, Selkoe DJ, Chen X, Stokin GB, Koo EH (1999) Mutagenesis identifies new signals for beta-amyloid precursor protein endocytosis, turnover, and the generation of secreted fragments, including Abeta42. *J Biol Chem* 274:18851–18856 Available at: <http://www.ncbi.nlm.nih.gov/pubmed/10383380> [Accessed October 25, 2017].

References

- Pérez Koldenkova V, Nagai T (2013) Genetically encoded Ca²⁺ indicators: Properties and evaluation. *Biochim Biophys Acta - Mol Cell Res* 1833:1787–1797 Available at: <http://dx.doi.org/10.1016/j.bbamcr.2013.01.011>.
- Peters A, Kaiserman-Abramof IR (1970) The small pyramidal neuron of the rat cerebral cortex. The perikaryon, dendrites and spines. *Am J Anat* 127:321–355 Available at: <http://www.ncbi.nlm.nih.gov/pubmed/4985058> [Accessed August 17, 2017].
- Petravicz J, Fiacco TA, McCarthy KD (2008) Loss of IP3 Receptor-Dependent Ca²⁺ Increases in Hippocampal Astrocytes Does Not Affect Baseline CA1 Pyramidal Neuron Synaptic Activity. *J Neurosci* 28:4967–4973 Available at: <http://www.ncbi.nlm.nih.gov/pubmed/18463250> [Accessed January 6, 2018].
- Picard M, Shirihai OS, Gentil BJ, Buelle Y (2013) Mitochondrial morphology transitions and functions: implications for retrograde signaling? *Am J Physiol Regul Integr Comp Physiol* 304:R393-406 Available at: <http://www.ncbi.nlm.nih.gov/pubmed/23364527> [Accessed July 23, 2017].
- Porter JT, McCarthy KD (1997) Astrocytic neurotransmitter receptors in situ and in vivo. *Prog Neurobiol* 51:439–455.
- Qiu WQ, Ferreira A, Miller C, Koo EH, Selkoe DJ (1995) Cell-surface beta-amyloid precursor protein stimulates neurite outgrowth of hippocampal neurons in an isoform-dependent manner. *J Neurosci* 15:2157–2167 Available at: <http://www.ncbi.nlm.nih.gov/pubmed/7891158> [Accessed October 26, 2016].
- Radzimanowski J, Simon B, Sattler M, Beyreuther K, Sinning I, Wild K (2008) Structure of the intracellular domain of the amyloid precursor protein in complex with Fe65-PTB2. *EMBO Rep* 9:1134–1140 Available at: <http://www.ncbi.nlm.nih.gov/pubmed/18833287> [Accessed October 26, 2016].
- Raffaello A, Mammucari C, Gherardi G, Rizzuto R (2016) Calcium at the Center of Cell Signaling: Interplay between Endoplasmic Reticulum, Mitochondria, and Lysosomes. *Trends Biochem Sci* 41:1035–1049 Available at: <http://www.ncbi.nlm.nih.gov/pubmed/27692849> [Accessed December 4, 2017].
- Ransom BR, Sontheimer H (1992) The neurophysiology of glial cells. *J Clin Neurophysiol* 9:224–251 Available at: <http://www.ncbi.nlm.nih.gov/pubmed/1375603> [Accessed July 25, 2017].
- Ransom CB, Ransom BR, Sontheimer H (2000) Activity-dependent extracellular K⁺ accumulation in rat optic nerve: the role of glial and axonal Na⁺ pumps. *J Physiol* 522 Pt 3:427–442 Available at: <http://www.ncbi.nlm.nih.gov/pubmed/10713967> [Accessed July

References

- 25, 2017].
- Reinhard C, Hébert SS, De Strooper B (2005) The amyloid-beta precursor protein: integrating structure with biological function. *EMBO J* 24:3996–4006 Available at: <http://www.ncbi.nlm.nih.gov/pubmed/16252002> [Accessed October 26, 2016].
- Retzius G (1894) *Die Neuroglia des Gehirns beim Menschen und bei Säugethieren* - Gustaf Retzius - Google Libri (Gustav Fischer, ed). Available at: https://books.google.de/books/about/Die_Neuroglia_des_Gehirns_beim_Menschen.html?id=JIKnMwAACAAJ&redir_esc=y [Accessed October 6, 2017].
- Reyes RC, Parpura V (2008) Mitochondria modulate Ca²⁺-dependent glutamate release from rat cortical astrocytes. *J Neurosci* 28:9682–9691 Available at: <http://www.ncbi.nlm.nih.gov/pubmed/18815254> [Accessed July 28, 2017].
- Reyes RC, Verkhratsky A, Parpura V (2012) Plasmalemmal Na⁺/Ca²⁺ exchanger modulates Ca²⁺-dependent exocytotic release of glutamate from rat cortical astrocytes. *ASN Neuro* 4 Available at: <http://www.ncbi.nlm.nih.gov/pubmed/22268447> [Accessed July 28, 2017].
- Ring S, Weyer SW, Kilian SB, Waldron E, Pietrzik CU, Filippov MA, Herms J, Buchholz C, Eckman CB, Korte M, Wolfer DP, Müller UC (2007) The secreted beta-amyloid precursor protein ectodomain APPs alpha is sufficient to rescue the anatomical, behavioral, and electrophysiological abnormalities of APP-deficient mice. *J Neurosci* 27:7817–7826 Available at: <http://www.ncbi.nlm.nih.gov/pubmed/17634375> [Accessed October 26, 2016].
- Rizzuto R, Brini M, Pinton P, King MP, Davidson M, Schon EA (1999) A calcium signaling defect in the pathogenesis of a mitochondrial DNA inherited oxidative phosphorylation deficiency. *Nat Med* 5:951–954 Available at: <http://www.nature.com/doi/10.1038/11396> [Accessed July 24, 2017].
- Rizzuto R, De Stefani D, Raffaello A, Mammucari C (2012) Mitochondria as sensors and regulators of calcium signalling. *Nat Rev Mol Cell Biol* 13:566–578 Available at: <http://dx.doi.org/10.1038/nrm3412>.
- Rizzuto R, Duchen MR, Pozzan T (2004) Flirting in little space: the ER/mitochondria Ca²⁺ liaison. *Sci STKE* 2004:re1 Available at: <http://www.ncbi.nlm.nih.gov/pubmed/14722345>.
- Roch JM, Jin LW, Ninomiya H, Schubert D, Saitoh T (1993) Biologically active domain of the secreted form of the amyloid beta/A4 protein precursor. *Ann N Y Acad Sci* 695:149–157 Available at: <http://www.ncbi.nlm.nih.gov/pubmed/8239274> [Accessed

References

- April 27, 2017].
- Rohan de Silva H a, Jen A, Wickenden C, Jen LS, Wilkinson SL, Patel AJ (1997) Cell-specific expression of beta-amyloid precursor protein isoform mRNAs and proteins in neurons and astrocytes. *Brain Res Mol Brain Res* 47:147–156 Available at: <http://www.ncbi.nlm.nih.gov/pubmed/9221912>.
- Russell JT (2011) Imaging calcium signals in vivo: a powerful tool in physiology and pharmacology. *Br J Pharmacol* 163:1605–1625 Available at: <http://www.ncbi.nlm.nih.gov/pubmed/20718728> [Accessed October 23, 2017].
- Sale A, Berardi N, Maffei L (2014) Environment and brain plasticity: towards an endogenous pharmacotherapy. *Physiol Rev* 94:189–234 Available at: <http://www.ncbi.nlm.nih.gov/pubmed/24382886> [Accessed October 27, 2016].
- Schettini G, Govoni S, Racchi M, Rodriguez G (2010) Phosphorylation of APP-CTF-AICD domains and interaction with adaptor proteins: signal transduction and/or transcriptional role--relevance for Alzheimer pathology. *J Neurochem* 115:1299–1308 Available at: <http://www.ncbi.nlm.nih.gov/pubmed/21039524> [Accessed October 27, 2016].
- Schindelin J, Arganda-Carreras I, Frise E, Kaynig V, Longair M, Pietzsch T, Preibisch S, Rueden C, Saalfeld S, Schmid B, Tinevez J-Y, White DJ, Hartenstein V, Eliceiri K, Tomancak P, Cardona A (2012) Fiji: an open-source platform for biological-image analysis. *Nat Methods* 9:676–682 Available at: <http://www.nature.com/doi/10.1038/nmeth.2019> [Accessed September 22, 2017].
- Schindelin J, Rueden CT, Hiner MC, Eliceiri KW (2015) The ImageJ ecosystem: An open platform for biomedical image analysis. *Mol Reprod Dev* 82:518–529 Available at: <http://doi.wiley.com/10.1002/mrd.22489> [Accessed July 3, 2017].
- Seabrook GR, Smith DW, Bowery BJ, Easter A, Reynolds T, Fitzjohn SM, Morton RA, Zheng H, Dawson GR, Sirinathsinghji DJ, Davies CH, Collingridge GL, Hill RG (1999) Mechanisms contributing to the deficits in hippocampal synaptic plasticity in mice lacking amyloid precursor protein. *Neuropharmacology* 38:349–359 Available at: <http://www.ncbi.nlm.nih.gov/pubmed/10219973> [Accessed October 30, 2017].
- Shariati SAM, De Strooper B (2013) Redundancy and divergence in the amyloid precursor protein family. *FEBS Lett* 587:2036–2045 Available at: <http://doi.wiley.com/10.1016/j.febslet.2013.05.026> [Accessed June 23, 2017].
- Sheng B, Niu Y, Zhou H, Yan J, Zhao N, Zhang X, Gong Y (2009) The mitochondrial function was impaired in APP knockout mouse embryo fibroblast cells. *Chinese Sci Bull* 54:1725–1731.

References

- Shigetomi E, Bushong EA, Haustein MD, Tong X, Jackson-Weaver O, Kracun S, Xu J, Sofroniew M V., Ellisman MH, Khakh BS (2013) Imaging calcium microdomains within entire astrocyte territories and endfeet with GCaMPs expressed using adeno-associated viruses. *J Gen Physiol* 141:633–647 Available at: <http://www.ncbi.nlm.nih.gov/pubmed/23589582> [Accessed September 26, 2017].
- Shigetomi E, Patel S, Khakh BS (2016) Probing the Complexities of Astrocyte Calcium Signaling. *Trends Cell Biol* 26:300–312 Available at: <http://linkinghub.elsevier.com/retrieve/pii/S096289241600009X> [Accessed October 30, 2017].
- Sholl DA (1953) Dendritic organization in the neurons of the visual and motor cortices of the cat. *J Anat* 87:387–406 Available at: <http://www.ncbi.nlm.nih.gov/pubmed/13117757> [Accessed September 25, 2017].
- Sisodia SS (1992) Beta-amyloid precursor protein cleavage by a membrane-bound protease. *Proc Natl Acad Sci U S A* 89:6075–6079 Available at: <http://www.ncbi.nlm.nih.gov/pubmed/1631093> [Accessed June 24, 2017].
- Skoff RP, Hamburger V (1974) Fine structure of dendritic and axonal growth cones in embryonic chick spinal cord. *J Comp Neurol* 153:107–147 Available at: <http://doi.wiley.com/10.1002/cne.901530202> [Accessed October 5, 2017].
- Slunt HH, Thinakaran G, Von Koch C, Lo AC, Tanzi RE, Sisodia SS (1994a) Expression of a ubiquitous, cross-reactive homologue of the mouse beta-amyloid precursor protein (APP). *J Biol Chem* 269:2637–2644 Available at: <http://www.ncbi.nlm.nih.gov/pubmed/8300594> [Accessed October 26, 2016].
- Slunt HH, Thinakaran G, Von Koch C, Lo AC, Tanzi RE, Sisodia SS (1994b) Expression of a ubiquitous, cross-reactive homologue of the mouse beta-amyloid precursor protein (APP). *J Biol Chem* 269:2637–2644 Available at: <http://www.ncbi.nlm.nih.gov/pubmed/8300594> [Accessed April 21, 2017].
- Soba P, Eggert S, Wagner K, Zentgraf H, Siehl K, Kreger S, Löwer A, Langer A, Merdes G, Paro R, Masters CL, Müller U, Kins S, Beyreuther K (2005) Homo- and heterodimerization of APP family members promotes intercellular adhesion. *EMBO J* 24:3624–3634 Available at: <http://www.ncbi.nlm.nih.gov/pubmed/16193067> [Accessed October 26, 2016].
- Spuch C, Ortolano S, Navarro C (2012) New insights in the amyloid-beta interaction with mitochondria. *J Aging Res* 2012.
- Srinivasan R, Huang BS, Venugopal S, Johnston AD, Chai H, Zeng H, Golshani P, Khakh

References

- BS (2015) Ca²⁺ signaling in astrocytes from *Ip3r2*^{-/-} mice in brain slices and during startle responses in vivo. *Nat Neurosci* 18:708–717 Available at: <http://www.nature.com/doi/10.1038/nn.4001>.
- Srinivasan R, Lu T-Y, Chai H, Xu J, Huang BS, Golshani P, Coppola G, Khakh BS (2016) New Transgenic Mouse Lines for Selectively Targeting Astrocytes and Studying Calcium Signals in Astrocyte Processes In Situ and In Vivo. *Neuron* 92:1181–1195 Available at: <http://www.ncbi.nlm.nih.gov/pubmed/27939582> [Accessed September 25, 2017].
- Stahl R, Schilling S, Soba P, Rupp C, Hartmann T, Wagner K, Merdes G, Eggert S, Kins S (2014a) Shedding of APP limits its synaptogenic activity and cell adhesion properties. *Front Cell Neurosci* 8:410 Available at: <http://www.ncbi.nlm.nih.gov/pubmed/25520622> [Accessed October 26, 2016].
- Stahl R, Schilling S, Soba P, Rupp C, Hartmann T, Wagner K, Merdes G, Eggert S, Kins S (2014b) Shedding of APP limits its synaptogenic activity and cell adhesion properties. *Front Cell Neurosci* 8:410 Available at: <http://www.ncbi.nlm.nih.gov/pubmed/25520622> [Accessed April 25, 2017].
- Stephen T-L, Gupta-Agarwal S, Kittler JT (2014) Mitochondrial dynamics in astrocytes. *Biochem Soc Trans* 42:1302–1310 Available at: <http://www.ncbi.nlm.nih.gov/pubmed/25233407> [Accessed December 4, 2017].
- Svoboda K, Yasuda R (2006) Principles of two-photon excitation microscopy and its applications to neuroscience. *Neuron* 50:823–839 Available at: <http://www.ncbi.nlm.nih.gov/pubmed/16772166> [Accessed March 10, 2017].
- Swerdlow RH, Jeffrey BM, Khan SM (2010) The AD mitochondrial cascade hypothesis. *Burns* 20:265–279.
- Szalai G, Krishnamurthy R, Hajnóczky G (1999) Apoptosis driven by IP(3)-linked mitochondrial calcium signals. *EMBO J* 18:6349–6361 Available at: <http://www.ncbi.nlm.nih.gov/pubmed/10562547> [Accessed July 24, 2017].
- Tait SWG, Green DR (2013) Mitochondrial regulation of cell death. *Cold Spring Harb Perspect Biol* 5 Available at: <http://www.ncbi.nlm.nih.gov/pubmed/24003207> [Accessed January 8, 2018].
- Tanzi RE, Gusella JF, Watkins PC, Bruns GA, St George-Hyslop P, Van Keuren ML, Patterson D, Pagan S, Kurnit DM, Neve RL (1987) Amyloid beta protein gene: cDNA, mRNA distribution, and genetic linkage near the Alzheimer locus. *Science* 235:880–884 Available at: <http://www.ncbi.nlm.nih.gov/pubmed/2949367> [Accessed April 21, 2017].

References

- Theer P, Mongis C, Knop M (2014) PSFj: know your fluorescence microscope. *Nat Methods* 11:981–982 Available at: <http://www.ncbi.nlm.nih.gov/pubmed/25264773>.
- Thinakaran G, Kitt CA, Roskams AJ, Slunt HH, Masliah E, von Koch C, Ginsberg SD, Ronnett G V, Reed RR, Price DL (1995) Distribution of an APP homolog, APLP2, in the mouse olfactory system: a potential role for APLP2 in axogenesis. *J Neurosci* 15:6314–6326 Available at: <http://www.ncbi.nlm.nih.gov/pubmed/7472397> [Accessed April 21, 2017].
- Thinakaran G, Koo EH (2008) Amyloid Precursor Protein Trafficking, Processing, and Function *. Available at: <http://www.jbc.org/content/283/44/29615.full.pdf> [Accessed October 25, 2017].
- Tian L, Hires SA, Mao T, Huber D, Chiappe ME, Chalasani SH, Petreanu L, Akerboom J, McKinney SA, Schreiter ER, Bargmann CI, Jayaraman V, Svoboda K, Looger LL (2009) Imaging neural activity in worms, flies and mice with improved GCaMP calcium indicators. *Nat Methods* 6:875–881 Available at: <http://www.ncbi.nlm.nih.gov/pubmed/19898485> [Accessed June 4, 2017].
- Timossi C, Ortiz-Elizondo C, Pineda DB, Dias JA, Conn PM, Ulloa-Aguirre A (2004) Functional significance of the BBXXB motif reversed present in the cytoplasmic domains of the human follicle-stimulating hormone receptor. *Mol Cell Endocrinol* 223:17–26 Available at: <http://www.ncbi.nlm.nih.gov/pubmed/15279907> [Accessed October 27, 2016].
- Turner PR, O'Connor K, Tate WP, Abraham WC (2003) Roles of amyloid precursor protein and its fragments in regulating neural activity, plasticity and memory. *Prog Neurobiol* 70:1–32 Available at: <http://www.ncbi.nlm.nih.gov/pubmed/12927332>.
- Tyan S-H, Shih AY-J, Walsh JJ, Maruyama H, Sarsoza F, Ku L, Eggert S, Hof PR, Koo EH, Dickstein DL (2012) Amyloid precursor protein (APP) regulates synaptic structure and function. *Mol Cell Neurosci* 51:43–52 Available at: <http://www.ncbi.nlm.nih.gov/pubmed/22884903> [Accessed February 9, 2017].
- Vasington FD, Murphy J V (1962) Ca⁺⁺ ion uptake by rat kidney mitochondria and its dependence on respiration and phosphorylation. *J Biol Chem* 237:2670–2677 Available at: <http://www.ncbi.nlm.nih.gov/pubmed/13925019> [Accessed January 24, 2018].
- Vella LJ, Cappai R (2012) Identification of a novel amyloid precursor protein processing pathway that generates secreted N-terminal fragments. *FASEB J* 26:2930–2940 Available at: <http://www.fasebj.org/cgi/doi/10.1096/fj.11-200295> [Accessed January 26, 2017].

References

- Verkhatsky A, Butt A (2013) Glial physiology and pathophysiology. John Wiley & Sons.
- Virchow R (1858) Die Cellularpathologie in ihrer Begründung auf physiologische und pathologische Gewebelehre, 1. Auflage. Berlin: Hirschwald. Available at: http://www.deutschestextarchiv.de/book/show/virchow_cellularpathologie_1858.
- Visch H-J, Rutter GA, Koopman WJH, Koenderink JB, Verkaart S, de Groot T, Varadi A, Mitchell KJ, van den Heuvel LP, Smeitink JAM, Willems PHGM (2004) Inhibition of mitochondrial Na⁺-Ca²⁺ exchange restores agonist-induced ATP production and Ca²⁺ handling in human complex I deficiency. *J Biol Chem* 279:40328–40336 Available at: <http://www.ncbi.nlm.nih.gov/pubmed/15269216> [Accessed January 24, 2018].
- von Bohlen und Halbach O (2009) Structure and function of dendritic spines within the hippocampus. *Ann Anat - Anat Anzeiger* 191:518–531 Available at: <http://linkinghub.elsevier.com/retrieve/pii/S0940960209001228> [Accessed August 17, 2017].
- von Lenhossek M (1895) Der Feinere Bau des Nervensystems im Lichte neuerer Forschung. Available at: http://www.networkglia.eu/sites/networkglia.eu/files/downloads/Bau_des_Nervensystems_VI.pdf [Accessed December 10, 2017].
- Wang B, Wang Z, Sun L, Yang L, Li H, Cole AL, Rodriguez-Rivera J, Lu H-C, Zheng H (2014) The amyloid precursor protein controls adult hippocampal neurogenesis through GABAergic interneurons. *J Neurosci* 34:13314–13325 Available at: <http://www.ncbi.nlm.nih.gov/pubmed/25274811> [Accessed February 9, 2017].
- Wang X, Lou N, Xu Q, Tian G-F, Peng WG, Han X, Kang J, Takano T, Nedergaard M (2006) Astrocytic Ca²⁺ signaling evoked by sensory stimulation in vivo. *Nat Neurosci* 9:816–823 Available at: <http://www.ncbi.nlm.nih.gov/pubmed/16699507> [Accessed May 15, 2017].
- Wang Y, Wu F, Pan H, Zheng W, Feng C, Wang Y, Deng Z, Wang L, Luo J, Chen S (2016) Lost region in amyloid precursor protein (APP) through TALEN-mediated genome editing alters mitochondrial morphology. *Sci Rep* 6:srep22244.
- Wang Z, Wang B, Yang L, Guo Q, Aithmitti N, Songyang Z, Zheng H (2009) Presynaptic and postsynaptic interaction of the amyloid precursor protein promotes peripheral and central synaptogenesis. *J Neurosci* 29:10788–10801 Available at: <http://www.ncbi.nlm.nih.gov/pubmed/19726636> [Accessed October 26, 2016].
- Wasco W, Bupp K, Magendantz M, Gusella JF, Tanzi RE, Solomon F (1992) Identification of a Mouse Brain cDNA that Encodes a Protein Related to the Alzheimer Disease-

References

- Associated Amyloid β Protein Precursor. *Proc Natl Acad Sci* 89:10758–10762 Available at: <http://www.ncbi.nlm.nih.gov/pubmed/1279693>.
- Wasco W, Gurubhagavatula S, Paradis MD, Romano DM, Sisodia SS, Hyman BT, Neve RL, Tanzi RE (1993) Isolation and characterization of APLP2 encoding a homologue of the Alzheimer's associated amyloid beta protein precursor. *Nat Genet* 5:95–100 Available at: <http://www.ncbi.nlm.nih.gov/pubmed/8220435> [Accessed October 26, 2016].
- Weyer SW, Zagrebelsky M, Herrmann U, Hick M, Ganss L, Gobbert J, Gruber M, Altmann C, Korte M, Deller T, Müller UC (2014) Comparative analysis of single and combined APP/APLP knockouts reveals reduced spine density in APP-KO mice that is prevented by APP α expression. *Acta Neuropathol Commun* 2:36 Available at: <http://www.ncbi.nlm.nih.gov/pubmed/24684730> [Accessed January 27, 2017].
- Willem M et al. (2015) η -Secretase processing of APP inhibits neuronal activity in the hippocampus. *Nature* 526:443–447 Available at: <http://www.nature.com/doi/10.1038/nature14864> [Accessed January 26, 2017].
- Woolfrey KM, Srivastava DP (2016) Control of Dendritic Spine Morphological and Functional Plasticity by Small GTPases. *Neural Plast* 2016:1–12 Available at: <http://www.hindawi.com/journals/np/2016/3025948/> [Accessed January 3, 2018].
- World Health Organization (2014) WHO | Dementia. 29/03/14:<http://www.who.int/mediacentre/factsheets/fs369/en> Available at: <http://www.who.int/mediacentre/factsheets/fs362/en/>.
- Wu S-Z, Bodles AM, Porter MM, Griffin WST, Basile AS, Barger SW (2004) Induction of serine racemase expression and D-serine release from microglia by secreted amyloid precursor protein (sAPP). *J Neuroinflammation* 1:2 Available at: <http://www.ncbi.nlm.nih.gov/pubmed/17627481> [Accessed October 27, 2016].
- Wu S, Barger SW (2004) Induction of serine racemase by inflammatory stimuli is dependent on AP-1. *Ann N Y Acad Sci* 1035:133–146 Available at: <http://www.ncbi.nlm.nih.gov/pubmed/15681805> [Accessed October 27, 2016].
- Xue Y, Lee S, Ha Y (2011) Crystal structure of amyloid precursor-like protein 1 and heparin complex suggests a dual role of heparin in E2 dimerization. *Proc Natl Acad Sci U S A* 108:16229–16234 Available at: <http://www.pubmedcentral.nih.gov/articlerender.fcgi?artid=3182750&tool=pmcentrez&rendertype=abstract> [Accessed May 28, 2013].
- Yoshikai S, Sasaki H, Doh-ura K, Furuya H, Sakaki Y (1990) Genomic organization of the human amyloid beta-protein precursor gene. *Gene* 87:257–263 Available at:

References

- <http://www.ncbi.nlm.nih.gov/pubmed/2110105> [Accessed April 25, 2017].
- Young P, Qiu L, Wang D, Zhao S, Gross J, Feng G (2008) Single-neuron labeling with inducible Cre-mediated knockout in transgenic mice. *Nat Neurosci* 11:721–728 Available at: <http://www.pubmedcentral.nih.gov/articlerender.fcgi?artid=3062628&tool=pmcentrez&rendertype=abstract>.
- Yuste R et al. (2011) Dendritic spines and distributed circuits. *Neuron* 71:772–781 Available at: <http://www.ncbi.nlm.nih.gov/pubmed/21903072> [Accessed October 26, 2016].
- Yuste R (2015) The discovery of dendritic spines by Cajal. *Front Neuroanat* 9:18 Available at: <http://journal.frontiersin.org/article/10.3389/fnana.2015.00018/abstract> [Accessed August 8, 2017].
- Zhang L, Trushin S, Christensen TA, Bachmeier B V., Gateno B, Schroeder A, Yao J, Itoh K, Sesaki H, Poon WW, Gylys KH, Patterson ER, Parisi JE, Diaz Brinton R, Salisbury JL, Trushina E (2016) Altered brain energetics induces mitochondrial fission arrest in Alzheimer's Disease. *Sci Rep* 6:18725 Available at: <http://www.nature.com/articles/srep18725>.
- Zhang Y, Thompson R, Zhang H, Xu H (2011) APP processing in Alzheimer's disease. *Mol Brain* 4:3 Available at: <http://www.ncbi.nlm.nih.gov/pubmed/21214928> [Accessed October 5, 2017].
- Zhang Z, Song M, Liu X, Su Kang S, Duong DM, Seyfried NT, Cao X, Cheng L, Sun YE, Ping Yu S, Jia J, Levey AI, Ye K (2015) Delta-secretase cleaves amyloid precursor protein and regulates the pathogenesis in Alzheimer's disease. *Nat Commun* 6:8762 Available at: <http://www.nature.com/doifinder/10.1038/ncomms9762> [Accessed January 26, 2017].
- Zheng H, Jiang M, Trumbauer ME, Sirinathsinghji DJS, Hopkins R, Smith DW, Heavens RP, Dawson GR, Boyce S, Conner MW, Stevens KA, Slunt HH, Sisoda SS, Chen HY, Van der Ploeg LHT (1995) beta-Amyloid precursor protein-deficient mice show reactive gliosis and decreased locomotor activity. *Cell* 81:525–531 Available at: <http://www.ncbi.nlm.nih.gov/pubmed/7758106> [Accessed October 27, 2016].
- Zorec R, Araque A, Carmignoto G, Haydon PG, Verkhratsky A, Parpura V (2012) Astroglial excitability and gliotransmission: an appraisal of Ca²⁺ as a signalling route. *ASN Neuro* 4:103–119 Available at: <http://www.pubmedcentral.nih.gov/articlerender.fcgi?artid=3310306&tool=pmcentrez&rendertype=abstract>.

References

- Zou C, Crux S, Marinesco S, Montagna E, Sgobio C, Shi Y, Shi S, Zhu K, Dorostkar MM, Müller UC, Herms J (2016) Amyloid precursor protein maintains constitutive and adaptive plasticity of dendritic spines in adult brain by regulating D-serine homeostasis. *EMBO J* 35:2213–2222 Available at: <http://www.ncbi.nlm.nih.gov/pubmed/27572463> [Accessed October 27, 2016].
- Zou C, Montagna E, Shi Y, Peters F, Blazquez-Llorca L, Shi S, Filser S, Dorostkar MM, Herms J (2015) Intraneuronal APP and extracellular A β independently cause dendritic spine pathology in transgenic mouse models of Alzheimer's disease. *Acta Neuropathol* 129:909–920 Available at: <http://www.ncbi.nlm.nih.gov/pubmed/25862638> [Accessed October 27, 2016].

11 LIST OF PUBLICATIONS

Montagna, E.*,Crux, S., Luckner, M., Herber, J., Colombo, VA. ,
Marinkovic, P., Tahirovic, S., Lichtenthaler, F S., Wanner, G., Müller, U.,
Sgobi, C.,Herms, J.,2018. “In vivo Ca²⁺ imaging of astrocytic microdomains reveals a critical
role of the amyloid precursor protein for mitochondria”; *Glia*, submitted.

Montagna, E., Dorostkar, MM. and Herms, J. 2017. “The Role of APP in Structural Spine
Plasticity.” *Frontiers in molecular neuroscience* 10: 136.

Zou, C., Crux, S. Marinesco, S., Montagna, E., Sgobio, C., Sh.Y., Shi, S., Zu, K., Dorostkar
MM., Müller, UC., Herms, J., 2016. “Amyloid Precursor Protein Maintains Constitutive and
Adaptive Plasticity of Dendritic Spines in Adult Brain by Regulating D-Serine Homeostasis.”
The EMBO journal.

Zou, C. Montagna, E., Shi, Y., Peters, F., Blazquez-Llorca, L., Shi, S., Filser, S., Dorostkar,
MM., Herms, J., 2015. “Intraneuronal APP and Extracellular A β Independently Cause
Dendritic Spine Pathology in Transgenic Mouse Models of Alzheimer’s Disease.” *Acta
Neuropathologica* 129(6).

Former publications

Giampà, C. C., Montagna, E., Dato, C., Melone, MA.,Bernardi, G., Fusco, FR., et al. 2013.
“Systemic Delivery of Recombinant Brain Derived Neurotrophic Factor (BDNF) in the R6/2
Mouse Model of Huntington’s Disease.” *PLoS ONE* 8(5).

Leuti, A., Laurenti, D., Giampà, C., Montagna, E., Dato, C., Anzilotti, S., Melone, MA.,
Bernardi, G.,Fusco, FR., 2013. “Phosphodiesterase 10A (PDE10A) Localization in the R6/2
Mouse Model of Huntington’s Disease.” *Neurobiology of Disease* 52.